

---

# 7 Hydrates in the Earth

## INTRODUCTION AND OVERVIEW

Only since 1965 has mankind recognized that the formation of *in situ* hydrates in the geosphere predated their artificial formation (ca. 1800) by millions of years. In addition to their age, it appears that hydrates in nature are ubiquitous, with some probability of occurrence wherever methane and water are in close proximity at low temperature and elevated pressures.

Because hydrates concentrate methane [at standard temperature and pressure (STP)] by as much as a factor of 164, and because less than 15% of the recovered energy is required for dissociation, hydrate reservoirs have been considered as a substantial future energy resource. While the total amount of hydrated gas is under some dispute, researchers in both the eastern (Makogon, 1988b) and western (Klauda and Sandler, 2005) hemispheres agree that the total amount of gas in this solid form may surpass the total conventional gas reserve, by an order of magnitude. Hydrates in the earth provide two additional applications, namely, (1) causes of current and ancient climate change and (2) geological hazards.

However, because there has been an overwhelming amount of information generated over the last decade on this topic, it may be well to provide an initial, conceptual overview or “reader’s guide” to this chapter alone, to structure the information. These eight concepts for hydrates in nature are considered, each in a chapter section as

- 7.1: The paradigm is changing: from assessment of amount to production of gas.
- 7.2: Ocean sediments with hydrates typically contain low amounts of biogenic methane.
- 7.3: Sediment lithology and fluid flow are major controls on hydrate deposition.
- 7.4: Remote methods enable an estimation of the extent of a hydrated reservoir.
- 7.5: Drilling logs and coring provide improved assessments of hydrated gas amounts.
- 7.6: Hydrate reservoir models indicate key variables for methane production.
- 7.7: Future hydrated gas production trends are from the permafrost to the ocean.
- 7.8: Hydrates play a part in climate change and geohazards.

Examples of these eight concepts are illustrated in four field case studies, the first two for assessment, and the second two for production: (1) Blake Bahama Ridge, (2) Hydrate Ridge, (3) Messoyakha, and (4) Mallik 2002. In choosing only four case studies for this chapter, the authors were restricted to regions with the broadest applications, in which many research groups have worked, reasoning for a consensus perspective, rather than that of a few groups. For example, interesting perspectives for hydrates in the Gulf of Mexico have evolved from excellent studies by Sassen, et al.; Roberts, et al.; and Paull et al. (all in Paull and Dillon, 2001) but as typical in emerging knowledge areas, several competing perspectives exist regarding the hydrate amounts and assessment. However, even with the consensus which exists in the following examples, the conceptual pictures are certain to be corrected in the future by more knowledgeable writers.

Several excellent volumes have been published over the last decade on hydrates in nature, to further guide the reader: The summaries below are in addition to individual ocean cruises and wells, to which the authors refer in the chapter,

1. *Hydrates of Hydrocarbons*, by Y.F. Makogon, 1997.
2. The *Proceedings of the International Gas Hydrate Conferences* contain state-of-the-art descriptions of hydrates, at three year intervals:
  - The first conference (New Paltz, New York, USA, 1993), edited by E.D. Sloan, J. Happel, and M.A. Hnatow, contains 61 papers by 130 authors.
  - The second conference (Toulouse, France, 1996), edited by J.-P. Monfort, contains 87 papers by 195 authors.
  - The third conference (Salt Lake City, Utah, USA, 1999), edited by G.D. Holder and P.R. Bishnoi, contains 104 papers by 258 authors.
  - The fourth conference (Yokohama, Japan, 2002), edited by Y.H. Mori, contains 204 papers by 500 authors.
  - The fifth conference (Trondheim, Norway, 2005), edited by T. Austvik, contains 247 papers by 683 authors.
3. *Gas Hydrates: Relevance to World Margin Stability and Climate Change*, edited by J.-P. Henriet and J. Minert, 1998.
4. *Submarine Gas Hydrates*, by G.D. Ginsburg and V.A. Soloviev, 1998.
5. *Natural Gas Hydrates: Occurrence, Distribution and Detection*, edited by C.K. Paull, and W.P. Dillon, 2001.
6. *Natural Gas Hydrates in Oceanic and Polar Environments*, edited by M.D. Max, 2003.
7. *Methane Hydrates in Quaternary Climate Change: The Clathrate Gun Hypothesis*, by J.P. Kennett, G. Cannariato, I.L. Hendy, R.J. Behl, 2003.
8. *Advances in the Study of Gas Hydrates*, edited by C.E. Taylor and J.T. Kwan, 2004.
9. *Economic Geology of Natural Gas Hydrates*, edited by A.H. Johnson, M.D. Max, and W.P. Dillon, 2006.

The above books represent years of effort by the authors/editors. For a conceptual picture of hydrates in nature, let us return to an exposition of the eight principles listed earlier.

## 7.1 THE PARADIGM IS CHANGING FROM ASSESSMENT OF AMOUNT TO PRODUCTION OF GAS

Makogon (1965) announced the presence of gas hydrates in the permafrost regions of the Soviet Union. Since that time there have been two extreme views of *in situ* hydrate reserves. In one view, they have been ignored, presumably because they were considered to be too dispersed and difficult to recover, relative to the conventional supply of gas. In the other view, they were thought to be pervasive in all regions of the earth with permafrost (23% of the land mass) and in thermodynamically stable regions of the oceans (90% of the oceans areal extent). With further exploration and production of gas from a hydrate reservoir, a third, more realistic estimate of the hydrate resource has evolved, as the basis for this chapter.

### 7.1.1 Extent of the Occurrence of *In Situ* Gas Hydrates

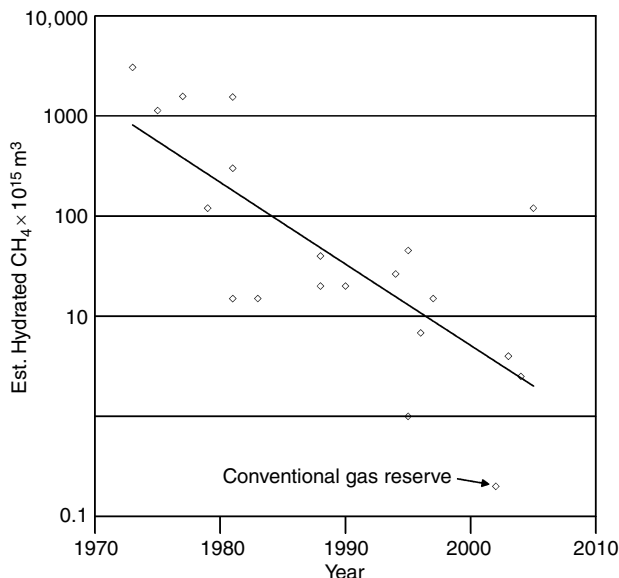
Knowledge of the occurrence of *in situ* gas hydrates is very incomplete, and is obtained from both indirect and direct evidence. For the most irrefutable evidence, there have been 23 locations where hydrate samples have been recovered, 3 in permafrost and 20 in ocean environments. In permafrost regions, hydrate evidence is limited to drillings and associated well logs, whereas the sonic reflection method is relatively inexpensive but much less direct and much less reliable means of sensing hydrate on oceanic continental margins. Economics is the determining factor promoting increasing interest in the larger, oceanic hydrate reservoirs.

Table 7.1 lists the estimates of natural gas in hydrates in the geosphere's gas hydrate stability zone (GHSZ). These estimates range from the maximum values of Trofimuk et al. (1973), who apparently assumed that hydrates could occur wherever satisfactory temperatures and pressures exist, to the minimum values of Soloviev (2002) who considered more limiting factors such as availability of methane, limited porosity, and percentages of organic matter, thermal history of various regions, and so on. All estimates of natural gas hydrates are not well defined, and therefore somewhat speculative. However, even the most conservative estimates suggest very large amounts of gas in hydrated form.

Table 7.1 illustrates that as man learns more about hydrates in the environment, estimates of the amount of hydrates decrease. As shown in Figure 7.1, this resulted in a steady reduction in the estimate of hydrated gas, since the initial estimates of  $3053 \times 10^{15} \text{ m}^3$  methane (STP) in by Trofimuk et al. (1973). The overwhelming size of this number may be realized by comparison to  $1 \times 10^{15} \text{ m}^3$ , which is the energy consumption of the United States for 1000 years at the current rate. In Figure 7.1, it should be noted that all of the estimates (except the estimate of Klauda and Sandler [2005]) were done in approximately the same way—a limited

**TABLE 7.1**  
**Estimates of *In Situ* Methane Hydrates**

Year	CH <sub>4</sub> amount 10 <sup>15</sup> m <sup>3</sup> STP	Citations
1973	3053	Trofimuk et al.
1977	1135	Trofimuk et al.
1982	1573	Cherskiy et al.
1981	120	Trofimuk et al.
1981	301	McIver
1974/1981	15	Makogon
1982	15	Trofimuk et al.
1988	40	Kvenvolden and Claypool
1988	20	Kvenvolden
1990	20	MacDonald
1994	26.4	Gornitz and Fung
1995	45.4	Harvey and Huang
1995	1	Ginsburg and Soloviev
1996	6.8	Holbrook et al.
1997	15	Makogon
2002	0.2	Soloviev
2004	2.5	Milkov
2005	120	Klauda and Sandler



**FIGURE 7.1** Estimates of amount of hydrated gas have generally decreased with time. Note the logarithmic scale of the ordinate.

amount of fairly well-known geological data on a local scale was extrapolated to a global level.

The Klauda and Sandler (2005) model is state-of-the-art as discussed in detail in Section 7.2.3.2.1 on hydrate formation. The model represents a singular advance because it alone enables prediction of 68 of the 71 occurrences of hydrates, with explanations for the three exceptions. The large amount of hydrates predicted by Klauda and Sandler includes both very deep hydrates and very dispersed hydrates, many of which are not accounted for by the other models or discovered by sampling due to dissociation. When only continental hydrates are considered, Klauda and Sandler predict  $4.4 \times 10^{16} \text{ m}^3$  (STP) of gas in hydrates, an estimate larger than those of Kvenvolden (1988) or Makogon (1997).

For simplicity, only estimates over the last decade are presented in Table 7.2, with assumptions or notable aspects that discriminate between the various models. Note that all estimates are comparatively large relative to estimates of the conventional gas reserve of  $0.15 \times 10^{15} \text{ m}^3$  methane (STP) (Radler, 2000).

Even the most conservative estimates of gas in hydrates in Table 7.1 indicate their enormous energy potential. Kvenvolden (1988) indicated that the 10,000 Gt (1 Gt =  $10^{15}$  g) carbon or  $1.8 \times 10^{16} \text{ m}^3$  of methane in hydrates may surpass the available, recoverable conventional methane by two orders of magnitude, or a factor of two larger than the methane equivalent of the total of all fossil fuel

**TABLE 7.2**  
**Assumptions in Models of the Last Decade of Hydrated Gas Amounts**

Model	Estimated amount $\times 10^{15} \text{ m}^3 \text{ CH}_4$	Assumptions or notable aspects
Harvey and Huang (1995)	23	<ol style="list-style-type: none"> <li>1. Limited to 250–3000 m H<sub>2</sub>O depth</li> <li>2. Interpolated seafloor temperature</li> <li>3. Required &gt;0.5 wt% organic carbon</li> <li>4. Reduced area arbitrarily by 25%</li> <li>5. 2.5–10% pore volume filling</li> </ol>
Dickens (2001)	4.9–25	<ol style="list-style-type: none"> <li>1. GHSZ is represented by Atlantic margin</li> <li>2. Isobath of 1 km used for span of global margins</li> <li>3. All continental margins contain hydrates</li> <li>4. Hydrated pore space is 1–5%</li> </ol>
Milkov (2004)	3	<ol style="list-style-type: none"> <li>1. Same approach as Dickens (above) with exceptions</li> <li>2. Only 20% of GHSZ contains hydrates</li> <li>3. Predicts overall (not local) amounts</li> <li>4. 1.2% of pore volume occupied</li> </ol>
Klauda and Sandler (2005)	120	<ol style="list-style-type: none"> <li>1. New thermomodel with pores and salt for GHSZ</li> <li>2. Measured seafloor T and organic carbon content</li> <li>3. Methanogenesis model matched to Blake-Bahama Ridge data</li> <li>4. Global average of 3.4% of pore volume filled</li> <li>5. Can predict 68 of 71 local hydrate sites</li> </ol>

deposits. He noted, based on Bolin (1983) and Moore and Bolin (1987), that global carbon cycle amounts were as follows: fossil fuel deposits (5,000 Gt), terrestrial soil, detritus, and peat (1960 Gt), marine dissolved materials (980 Gt), terrestrial biota (830 Gt), the atmosphere (3.6 Gt), and marine biota (3 Gt). Relative to hydrates, the only larger pool of inorganic and organic carbon is that disseminated in sediments and rocks (20,000,000 Gt), which is unrecoverable as an energy resource.

Ginsburg and Soloviev (1995) and Milkov (2004) suggested that hydrates may be two orders of magnitude less than the previous consensus. They suggested that both the high contents of sediments and the concept of continuous regional distribution were overstated in past estimates. However, even with more conservative estimates, they indicated that the gas content in hydrates was  $10^{15} \text{ m}^3$ , accurate to one order of magnitude. It was difficult to reconcile the original Ginsburg and Soloviev (1995) local hypothesis with a continuous distribution shown by bottom simulating reflectors (BSRs), so modifications were made to account for both diffusion and water migration (Ginsburg and Soloviev, 1997; Soloviev and Ginsburg, 1997).

A second concern for the large estimates of methane in hydrate results from the Leg 164 drilling by Holbrook et al. (1996) who suggest downscaling the estimates in [Table 7.1](#) by as much as a factor of three. However, even if such errors are real, the amount of gas in hydrates remains enormous. Ginsburg and Soloviev note that most resource estimates in Table 7.1 rely upon the equation  $Q = S \times h \times K \times Z \times E$ , where  $Q$  = gas content ( $\text{m}^3$ ),  $S$  = hydrate area ( $\text{m}^2$ ),  $h$  = hydrate thickness (m),  $K$  = sediment porosity (%),  $Z$  = fractional pore filling, and  $E$  = gas expansion (164 vol. gas/vol. hydrate).

The most detailed method of U.S. hydrate resource estimation has been by Collett (1995, 1996). He assigned probabilities to 12 different factors to estimate the hydrate resources within the United States at  $9 \times 10^{15} \text{ m}^3$  of gas. Collett (1995) notes the high degree of uncertainty places the above mean value between the 95% probability level ( $3 \times 10^{15} \text{ m}^3$ ) and the 5% probability level ( $19 \times 10^{15} \text{ m}^3$ ). However, in the United States, the mean hydrate value indicates 300 times more hydrated gas than the gas in the total remaining recoverable conventional reserves.

After concluding that the hydrated reserves are enormous, a second major point is that the amount of hydrates in the ocean surpasses that in the permafrost by two orders of magnitude. This oceanic amount is larger than would be expected, even though the oceans comprise 70% of the earth's surface, while the permafrost (regions with the land hydrates) comprise only 23% of the earth's land mass. In the relative hydrate amounts in the ocean and permafrost ([Table 7.3](#)), note that the estimates of the oceanic hydrate reserves are so large that a 1% error in ocean approximations could encompass the entire permafrost hydrate reserves. It should be noted that methane accumulates to form hydrates in continental margin sediments for the following two reasons: (1) the flux of organic carbon to the seafloor is the greatest and (2) the sedimentation rates are the highest (Dillon and Max, 2001).

The major difficulty in considering hydrates as actual reserves stems from the solid, dispersed character of the hydrates in locations that are difficult to

**TABLE 7.3**  
**Estimates of Relative Hydrated Methane in the Permafrost and the Ocean**

Permafrost hydrated methane ( $10^{14} \text{ m}^3$ )	Oceanic hydrated methane ( $10^{16} \text{ m}^3$ )	References
0.57	0.5–2.5	Trofimuk et al. (1977)
0.31	0.31	McIver (1981)
340	760	Dobrynin et al. (1981)
1.0	1.0	Makogon (1988)
7.4	2.1	MacDonald (1990)

access, such as permafrost and deep oceans. The most recent estimate (Klauda and Sandler, 2005) determined that there is a global average value of 3.4% of the pore space filled, compared to the common a priori assumption of an overall global value of 5%.

Due to this low pore filling and long formation times, hydrates should be considered a nonrenewable resource from which the recovery of gas is much more difficult than that from a normal gas reservoir. In addition, while an energy balance of the dissociation of pure hydrates is highly favorable, hydrates may be sparsely dispersed in sediment so economic recovery will be problematic. However, before turning to the production of gas from hydrates, consider first the locations of hydrate reserves, and requirements for formation.

Kvenvolden (Personal Communication, November 28, 2005) compiled 89 hydrate sites shown in Figure 7.2, with a complete listing in Tables 7.4 and 7.5. In those locations hydrates were either:

1. Recovered as samples (23 locations),
2. Inferred from BSRs (63 locations), decrease in pore water chlorinity (11 locations), well logs (5 locations), and slumps (5 locations), or
3. Interpreted from geologic settings (6 locations).

In the above hydrate evidence, some locations are double-listed because they had more than one piece of evidence. It is interesting that 63 BSR locations provide the most evidence for hydrates—a factor of almost 3 larger than the 23 sample locations with the most irrefutable evidence. As will be demonstrated later in the Blake-Bahama Ridge and Hydrate Ridge Case Studies and Section 7.4.2, BSR evidence is not totally reliable, but provides a first approximation of hydrated subsurface depth and area extent.

The hydrates-in-nature paradigm is currently changing. The above tables and quantity estimates indicate that much of the natural gas containing hydrates is in the ocean bottom, and while production of gas from such deep-lying hydrates is now too expensive, it is likely that in the near future mankind will need to

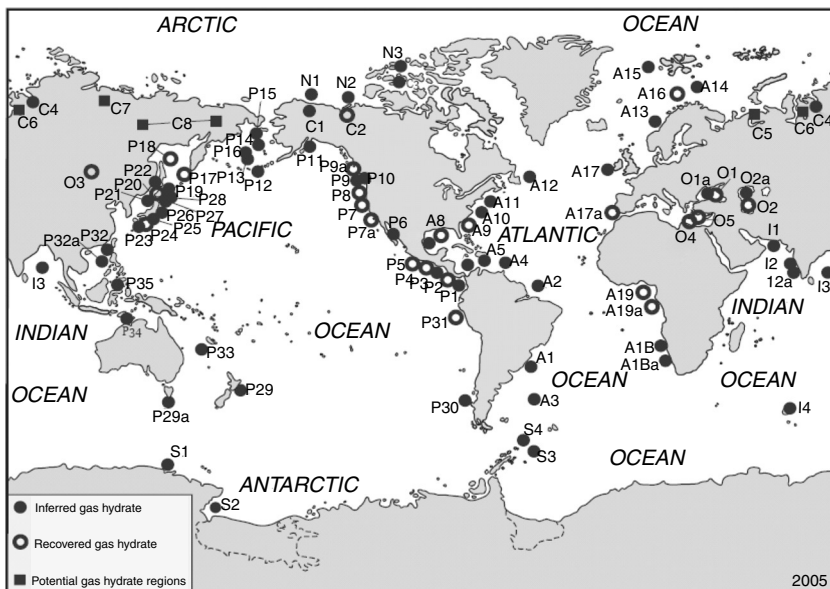


**FIGURE 7.2** Inferred (63), Recovered (23), and Potential (5) hydrate locations in the World. (Courtesy of K. Kvenvolden, Personal Communication November 28, 2005.)

tap that fuel source to meet growing energy demands. However, the conceptual paradigm is changing from assessment of the energy resource, as in the two initial case studies of the Blake-Bahama Ridge and Hydrate Ridge, to the conceptual proof of energy production from hydrates, as shown in the two case studies of the Messoyakha field and the Mallik 2002 field, with all four case studies given at the chapter conclusion. The next step will be extended production testing in permafrost-associated hydrates.

This paragraph summarizes the preceding first principle of hydrates in nature. Very large amounts of hydrated methane exist in nature, perhaps, as much as twice that of all other fossil fuels combined. Such a large resource finds major applications in energy, climate, and geohazards. Of the two geologic types of reservoirs, the amount of hydrates in the ocean overshadows that in the permafrost, by two orders of magnitude. Except for anecdotal instances, hydrates are distributed in very low concentrations over very large areas. The reader should be cautioned that it is very unlikely that any reservoirs similar to the Blake Ridge (see Case Study 1) will ever be exploited. Kleinberg (Personal Communication, July 27, 2006) cautions, “There will be windmills on the roofs of Charleston before the Blake Ridge is drilled for gas.” Hydrated reservoirs should be considered as a nonrenewable resource, because they require geologic times to accumulate, as will be demonstrated in the remainder of this chapter. The hydrate paradigm is changing—moving from locating and quantifying amounts of hydrates in reservoirs to conceptual production and production testing.

**TABLE 7.4**
**Summary of Known and Inferred Subaqueous Gas-Hydrate Occurrences in Atlantic Ocean, Polar Oceans, Continents, and in Inland Seas and Lakes**

Designation	Location offshore	Evidence	References
<b>Atlantic ocean</b>			
A1	(Pelotas Basin)	BSR	Fontana and Mussemeci (1994)
A2	Brazil (Amazon Fan)	BSR	Manley and Flood (1988)
A3	Argentina (Central Argentine Basin)	BSR	Manley and Flood (1988)
A4	Barbados (Barbados Ridge)	BSR	Ladd et al. (1982)
A5	Southern Caribbean Sea	BSR	Ladd et al. (1984)
A6	Panama and Colombia (Colombia Basin)	BSR	Shipley et al. (1979)
A7	Gulf of Mexico (off Mexico, western area)	BSR	Shipley et al. (1979)
A8	(off USA, northern area)	Samples	Brooks et al. (1985, 1986); Sassen and MacDonald (1994, 1997a,b)
A9	Southeastern USA (Blake-Bahama Ridge) (DSDP Leg 76)	BSR Slumps Samples	Markl et al. (1970); Shipley et al. (1979) Carpenter (1981); Dillon et al. (1996) Kvenvolden and Barnard (1983)
	(ODP Leg 164)	<Cl <sup>-</sup>	Jenden and Gieskes (1983)
	(ODP Leg 164)	BSR	Holbrook et al. (1996)
A10	Eastern USA (Carolina Trough)	Samples	Paull et al. (1996)
A11	Eastern USA (Continental Rise)	BSR	Dillon and Paull (1983)
			Tucholke et al. (1977); Dillon et al. (1993, 1995)
A12	Newfoundland, Canada (Laborador Shelf)	BSR	Taylor et al. (1979)
A13	Norway (Storegga Slide) (ODP Leg 104)	BSR Slumps <Cl <sup>-</sup> CH <sub>4</sub> , <Cl <sup>-</sup>	Bugge et al. (1987); Mienert et al. (1998) Jansen et al. (1987); Bugge et al. (1987) Hesse and Harrison (1981) Kvenvolden et al. (1989)

(Continued)

**TABLE 7.4**  
**Continued**

<b>Designation</b>	<b>Location offshore</b>	<b>Evidence</b>	<b>References</b>
A14	(Barents Sea)	BSR	Andreassen et al. (1990)
A15	(off Svalbard)	BSR	Posewang and Mienert (1999)
A16	(Haakon-Mosby mud volcano)	Samples	Ginsburg et al. (1999)
A17	Ireland (Porcupine Basin)	Geophysics	Henriet et al. (1998)
A17a	Spain (Gulf of Cadiz)	Sample	Mazurek et al. (2002)
A18	Africa (S.W. Africa)	Slumps	Summerhayes et al. (1979)
A18a	South Africa (S.W. continental margin)	BSR	Ben-Avraham et al. (2002)
A19	Nigeria (continental slope)	Samples	Brooks et al. (1994)
A19a	Congo/Angola (Congo–Angola Basin)	Samples	Charlou et al. (2004)
<b>North (Arctic)</b>			
N1	Alaska (Beaufort Sea)	BSR	Grantz and Dinter (1980); Kvenvolden and Grantz (1990)
		Slumps	Kayen and Lee (1991)
N2	Canada (Beaufort Sea)	Logs	Weaver and Stewart (1982)
N3	Canada (Sverdrup Basin)	Logs	Judge (1982)
<b>South (Antarctic)</b>			
S1	Antarctica (Wilkes Land Margin)	BSR	Kvenvolden et al. (1987)
S2	(Ross Sea)	CH <sub>4</sub>	McIver (1975)
		<Cl <sup>-</sup>	Mann and Gieskes (1975)
S3	(Weddell Sea)	BSR	Lonsdale (1990)
S4	(South Shetland margin)	BSR	Lodolo et al. (1993)

**Other (inland seas and lakes)**

O1	Black Sea, Russia	Samples	Yefremova and Zhizhchenko (1974); Ginsburg et al. (1990)
O1a	Black Sea, Russia	BSR	Zillmer et al. (2005)
O2	Caspian Sea, Russia	Samples	Yefremova and Gritchina (1981); Ginsburg et al. (1992)
O2a	Caspian Sea, Russia	BSR	Diaconescu et al. (2004)
O3	Lake Baikal, Russia	BSR	Hutchinson et al. (1991)
		Samples	Kus'min et al. (1998)
O4	Mediterranean Sea (ODP Leg 160)	<Cl <sup>-</sup> , CH <sub>4</sub>	DeLange and Brumsack (1998)
O5	Turkey (Kula mud volcano)	Sample	Woodside et al. (1998)

**Continental**

C1	Alaska (North Slope)	Logs	Collett (1993)
		PCS	Summary by Collett (1993)
C2	Canada (Mackenzie Delta)	Logs	Bily and Dick (1974)
		Samples	Dallimore et al. (1999)
C3	(Arctic Islands)	Logs	Davidson et al. (1978); Judge (1982)
C4	Russia (Messoyakah Field)	CH <sub>4</sub>	Makogon et al. (1972)
C5	(Timan-Pechora Province)	Interpretation	Cherskiy et al. (1982)
C6	(Western Siberian Platform)	Interpretation	Cherskiy et al. (1982)
C7	(Eastern Siberian Craton)	Interpretation	Cherskiy et al. (1982)
C8	(Northeast Siberia)	Interpretation	Cherskiy et al. (1982)

*Note:* BSR, Bottom-Simulating Reflection; <Cl<sup>-</sup>, Low Chloride Content of Pore Water; CH<sub>4</sub>, High Methane Content; Logs, Well-Log Response; PCS, Pressure Core Sample; Geophysical, Seismic Evidence of Past Occurrence of Gas Hydrate.

*Source:* From Kvenvolden, Personal Communication, November 28, 2005.

**TABLE 7.5**  
**Summary of Known and Inferred Subaqueous Gas–Hydrate Occurrences in the Pacific and Indian Oceans**

Designation	Location offshore	Evidence	References
<b>Pacific ocean</b>			
P1	Panama	BSR	Shipley et al. (1979)
P2	Costa Rica (Middle America Trench) (DSDP Leg 84)	BSR Samples	Shipley et al. (1979) Kvenvolden and McDonald (1985)
	(ODP Leg 170)	Samples	Shipboard Scientific Party (1997)
P3	Nicaragua (Middle America Trench)	BSR	Shipley et al. (1979)
P4	Guatemala (Middle America Trench) (DSDP Leg 67)	BSR Samples <Cl <sup>-</sup>	Shipley et al. (1979) Harrison and Curiale (1982) Hesse and Harrison (1981); Harrison et al. (1982)
	(DSDP Leg 84)	Samples Logs	Kvenvolden and McDonald (1985) Kvenvolden and McDonald (1985)
P5	Mexico (Middle America Trench) (DSDP Leg 66)	BSR Samples	Shipley et al. (1979) Shipley and Didyk (1982)
P6	Mexico (Gulf of California, Guaymas Basin)	BSR	Lonsdale (1985)
P7	California, USA (Eel River Basin)	BSR	Field and Kvenvolden (1985)
P7a	(Santa Monica Basin)	Samples	Brooks et al. (1991)
P8	Oregon, USA (Cascadia Basin) (ODP Leg 146)	BSR Samples	Normark et al. (2003) Moore et al. (1992)
	(Hydrate Ridge)	Samples	Whiticar et al. (1995); Kastner et al. (1998)
P9	Canada (Cascadia Basin)	BSR	Suess et al. (1999a,b) Davis et al. (1990); Hyndman and Spence (1992)
P9a	Northern Cascadia Margin	Samples	Pohlman et al. (2005)
P10	(Fjords of British Columbia)	Slumps	Bornhold and Prior (1989)
P11	Alaska, USA (Eastern Aleutian Trench)	BSR	Kvenvolden and von Huene (1985)
P12	Alaska, USA (Middle Aleutian Trench)	BSR	McCarthy et al. (1984)
P13	Bering Sea (Alaska, USA)	<Cl <sup>-</sup> VAMPs	Hesse and Harrison (1981) Scholl and Cooper (1978)

**TABLE 7.5**  
**Continued**

Designation	Location offshore	Evidence	References
P14	(USA, Bering Sea Shelf)	BSR	Hammond and Gaither (1983)
P15	(USA/Russia, Navarin Margin)	BSR	Carlson et al. (1985)
P16	Russia (Shirshov Ridge)	BSR	Saltykova et al. (1987)
P17	Okhotsk Sea (Paramushir Island, Russia)	Samples	Zonenshayn et al. (1987)
P18	(Sahkalin Island, Russia)	Samples	Ginsburg et al. (1993)
P19	(Off Abashiri, Kitami-Yamato Mount, Japan)	BSR	Matsumoto et al. (1994); Sato (1994)
P20	Japan, Japan Sea (DSDP Leg 57) (Okushiri Ridge) (ODP Leg 127)	<Cl <sup>-</sup> Sample BSR	Moore and Gieskes (1980) Shipboard Scientific Party (1990) Kuramoto and Okamura (1995)
P21	(Western Tsugaru Basin)	BSR	Sato (1994)
P22	(Tatar Trough)	BSR	Sato (1994)
P23	Japan, Nankai Trough (off eastern Miyazaki)	BSR	Aoki et al. (1983); Tamano et al. (1984)
P24	(off southern Shikoku) (ODP Leg 131)	BSR Sample	Shipboard Scientific Party (1991) Shipboard Scientific Party (1991)
P25	(Muroto Trough)	BSR	Sato (1994); Matsumoto et al. (1994)
P26	(Kumano-nada off Omaezaki Cape)	BSR	Okuda (1995); Gas Epoch (1995)
P27	Japan, Offshore Chiba Basin	CH <sub>4</sub> , <Cl <sup>-</sup> BSR	JNOC press release (2000) Arato et al. (1995)
P28	Japan, Kuril Trench (off Tokachi/Hidaka)	BSR	Sato (1994)
P29	New Zealand (Hikurangi Trough)	BSR	Katz (1981)
P29a	Tasmania (South Tasman Rise)	BSR	Stagg et al. (2000)
P30	Chile (Peru-Chile Trench)	BSR	Cande et al. (1987)
P31	Peru (Peru-Chile Trench) (ODP Leg 112)	CH <sub>4</sub> , <Cl <sup>-</sup> BSR Samples	Froelich et al. (1995) Miller et al. (1991) Kvenvolden and Kastner (1990)
P32	Taiwan (South China Sea)	BSR	Chi et al. (1998)
P32a	South China Sea	BSR	Wu et al. (2005)
P33	Australia (Tasman Sea, Lord Howe Rise)	BSR	Exon et al. (1998)
P34	(Timor Trough)	CH <sub>4</sub>	McKirdy and Cook (1980)
P35	Indonesia (Celebes Sea)	BSR	Neben et al. (1998)
<b>Indian Ocean</b>			
I1	Oman (Gulf of Oman, Makran Margin)	BSR	White (1979)
I2	India (Arabian Sea)	BSR	Veerayya et al. (1998)

(Continued)

**TABLE 7.5**  
**Continued**

Designation	Location offshore	Evidence	References
I2a	(Western continental margin)	BSR	Rao et al. (2001)
I3	(Bay of Bengal)	BSR	Rastogi et al. (1999)
I4	Kerguelen Plateau (Labuan Basin)	BSR	Stagg et al. (2000) P29a

*Note:* BSR, Bottom simulating reflection;  $<\text{Cl}^-$ , low chloride content of pore water;  $\text{CH}_4$ , high methane content; VAMPs, velocity amplitude pulldowns; Logs, well-log response.

*Source:* From Kvenvolden, Personal Communication, November 28, 2005.

## 7.2 SEDIMENTS WITH HYDRATES TYPICALLY HAVE LOW CONTENTS OF BIOGENIC METHANE

The rule of thumb in the title is shown in the following six points, which comprise the subsections of 7.2:

1. As a heuristic, methane availability limits hydrate formation in reserves. Of the two sources of methane (biogenic and thermogenic) in natural hydrates, most of the gas is biogenic, that is, from bacterially generated methane, with anecdotal exceptions.
2. Hydrates result from two types of reservoirs: (1) the large majority of cases are for slow flux or in-place generation of methane dissolved in water, as shown in the case study of the Blake Bahama Ridge and (2) fast fluxes of dissolved and free gas from deeper in the earth, as shown in the Hydrate Ridge case study, with other examples being the Black and Okhotsk Seas. Exceptions to this rule of thumb are shown via thermogenic gas examples from the Gulf of Mexico, Barkley Canyon and the Caspian Sea, which also have fast fluxes.
3. The biogenic methane is generated from anaerobic degradation, accompanied by a sulfate–methane interface (SMI), which can be used to determine the upper boundary of hydrate formation depth (Paull et al., 2005).
4. Another heuristic (Roberts, 2001) is that intermediate fluxes of gas result in hydrates, while very fast fluxes result in mud volcanoes and very slow fluxes result in mineralization, or carbonates.
5. With anecdotal exceptions, the hydrate content is usually low, typically averaging 3.5% of pore volume.
6. Current hydrated gas estimates are made for biogenic gas associated with in-place generation that tends to be more uniformly distributed. We have no general factual data about the extent of hydrate distribution in the vicinity of submarine seepages (Ginsburg and Soloviev, 1998, p. 165).

After the section summary in the preceding six statements, let us consider the evidence for such judgments. Methane availability is one of the most critical issues controlling the occurrence of natural gas hydrates (Xu and Ruppel, 1999). In the thermodynamic regime of temperature and pressure in the ocean or permafrost, water is seldom the limiting chemical; therefore several of the markers of hydrate formation are related to the generation of methane. The origins of the gases in hydrate are mostly biogenic but there is anecdotal evidence of thermogenic gases, as in the Gulf of Mexico and Caspian Sea. Kvenvolden and Lorenson (2001) state that more than 99% of the hydrates on earth contain methane formed by biogenic processes. We will consider the gas source (Section 7.2.1), before qualitative hydrate formation (Section 7.2.2) and the mechanism (Section 7.2.3) is investigated.

### 7.2.1 Generation of Gases for Hydrate Formation

For details of methane hydrates *in situ* geochemistry beyond the overview in this section, the reader is referred to the review by Kvenvolden (1995). While they are not typical in hydrates, thermogenic gases are more common in normal natural gas reservoirs, and thermogenic generation has been reviewed thoroughly in a number of references (see for example, Hunt, 1979, 163 ff.). The thermogenic gases are produced by a catagenesis process characterized by high temperatures ( $>450$  K), producing relatively large amounts of ethane and higher hydrocarbons. However, because biogenic gases dominate in hydrates, organic diagenesis will be briefly reviewed, with its low temperature mechanism.

The words “organic diagenesis” (sometimes called bacterial methanogenesis) are used to denote the low temperature, biogenic conversion of organic matter to methane, which is subsequently transformed to hydrate. Organic diagenesis is usually enhanced by high values of the clastic/organic flux to the seafloor. Kvenvolden (1985a) suggested sedimentation rates between  $30\text{ m}/10^6\text{ yr}$  and  $300\text{ m}/10^6\text{ yr}$  are necessary for hydrate formation. Collett (1996) and Klauda and Sandler (2005) assign probabilities of zero to hydrate formation if the total organic carbon (TOC) present is less than 0.5% and 0.4%, respectively. Collett assigns a probability of unity if the TOC is greater than 2%, as an upper bound.

The following discussion is derived almost entirely from the classic review of organic diagenesis by Hesse (1986). He modified the work of Claypool and Kaplan (1974), to suggest six stages (diagrammed in Figure 7.3) through which organic matter passes in anaerobic sediments. At each stage the change in the standard Gibbs free energy of reaction is more negative (favorable) than the reaction mechanism of the stages above it.

In stage one of Figure 7.3 the organic matter (containing carbon, nitrogen, and phosphorus in the ratio 106:16:1) is oxidized by dissolved oxygen. With somewhat deeper sediments, the organic matter is reduced in the second stage by nitrates, primarily in the form of nitric acid. More typically, oceans are anaerobic where hydrates are found, and follow the systems on the right of Figure 7.3. However, from the third stage onward, both the ventilated basin (on the left of Figure 7.3)

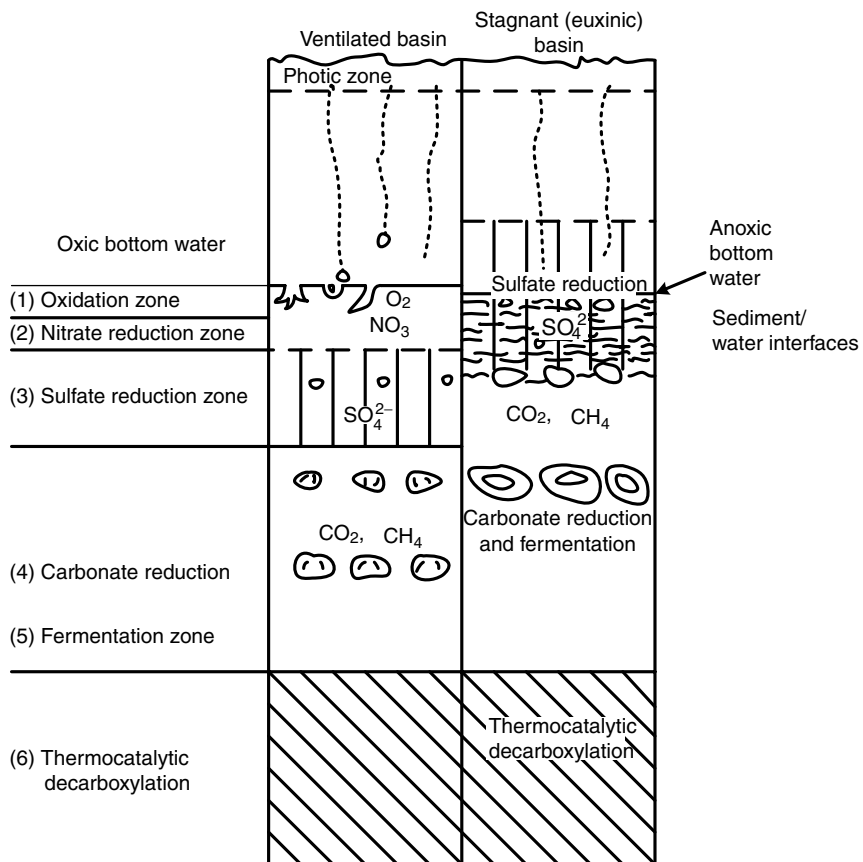
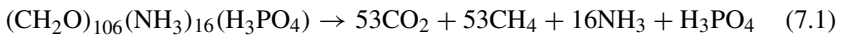


**FIGURE 7.3** Stages of organic matter oxidation in anoxic sediments. (Reproduced from Hesse, R., *Geosci. Can.*, **14**, 165 (1986). With permission from the Geological Association of Canada.)

and anaerobic or anoxic basins (on the right) follow similar mechanisms. The third stage is characterized by sulfate ion reduction. Immediately below is the fourth stage of carbonate reduction, which generates methane for hydrate formation. Whiticar et al. (1986) demonstrated that methane is generated by microbial reduction of  $CO_2$  after the sulfate has been reduced. Without giving the complete carbonate mechanism, the overall reaction for the production of methane from an organic is



Below the stage of methane production is the fermentation (fifth) stage, followed by the sixth, thermocatalytic stage at still greater depths. The initial five stages require the presence of bacteria; below stage five, bacterial activity ceases

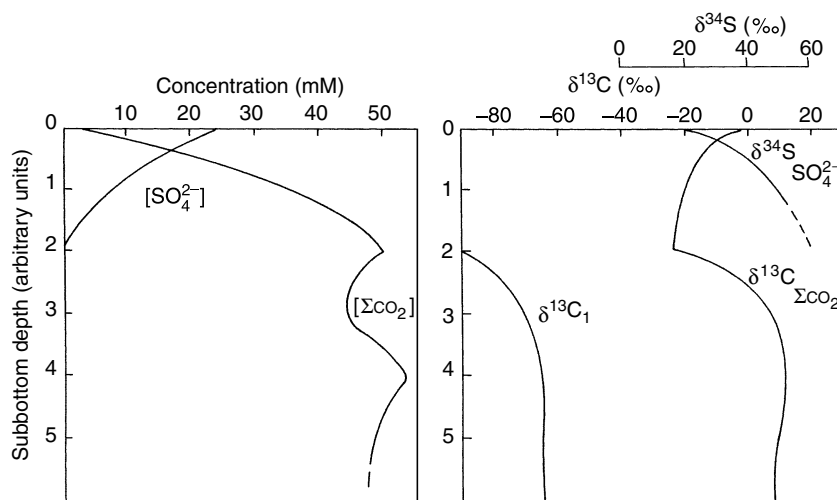


**FIGURE 7.4** Generalized profiles of concentration and isotope ratio changes for dissolved sulfate and carbon species in anoxic marine sediments. Depth scale is arbitrary with depth units ranging from  $10^{-1}$  to  $10^2$  m. (Reproduced from Claypool, G.E., Kvenvolden, K.A., *Ann. Rev. Earth Planet Sci.*, **11**, 299 (1983). With permission from Annual Reviews, Inc.)

and the more usual thermocatalytic reactions begin, which are associated with hydrocarbon production. The main chemical species released to the pore water from the microbial breakdown of organic matter are the carbonate species listed as  $\Sigma\text{CO}_2$ , which include  $\text{CO}_2$ ,  $\text{H}_2\text{CO}_3$ ,  $\text{HCO}_3^-$ , and  $\text{CO}_3^{2-}$  as shown in Figure 7.4.

Carbonates are generated in all of the zones, but they are consumed only below the third stage. After the depletion of more than 80% of the sulfate, the components of  $\Sigma\text{CO}_2$  become oxidants, leading to the production of methane. It is possible to distinguish between the  $\text{CO}_2$  produced and the  $\text{CO}_2$  consumed, determining the extent of carbon isotopic fractionation, particularly associated with the methane production in stage four.

The way of discriminating gas source is via the isotope  $^{13}\text{C}$ , which is distributed through sediments of all geological ages; the  $^{13}\text{C}$  difference in mass relative to  $^{12}\text{C}$  is brought about through fractionation by both biological and physical processes. The fractionation is measured relative to a standard sample of Pee Dee Belemnite (PDB), with the units of parts per thousand (‰). The ratio difference ( $\delta$ ) of  $^{13}\text{C}$  to  $^{12}\text{C}$  may be measured spectrometrically, and is defined by

$$\delta^{13}\text{C} \equiv \left[ \frac{[^{13}\text{C}] / [^{12}\text{C}]_{\text{sample}}}{[^{13}\text{C}] / [^{12}\text{C}]_{\text{PDB}}} - 1 \right] \times 10^3 \quad (7.2)$$

Methane formed by biogenic processes ranges in  $\delta^{13}\text{C}$  from about  $-60\text{‰}$  to  $-85\text{‰}$ , while methane from thermogenic processes ranges from  $-25\text{‰}$  to  $-55\text{‰}$  (Hunt 1979, p. 25).

During the first three stages of organic matter decomposition in Figure 7.3, negligible carbon isotopic fractionation occurs. However, in the fourth stage, methane generated from carbonates has an isotopic composition that is about 70‰ lighter than the carbon of the parent material (Hesse, 1986). The residual CO<sub>2</sub> consequently becomes enriched in  $\delta^{13}\text{C}$  reaching positive values as high as +15–25‰.

Figure 7.4 shows the reduction in sulfates and the corresponding growth of both the parent carbonates and the offspring methane with subbottom depth. The methane production is parallel but lower in isotope production than the carbonates. In Figure 7.4 the sulfur isotope ( $\delta^{34}\text{S}$ ) content is defined in an identical manner to Equation 7.2 with the replacement of the fraction  $^{13}\text{C}/^{12}\text{C}$  by  $^{34}\text{S}/^{32}\text{S}$  in both the numerator and the denominator, using Cañon Diablo meteoritic troilite as a standard. The  $\delta^{34}\text{S}$  value increases from 20–60‰ before substantial biogenic methane is produced.

A second heuristic differentiating biogenic and thermogenic gas is the ratio of methane to heavier hydrocarbons. Biogenic gas typically has values greater than 10<sup>3</sup> for the ratio of methane to the sum of ethane and propane [C<sub>1</sub>/(C<sub>2</sub> + C<sub>3</sub>)] while for thermogenic gas this ratio is usually less than 100 (Bernard et al., 1976). Figure 7.5 is a plot of the ratio of C<sub>1</sub>/(C<sub>2</sub> + C<sub>3</sub>) against isotopic composition for

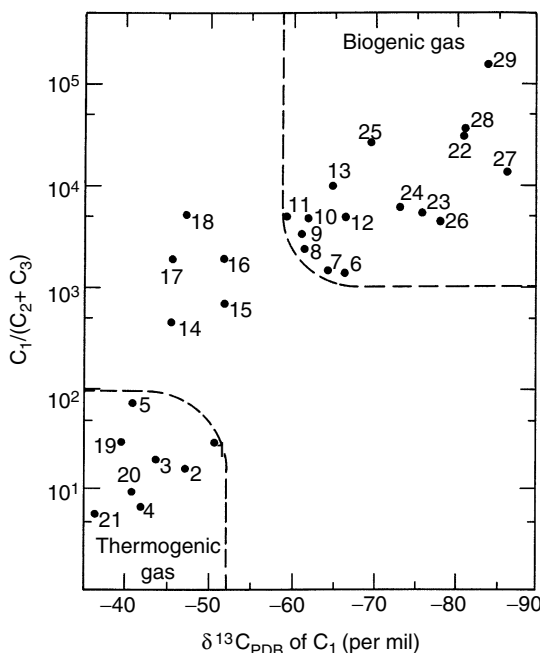


**FIGURE 7.5** Plot of C<sub>1</sub>/(C<sub>2</sub> + C<sub>3</sub>) against isotopic composition of C<sub>1</sub> to distinguish biogenic and thermogenic gas. (Reproduced from Claypool, G.E., Kvenvolden, K.A., *Ann Rev Earth Planet. Sci.*, **11**, 299 (1983). With permission.)

**TABLE 7.6**  
**Gas Characteristics of Gulf of Mexico and Caspian Sea Hydrate Samples**

Site	$\delta^{13}\text{C}$	Composition of gas, mol%						
		CH <sub>4</sub>	C <sub>1</sub>	C <sub>2</sub>	C <sub>3</sub>	i-C <sub>4</sub>	n-C <sub>4</sub>	CO <sub>2</sub>
<b>Biogenic hydrate samples</b>								
Orca Basin	-71.3	99.1	0.34	0.28			0.24	159
Garden Banks-388	-70.4	99.5	0.12				0.26	829
Green Canyon-257	-69.2	99.7					0.26	>1000
Green Canyon-320	-66.5	99.7	0.08				0.12	1246
<b>Thermogenic gas hydrates</b>								
Green Canyon-184	-44.6	70.9	4.7	15.6	4.4	0.3	4.1	3.2
Green Canyon-204	-56.5	61.9	9.2	22.8	4.5	1.3	0.2	1.9
Green Canyon-234	-43.2	74.3	4.0	13.0	3.2	0.86	4.6	4.4
Mississippi Canyon	-48.2	93.4	1.2	1.3			4.0	37.4
Buzdag (Caspian)	-44.8	74.7	17.4	2.4	0.4	1.1	3.6	3.77
Buzdag (Caspian)	n.a.	76.0	19.3	2.4	0.6	0.3	1.2	3.50
Elm (Caspian)	-56.0	95.3	0.6	1.6	1.7	n.d.	0.9	43.3
Elm (Caspian)	n.a.	81.4	15.3	1.6	0.2	0.7	0.8	4.81

Source: From Brooks, J.M., et al., *Org. Geochem.*, **10**, 221, 1986, Ginsburg, G.D., Soloviev, V.A., *Bull. Geol. Soc of Denmark*, Copenhagen, **41**, 95, 1994. With permission.

several gas seep samples as a principal means to distinguish the gas source. Note in Figure 7.5 that samples 14 through 18 are derived from mixtures of thermogenic and biogenic gases.

Table 7.6 quantifies the isotope and composition differences for biogenic and thermogenic hydrate samples in the Gulf of Mexico (Brooks et al., 1986), as well as for thermogenic hydrates from the Caspian Sea (Ginsburg and Soloviev, 1994). Note that there is usually between 1 mol% and 20% propane in thermogenic hydrates, compared against propane's relative absence in biogenic hydrates. These amounts are consistent with the phase equilibrium heuristics of Chapter 4 which suggest that propane should be concentrated in the hydrate phase. One would not expect a small (e.g., ppm) propane concentration in hydrates for a thermogenic gas.

### 7.2.2 The SMI, the Hydrate Upper Boundary, and the SMI Rule-of-Ten

As shown in the discussion accompanying Figure 7.4, sulfate is reduced before methane is generated in the diagenesis process. At the subsediment SMI, sulfate from the seawater above, and methane from the dissolved (or free) gas below, are consumed to produce carbonate and hydrogen sulfide. The anaerobic reaction for

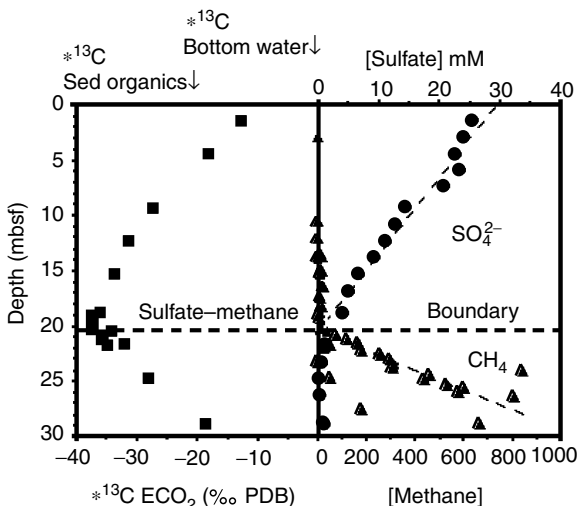
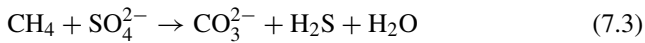


**FIGURE 7.6** Samples from ODP Leg 164 Hole 994 at Blake Bahama Ridge, showing the sub-bottom reduction in sulfate until the depth of the Sulfate–Methane Interface (SMI), and the increase in methane concentrations below the SMI. (Paull, Personal Communication, October 25, 2001.)

the consumption of methane and sulfate resulting in the production of carbonates for subsea ridges, chimneys, or chemoherms, and hydrogen sulfide as a substrate for chemosynthetic communities (see the Hydrate Ridge case study) is



As one of many examples of the relative sulfate and methane concentrations with depth, Paull et al. (1996) measured samples (Figure 7.6) from the Blake-Bahama Ridge ODP Leg 164 hole 994.

Recently, based upon 435 samples on 25 long cores (up to 37 m) in the Gulf of Mexico and multiple samples in the Blake-Bahama Ridge, Paull et al. (2005) offered the following rule of thumb, which might be called the SMI Rule of 10: the methane concentration is insufficient to form hydrates, until a depth of a factor of 10 times the SMI depth. For example, at Blake-Bahama Ridge, the average SMI was at 20 mbsf and the top of the hydrate zone was at 200 mbsf. Similarly in the Gulf of Mexico west of the Mississippi Canyon, the average SMI is at 12 mbsf so hydrates should be stable beginning at 120 mbsf in those locations. Figure 7.6 shows the concentration changes of sulfate, methane, and carbonates around the SMI (Paull et al., 1996). As with all rules of thumb, there are exceptions to the general case, particularly where the methane flux is very high, such as at the Hydrate Ridge where hydrates appear in the uppermost 25 m, and in the Gulf of Mexico sites that have surface hydrate outcrops, indicating fast flows.

For the average case, however, the SMI Rule of 10 can bound the top of the hydrate zone, when the gas flux is small enough to reduce a significant amount of sulfate. Ten times the depth of the SMI is the approximate initiation depth for hydrate formation. This new and largely unrecognized heuristic provides a convenient upper bound to hydrates in sediments just as, in the next section, the lower bound of hydrate stability will be shown to be the intersection of the phase boundary and the geothermal gradient, also complemented in Section 7.4 by the Bottom Simulating Reflector (BSR). Another suggestion is that the tenfold depth of the SMI may coincide with the gas solubility required to form hydrates in seawater, as indicated at the conclusion of Section 7.4.

### 7.2.3 Mechanisms for Generation of Hydrates

Methane, either from biogenic or thermogenic sources, combines with water in sediments to form hydrates. While biogenic gas in the majority of the cases is in the ocean (Dillon and Max, 2000), in the northern Gulf of Mexico, Brooks (Personal Communication, June 29, 1988) estimated that approximately equal numbers of hydrate samples were recovered from each type of gas source. Due to the high temperature requirements for its production, thermogenic gas must migrate along sediment faults from its source at depth to the cooler hydrate stability region.

Thermogenic gas migration occurs via channels and faults (e.g., salt diapirs) that are common to regions such as the Gulf of Mexico or mud volcanoes in the Caspian Sea (Ginsburg and Soloviev, 1994). Thermogenic, massive hydrates are associated with faults in fine-grained sediments rather than biogenic, dispersed hydrates in course-grained rocks, as shown, for example, in the ODP Leg 146 results (Westbrook et al., 1994) and in the gas hydrate samples database (Booth et al., 1996).

Thermogenic gas hydrates associated with faults are generally more localized than biogenic hydrates which are normally indicated by widespread BSRs. Consequently, hydrate resource estimates (Collett, 1995; Kvenvolden, 1995) are based principally on biogenic gas properties and phase equilibria. Thermogenic hydrates are considered to be anecdotal in nature, due to their association with faults that act as conduits for deeper gas. Paull et al. (2005) suggest that such conduits cause thermogenic hydrates to be localized in the pathway vicinity, rather than be dispersed over wide areas, and that such localization may be responsible in the Gulf of Mexico for the lack of BSRs discussed in Section 7.4.

For Prudhoe Bay permafrost hydrates, Collett et al. (1988) suggested that thermogenic gas migrated along faults from deeper regions, where it was mixed with biogenic gas and either directly converted to gas hydrate or first concentrated in existing structural/stratigraphic traps, and later converted to hydrate.

Similarly, if channels are available, biogenic gas may migrate to regions within the hydrate stability envelope. Most of the gas was of biogenic origin in the hydrate core recovered from the Northwest Eileen State Well Number 2, one of the first wells to recover hydrates (Collett, 1983). The biogenic source is likely to predominate for hydrates in permafrost (Kvenvolden, Personal Communication,

October 19, 1988), in addition to biogenic dominance in ocean hydrates (Dillon and Max, 2000), with sporadic mixtures of biogenic and thermogenic gas in Alaska, Russia, offshore Canada, and the Gulf of Mexico. It is possible to have both means (in place generation and fast fluxes) of supplying biogenic gas, indicated by Kvenvolden et al. (1984) and Kvenvolden and Claypool (1985) at DSDP Site 570 in the Middle America Trench.

### 7.2.3.1 Hydrate formation in the two-phase region

Because free gas (or gas-saturated water) is less dense than either water or sediments, it will percolate upward into the region of hydrate stability. Kvenvolden suggested that a minimum residual methane concentration of 10 mL/L of wet sediment was necessary for hydrate formation. The upward gas motion may be sealed by a relatively impermeable layer of sediment, such as an upper dolomite layer (Finley and Krason, 1986a) or the upper siltstone sequence, as in the North Slope of Alaska (Collett et al., 1988). Alternatively, permafrost or hydrate itself may act as an upper gas seal. These seals can also provide traps for free gas that has exsolved from solution, and the seals can subsequently act to provide sites for hydrate formation from the free gas.

In addition the extensive hydrate exploration experience of Collett (Personal Communication, May 25, 2006) suggests that the container can control the amount of hydrate present. For example, when the container is relatively porous, grain-supported sand, the hydrate content can be high (as much as 70–80% of the pore volume). However, for low porosity shales the content may be much lower (e.g., 3% of the pore volume).

Hydrate formation from free gas will likely initiate at a gas–liquid interface, as observed in the laboratory experiments of Chapter 6. As indicated in Chapter 3, either initial hydrate formation or a solid phase can serve as nucleation sites for additional formation from the gas and aqueous liquid phases. However, most geochemists (Claypool and Kaplan, 1974; Finley et al., 1987, etc.) suggest hydrates form from gas (either at equilibrium or supersaturated) dissolved in the liquid phase, without a free gas.

Using innovative experiments, Tohidi and coworkers (2001) and Anderson et al. (2001) have shown that hydrates can be formed in artificial glass pores from saturated water, without a free gas phase. They found that with significant subcooling the amount of hydrate formation was proportional to the gas solubility; carbon dioxide formed more hydrates from a saturated solution than did methane. Further, the maximum amount of methane hydrate formation was fairly low—about 3% of the pore volume—a value consistent with the amount of hydrates in sediment.

While hydrate formation from a saturated water phase may be possible, substantial accumulation will require geologic-like times because the concentration of dissolved gas in water is extremely low—only  $0.5\text{--}2.5 \times 10^{-3}$  methane mole fraction in water and brines at depths from 300 to 5000 m (Hunt, 1979). The concentration of gas in the hydrate (one molecule of gas per six molecules of water)

is much higher than the methane solubility in water ( $2.5 \times 10^{-3}$  mol fraction methane) at typical ocean hydrate conditions.

However, as shown in the phase diagrams and accompanying discussion in Chapter 4, hydrate stability is thermodynamically possible in equilibration with only saturated seawater. In the following section it is shown that Klauda and Sandler (2005) calculated the period for hydrate formation to be very long (1–10 million years). Similarly Rempel (1994) provided a model for the formation and accumulation of hydrates, using a moving boundary mathematical technique similar to the Yousif et al. (1988) model. Rempel's model predicts a time period required of  $2 \times 10^5$  years for a 1% accumulation of hydrates. Xu and Ruppel (1999) showed the time to be greater than  $1 \times 10^6$  years to generate a substantial hydrate mass using only diffusive fluxes.

Booth et al. (1996) compiled the data for all recovered hydrate samples and determined that 70% of the recovered samples were in the two-phase region, that is, at pressures higher (or temperatures lower) than the three-phase boundary, as shown in Figure 7.7. This result gives validity to the suggestion that

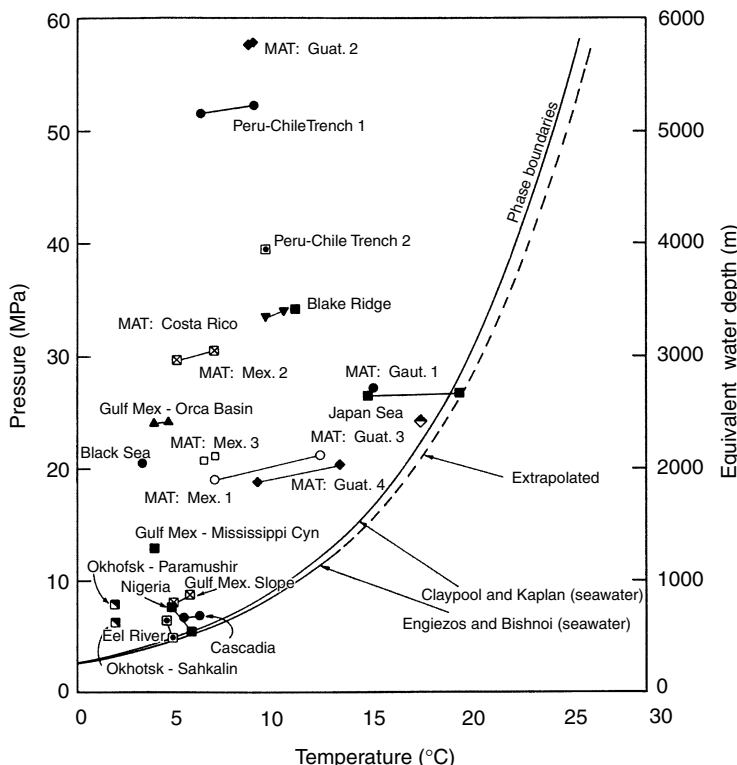


**FIGURE 7.7** Compilation of data for recovered hydrate samples in relation to the three-phase boundary. (Courtesy of Booth et al., 1996.)

hydrates form from methane-saturated water. It is unlikely that 70% of the recovered hydrates formed at the three-phase line and then moved into the two-phase region. The two-phase hydrate formation mechanism is discussed further in Section 7.2.3.2.3.

More importantly, the result of Booth et al. also suggests that only massive hydrate samples can survive the trip from the bottom of the ocean to ship deck. For example, if the massive MAT: Guatemala 2 sample (topmost in Figure 7.7) were recovered at constant pressure, the temperature would need to rise more than 16°C before the sample reached the three-phase line, where dissociation would begin. This result is consistent not only with laboratory determinations for dispersed hydrates (Kumar et al., 2004; Paull et al., 2005; Wright and Dallimore, 2005) but also shows the parallel of recovered core dissociation with radial dissociation due to depressurization in pipelines, modified for sediment content (Davies and Sloan, 2006).

This requirement for a large increase in temperature below the phase boundary may have enabled the MAT: Gautamala 2 sample to survive the trip from seafloor to shipboard. However, upon recovery and heating of smaller, more dispersed *in situ* samples at the three-phase condition, dissociation will begin almost immediately, so that the sample may not survive nonpressurized recovery. In contrast to small hydrates, massive hydrates are aided in slow dissociation by a low surface to volume ratio, together with the protective formation of an ice layer by the dissociated water (Yakushev and Istomin, 1991; Gudmundsson and Parlaktuna, 1992).

The smaller dispersed hydrates, which are considered more pervasive, may be heated to the three-phase boundary more readily due to the high surface to volume ratio of small particles. Small particles may decompose before they are recovered, as suggested by Paull et al. (2005) and by Klauda and Sandler (2005). Thus the amount of hydrates may be underestimated via the method of gas evolution from nonpressurized cores. Much of the dispersed hydrates may have dissociated on the trip from the seafloor to shipboard (Paull et al., 2005).

### 7.2.3.2 Models for *in situ* hydrate formation

Based upon an overview of several years of research sponsored by the U.S. Department of Energy, R.D. Malone (1985) suggested that hydrates occur in four types, each of which is depicted in Figure 7.8:

1. The first type of hydrate is finely disseminated. Due to their disseminated nature, these hydrates may dissociate rapidly, frequently within the time span of a core's trip from the seafloor to shipboard, leaving residual traces of pore water freshening, or low temperatures, because of the endothermic heat of dissociation. As discussed in this section, disseminated hydrates represent the large majority of hydrates in the ocean.

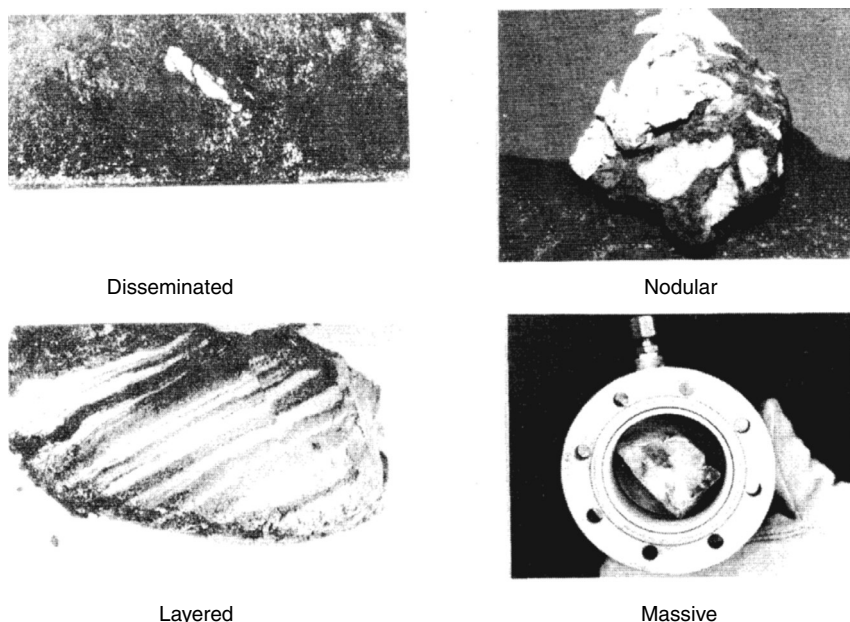


FIGURE 7.8 Photographs of four types of hydrates. (R.D. Malone, courtesy of W.F. Lawson, U.S. Department of Energy, 1988.)

2. Nodular hydrates up to 5 cm in diameter may occur, such as found in the Green Canyon Gulf of Mexico; the gas in these hydrates may be of thermogenic origin that migrated from depth.
3. Layered hydrates are separated by thin layers of sediments, such as cores recovered from the Blake-Bahama Ridge. Such hydrates probably occur both offshore and in permafrost regions.
4. Massive hydrates, such as the one recovered from Site 570 of DSDP Leg 84 off the MAT, may be as thick as 3–4 m and contain more than 95% hydrate. While there is some question as to whether this sample is of biogenic origin (Kvenvolden and Claypool, 1985) or thermogenic origin (Finley and Krason, 1986a), it appears that much of the gas migrated to the hydrate site, and either formed along a fault, or pushed aside sediments as the massive hydrate grew, using the pressure of crystallization indicated by Torres et al. (2004) and Sassen et al. (2004).

Brooks et al. (1985) suggested that since most Gulf of Mexico hydrates were found to be biogenic, if disseminated, and thermogenic, if more massive. Thermohydrates may have a greater supply of gas through faults and diapirs. They note, however, that hydrate formation is influenced by a number of other factors, among which are sediment texture, formation of authigenic carbonate rubble, and shallow faulting and fracturing of the sediments.

Figure 7.9 (from Roberts, 2001) gives an overview mechanism of hydrate formation in the Gulf of Mexico as a function of the flux of methane through sediments:

1. Low gas fluxes result in mineralization, such as carbonate mounds, cones, and chimneys, with very localized and poorly developed chemosynthetic communities, and highly biodegraded hydrocarbons.
2. Moderate gas fluxes result in gas hydrate mounds, dense diverse chemosynthetic communities, (Beggiatoa, tube worms, clams), and moderately degraded hydrocarbons.
3. Rapid gas fluxes result in mud volcanoes and vents, localized bacterial mats and clams, and nonbiodegraded hydrocarbons.

Such a summary overview for the Gulf of Mexico, also finds a clear example in the case study of Hydrate Ridge. While Roberts provided a qualitative summary of the three ranges of gas fluxes, his conceptual picture evolved from a career of field experiments, serves as a basis for quantification, such as in the following models.

There are three current models of hydrate formation in the literature: (1) *in situ* formation from biogenic methane, (2) formation from free (perhaps recycled) gas traveling upward, and (3) formation by upward mobile water which exsolves the gas used for hydrate formation. Each model is discussed briefly in Sections 7.2.3.2.1–7.2.3.2.3.

#### 7.2.3.2.1 *Hydrate formation by in-place biogenic methane*

Kvenvolden and Barnard (1983) and Brooks et al. (1985) followed the Claypool and Kaplan (1974) suggestion that free methane can be generated in place using the diagenetic mechanism indicated above. Brooks et al. (1987) indicate that twice the methane solubility amount can be achieved by *in situ* production.

However, other researchers suggest that considerably less methane can be generated by *in situ* hydrate production. Hyndman and Davis (1992) indicated that an unaccountably high concentration of gas was required for hydrate formation. Minshull et al. (1994), Paull et al. (1994), and Klauda and Sandler (2005) suggest that for in-place formation, under the best conditions the maximum amount of hydrate that can fill the sediments is 3%.

Hydrate generation by in-place diagenesis is thought to produce the most uniform layers and may be responsible for uniform seismic responses, such as BSRs (Ginsburg and Soloviev, 1998, p. 151). However, as shown in Section 7.4.2, BSRs are only a first-order tool for hydrate prospecting and have a substantial number of false indications, both positive and negative. Consider the conceptual picture of in-place hydrate formation. Carbon-containing components fall to the bottom of the ocean and are buried. The diagenesis occurs producing methane below the SMI. Finally hydrates form with the produced biogenic methane. The process is very slow, because the temperature is very low (typically 277 K) relative to most man-made chemical reactions.

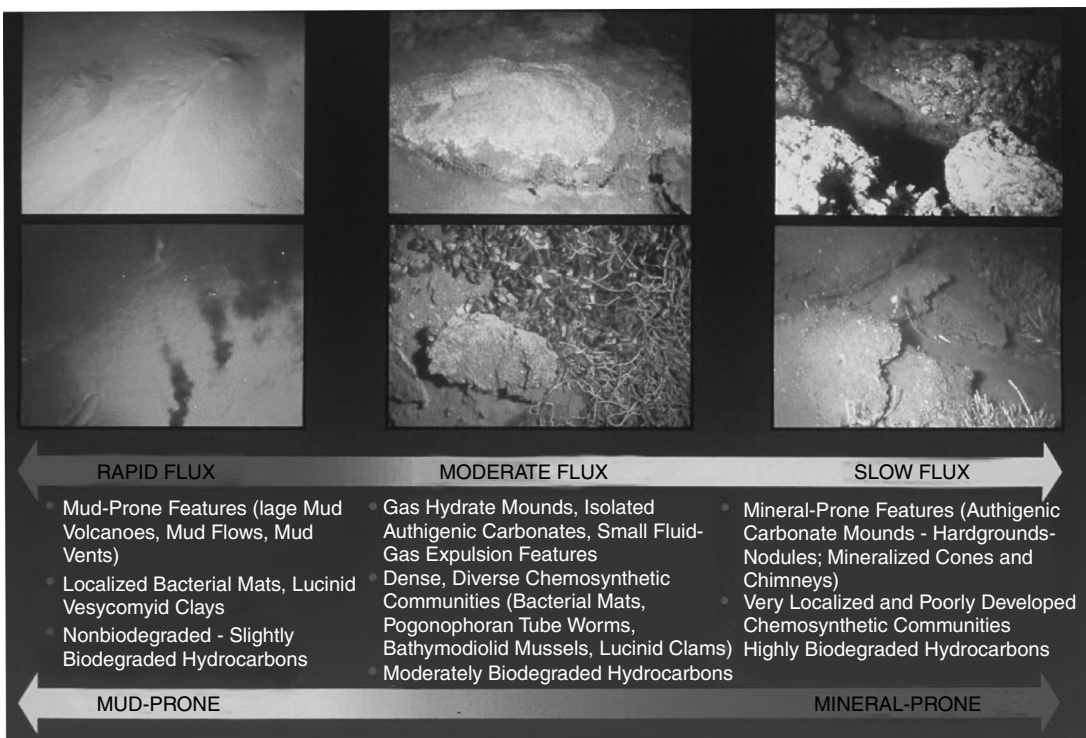


**FIGURE 7.9** (See color insert following page 390.) Qualitative relationships between fluid fluxes and geologic–biologic response. Each picture has a field of view 3–4 m across. (From Roberts, H.H., in *Natural Gas Hydrates: Occurrence, Distribution and Detection*, (Paull, C.K., Dillon, W.P., eds.) p. 145. American Geophysical Union, Washington, DC (2001). With permission.)

Consider the recent model of Klauda and Sandler (2005) for in-place hydrate formation. Their hydrated gas estimate [ $120 \times 10^{15} \text{ m}^3$  methane (STP)] was made using a different method from those of all preceding estimates. First a new *ab initio* thermodynamic model was generated to include effects of pores and salt. Then measured local temperatures and gradients in each of the world's oceans were used to determine the intersection of the geothermal gradient with the phase boundary, without restriction to depth. Measured local organic sediment contents were also used to serve as input to the methanogenesis mass transfer model of Davie and Buffett (2001, 2003), which was matched to the Blake-Bahama Ridge data of ODP Leg 164 to determine a minimum organic content of >0.4 wt% carbon was required and that a global pore volume average of 3.4% of hydrate existed.

The above summary suggests that hydrates were generated *in situ*, by the decomposition of organic matter. It is interesting to note that the model of Klauda and Sandler (2005) provides local estimates that sum to a large global value of  $1.2 \times 10^{17} \text{ m}^3$  methane (STP) but that estimate includes very deep hydrates, as well as dispersed small concentrations of hydrates that may dissociate during core recovery. When only continental margins are considered (as with the geoscience models) Klauda and Sandler reduce the estimate to  $4.4 \times 10^{16} \text{ m}^3$  methane (STP), more comparable to other recent estimates.

The Klauda and Sandler model can be used to predict the uniformly distributed hydrates that form in place on the seafloor with a resulting BSR, rather than those associated with rapid convective fluxes, which tend to be associated with faults, and thus more anecdotal in nature. Klauda and Sandler note that their model can be used to predict 68 of 71 local occurrences where hydrates have been found around the world, and explain the three exceptions. The ability to predict hydrate occurrences is a significant step in model verification.

#### 7.2.3.2.2 Hydrate formation by migration of free gas

Paull et al. (1994) and Minshull et al. (1994) proposed models dealing with hydrate formation by the upward migration of free gas. The rudiments of the model suggest that free gas from below the hydrates migrates through fissures or permeable sediments and forms hydrates at nucleation/growth sites. Gas may come from either free biogenic gas or from dissociated hydrates.

Paull et al. (1994) provided a model for hydrate formation from free and recycled gas, as shown in [Figure 7.10](#). In this model, the base of the gas hydrate stability (BGHS) field moves upward with progressive burial/subsidence through times 1, 2, and 3. Shown in Figure 7.10 at time 2, the former BGHS has been displaced upward, leading to decomposing hydrates. As hydrates decompose, the methane solubility limit is surpassed, so that so-called recycled rising gas bubbles permeate fissures in the overlying hydrate stability layer. At time 3 a higher gas stability zone and layer is achieved.

Two independent experiments have formed hydrates from free gas bubbles at the ocean bottom. Sassen and McDonald (1997) in the Gulf of Mexico and Brewer et al. (1997) off California have performed undersea experiments to show that hydrates readily form from artificial methane and carbon dioxide in sea water.

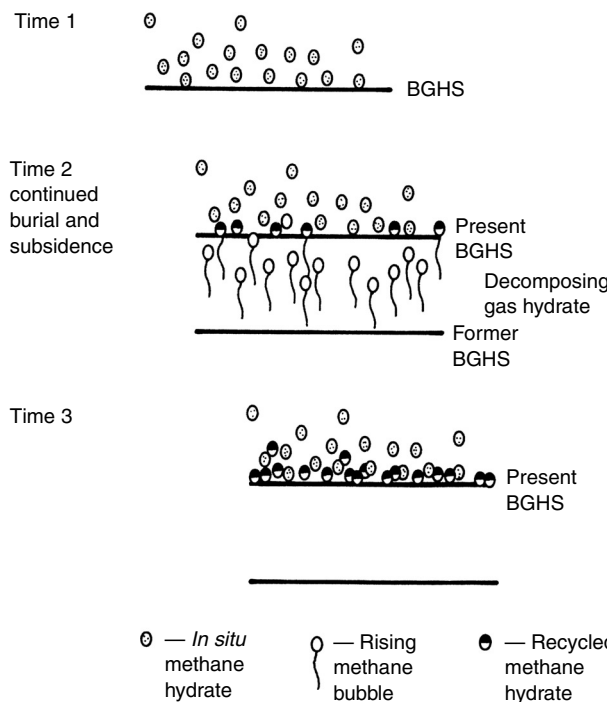


**FIGURE 7.10** Proposed model of hydrate formation by upward migration and recycling of gas. (Reproduced from Paull, C.K., Ussler, W., Borowski, W.S., in *Proc. First International Conference on Natural Gas Hydrates*, **715**, 392 (1994). With permission from the New York Academy of Sciences.)

#### 7.2.3.2.3 Hydrate formation from gas dissolution of rising water

Hyndman and Davis (1992) proposed that as methane-unsaturated water rises, it becomes saturated at lower pressures. As the saturated (or supersaturated) water passes through the phase stability zone, hydrate formation occurs without a free gas zone. This model results in a maximum hydrate concentration at the three-phase (BSR) boundary with a successively lower hydrate amounts above the BSR as was shown to be the case in Cascadia Margin ODP Drill Sites 889 and 890 by Hyndman et al. (1996).

From Chapters 4, 5 and 6 thermodynamic data and predictions, the maximum methane concentration (solubility) occurs in the aqueous liquid at equilibrium with hydrates. In order for methane to exsolve the liquid, the solubility must change rapidly as the water rises with corresponding decreases in pressure and temperature. Solubility calculations (Handa, 1990) indicate a change in methane concentration too gradual to account for a significant hydrate amount. Solubility data are needed at conditions of hydrate formation, in order to confirm this model. Preliminary solubility data are available from Besnard et al. (1997).

Rempel (1994) provided a model for the formation and accumulation of hydrates, using a moving boundary mathematical technique similar to the

Yousif et al. (1988) model. Rempel's model predicts a hydrate volume fraction of less than 1%, with a time period required of  $2 \times 10^5$  years for a 1% accumulation of hydrates.

Xu and Ruppel (1999) solved the coupled mass, heat, and momentum equations of change, for methane and methane-saturated fluxes from below into the hydrate stability region. They show that frequently methane is the critical, limiting factor for hydrate formation in the ocean. That is, the pressure–temperature envelope of the Section 7.4.1 only represents an outer bound of where hydrates might occur, and the hydrate occurrence is usually less, controlled by methane availability as shown in Section 7.4.3. Further their model indicates the fluid flow (called advection or convection) in the amount of approximately 1.5 mm/yr (rather than diffusion alone) is necessary to produce significant amount of oceanic hydrates.

### 7.3 SEDIMENT LITHOLOGY AND FLUID FLOW ARE MAJOR CONTROLS ON HYDRATE DEPOSITION

In a recent ocean hydrate formation state-of-the-art summary, Tréhu et al. (2006) listed the effects of fluid flow and sediment lithology. Ocean hydrate deposits are distributed on a spectrum between two types in ocean sediments: (1) focused high flux (FHF) gas hydrates, and (2) distributed low flux (DLF) gas hydrates. In FHF hydrates the gas comes from a large sediment volume channeled through a high-permeability sand to the point of hydrate formation, and these hydrates are typically in the upper tens of meters of the sediment. In contrast, the DLF hydrates are generated near where the hydrates are formed, and fluid flow is responsible for movement of the gas within the gas hydrate occurrence zone (GHOZ).

Table 7.7 contrasts FHF and DLF hydrates. It should be emphasized that both hydrates are end-member types with the frequent occurrence of mixed types. For example, while Table 7.7 typifies Blake Ridge as DLF hydrates and Barkley Canyon as FHF hydrates, there is often a mixture of both types as shown in the Leg 204 study in the Cascadia Margin. As a second example, while the Gulf of Mexico is normally known for FHF hydrate deposits, Hutchinson et al. (2004) provide evidence for some elements that have DLF characteristics.

### 7.4 REMOTE METHODS ENABLE AN ESTIMATION OF THE EXTENT OF A HYDRATED RESERVOIR

In addition to the thermodynamic and kinetic models shown above, which use parameters such as temperature, pressure, and carbon content, three initial detection tools enable initial estimates of hydrates in an ocean geologic setting: (1) the thermodynamic pressure–temperature stability data of Chapters 5 and 6, combined with the geothermal gradient, determine the maximum stability depth, (2) seismic methods such as BSR provide tentative assessments of the area and the maximum depth (lower boundary) of hydrate formation, and (3) methane solubility that determines the top and bottom stability within the P–T region of item (1). These are considered in Sections 7.4.1, 7.4.2, and 7.4.3, respectively.

**TABLE 7.7**  
**Two End-Member Hydrate Deposits**

FHF gas hydrates	DLF gas hydrates
Rich, localized hydrate deposits	Broadly distributed, lean hydrate deposits
Related to mounds, vents, pockmarks	Related to dispersed, low concentrations
CH <sub>4</sub> /H <sub>2</sub> O from kilometers below seafloor	CH <sub>4</sub> generated near hydrate deposit
High-permeability conduits	Low-permeability flow
Frequently are deposited in sands	Frequently are deposited in shales
Forming flow rapid: convective and diffusive	Forming flow is slow; frequently diffusive
Form within tens of meters of mud line	Form deeper in occurrence zone GHOZ
Represent a small amount of hydrates	Represent the majority of hydrate
Not normally predicted by models	Frequently modeled
Can be massive gas hydrates	Hydrates dispersed less than—5% of pore volume
Found by seafloor imaging and protrusions	Found by BSR and GHOZ zones
Can be structure I, II, or H hydrates	Usually structure I, biogenic gas hydrates
Can have complex fauna with them	Usually associated with shales, not fauna
Represented by Barkley Canyon hydrates	Represented by Blake Ridge hydrates

#### 7.4.1 The Hydrate Pressure–Temperature Stability Envelope

There are four requirements for generation of natural gas hydrates: (1) low temperature, (2) high pressure, (3) the availability of methane or other small nonpolar molecules, and (4) the availability of water. Without any one of these four criteria, hydrates will not be stable. As indicated in both the previous section and in Section 7.4.3, the third criteria for hydrate stability—namely methane availability—is the most critical issue controlling the occurrence of natural gas hydrates. Water is ubiquitous in nature so it seldom limits hydrate formation. However, the first two criteria are considered here as an initial means of determining the extent of a hydrated reservoir.

Figures 7.11a,b are arbitrary examples of the depths of hydrate phase stability in permafrost and in oceans, respectively. In each figure the dashed lines represent the geothermal gradients as a function of depth. The slopes of the dashed lines are discontinuous both at the base of the permafrost and the water–sediment interface, where changes in thermal conductivity cause new thermal gradients. The solid lines were drawn from the methane hydrate  $P$ – $T$  phase equilibrium data, with the pressure converted to depth assuming hydrostatic conditions in both the water and sediment. In each diagram the intersections of the solid (phase boundary) and dashed (geothermal gradient) lines provide the lower depth boundary of the hydrate stability fields.

In Figure 7.11a, it is important to note that in the region between the three-phase line and the geothermal gradient, hydrates are stable with only one other phase. The second phase is in excess—in most cases, liquid water containing

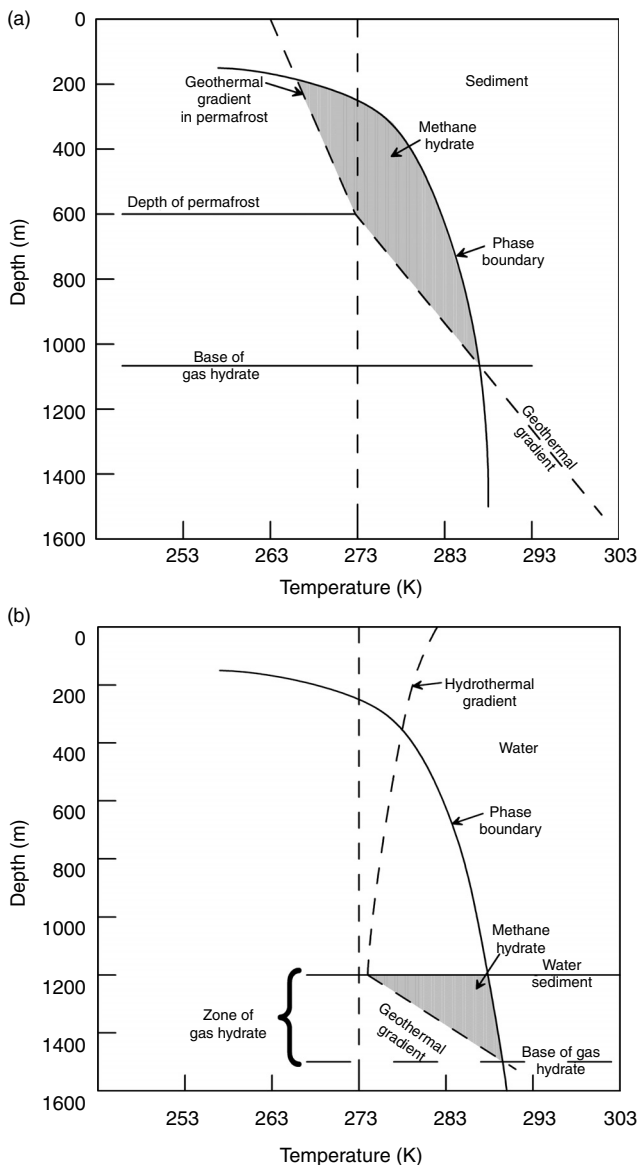


**FIGURE 7.11** Envelopes of methane hydrate stability (a) in Permafrost and (b) in Ocean sediment. (Reproduced from Kvenvolden, K.A., *Chem. Geol.*, **71**, 41 (1988). With permission from Elsevier Science Publishers.)

dissolved methane. Once hydrates are initiated, further nucleation can occur in the two-phase region with increases in pressure, decreases in temperature, or addition of methane as determined by the solubility limits. Quantitative two-phase  $P-T$ -solubility conditions are provided in Chapter 6.

In [Figure 7.11b](#) one would not expect hydrates to be stable in the region above the seafloor sediment due to an absence of means to concentrate gas in water and a means of retaining the hydrates, because hydrate density (sp. gr. 0.9) is less than that of seawater. In both Figures 7.11a,b, a small addition of heavier natural gas components, such as ethane, propane, or isobutane, will cause the hydrate stability depth to increase due to a displacement of the phase boundary line away from the geothermal gradient. In neither case, however, have hydrates been found at depths greater than about 2000 m below the surface, due to the high temperatures resulting from the geothermal gradient.

For methane hydrate, the minimum water depth is 381 m in freshwater and up to 436 m in seawater, respectively, at 277 K. In the world's oceans at water depths greater than 600 m, the temperature is typically uniform at 277 K, due to the density maximum in seawater. Lower bottom water temperature exceptions can be found with strong subbottom currents from Antarctic and Arctic environments such as the north of Norway or Russia. Methane-phase equilibrium data in [Chapter 6](#), indicate that 3.81 MPa are required to stabilize methane hydrates at 277.1 K. Using the rule of thumb 1 MPa = 100 m water, hydrates in pure water would be stable at depths greater than 381 m.

At a sea salt concentration totaling 3.5 wt%, using the thermodynamic data of Dholabhai et al. (1991) in Chapter 6, a pressure of 4.364 MPa (a minimum seawater depth of 436 m—about 55 m deeper than in pure water) is required to stabilize hydrates at 277 K. Further corrections to the phase boundary are required considering effects of (1) hydrocarbons other than methane, (2) salt concentrations other than 3.5 wt%, and (3) sediment pores or capillary pressure, as indicated in [Chapter 5](#).

Two final points should be made regarding the hydrate pressure–temperature limits shown in Figures 7.11a,b. The intersection of the phase boundary with the geothermal gradient limits the lower stability depth of hydrates. In Section 7.4.2, it will be shown that this intersection usually coincides with the BSR, an approximate exploration tool, which is caused by a seismic velocity decrease from hydrates above, to gas below the reflector.

Second, the hydrates at the lower stability depth are the most easily dissociated because they are at the phase boundary. At some constant depth, above the lower intersection of the two lines, the hydrates (along with their encasing sediments) that exist at the geothermal gradient must be heated to the phase boundary resulting in a loss of recovery efficiency, due to the requirement of heating the hydrated sediment before dissociation.

---

### Example: What Fraction of Hydrate Reserves are Economical to Recover for Energy?

If we assume that the temperatures and pressures of the hydrate samples in [Figure 7.7](#) are representative of worldwide hydrate reservoirs, we can use the principles of Figure 7.11 to estimate what fraction of hydrated reservoirs

are economical for energy recovery. At 100% efficiency, the energy obtained from the gas, as measured by the heat of combustion, must equal to or be greater than the sensible energy to bring the hydrates from the geothermal line to the phase boundary in Figure 7.11, and the energy of dissociation. This can be expressed as enthalpy (energy corrected for pressure and volume).

$$\Delta H^{\text{combustion}} = \Delta H^{\text{sensible}} + \Delta H^{\text{dissociation}} \quad (7.4)$$

The values in Equation 7.4 may be calculated, assuming that hydrates occupy 3% of the typical pore volume of 30%, as determined by field studies. Using Equation 7.4 one may perform the following calculation (Gupta, A.R., Personal Communication, January 13, 2006):

#### *Assumptions*

1. Basis: 1 m<sup>3</sup> of reservoir of 30% porosity, with 3% of the pore volume as hydrates
2. Volume of rock in 1 m<sup>3</sup> with 30% porosity = 0.7 m<sup>3</sup>
3. Volume of hydrates (seawater) in 1 m<sup>3</sup> of reservoir = 0.009 m<sup>3</sup><sub>hydrate</sub>, (0.291 m<sup>3</sup><sub>seawater</sub>)
4. Only hydrates and seawater exist in the pore volume
5. Heat of methane combustion = 37,250 kJ/m<sup>3</sup> of gas
6. Heat of hydrate dissociation = 368,803 kJ/m<sup>3</sup> of hydrate
7. Heat capacity of hydrate, seawater, and rock is 2500, 4180, 2240 kJ/m<sup>3</sup> K, respectively

*Step 1:* Calculate the energy gained from combustion ( $\Delta H^{\text{combustion}}$  in Equation 7.4)

$$\frac{37,250 \text{ kJ}}{\text{m}^3 \text{ gas}} \times \frac{170 \text{ m}^3 \text{ gas}}{\text{m}^3 \text{ hydrate}} \times \frac{0.009 \text{ m}^3 \text{ hydrate}}{\text{m}^3 \text{ reservoir}} = 56,992.5 \frac{\text{kJ}}{\text{m}^3 \text{ reservoir}}$$

*Step 2:* Calculate the energy required to dissociate hydrate

(2a) Calculate the sensible heat required to move reservoir to three-phase temperature at constant pressure ( $\Delta H^{\text{sensible}}$  in Equation 7.4), that is,

$$\begin{aligned} &= \left( \frac{0.7 \text{ m}^3 \text{ rock}}{\text{m}^3 \text{ reservoir}} \times \frac{2240 \text{ kJ}}{\text{m}^3 \text{ rock-K}} + \frac{0.291 \text{ m}^3 \text{ water}}{\text{m}^3 \text{ reservoir}} \times \frac{4180 \text{ kJ}}{\text{m}^3 \text{ water-K}} \right. \\ &\quad \left. + \frac{0.009 \text{ m}^3 \text{ hydrate}}{\text{m}^3 \text{ reservoir}} \times \frac{2500 \text{ kJ}}{\text{m}^3 \text{ hydrate-K}} \right) \times (T_{\text{eqm}} - T_{\text{sys}}) \\ &= \left( \frac{2806.88 \text{ kJ}}{\text{m}^3 \text{ reservoir}} \right) \times (T_{\text{eqm}} - T_{\text{sys}}) \end{aligned}$$

- (2b) Calculate the energy of hydrate dissociation ( $\Delta H^{\text{dissociation}}$  in Equation 7.4), that is,

$$\frac{368,803 \text{ kJ}}{\text{m}^3 \text{ hydrate}} \times \frac{0.009 \text{ m}^3 \text{ hydrate}}{\text{m}^3 \text{ reservoir}} = 3,319.22 \frac{\text{kJ}}{\text{m}^3 \text{ reservoir}}$$

Total heat input to dissociate hydrate

$$= \left( \frac{2,806.88 \text{ kJ}}{\text{m}^3 \text{ reservoir}} \right) \times (T_{\text{eqm}} - T_{\text{sys}}) + \left( \frac{3,319.22 \text{ kJ}}{\text{m}^3 \text{ reservoir}} \right)$$

*At break-even point:*

Heat input = Heat output

$$\left( \frac{2,806.88 \text{ kJ}}{\text{m}^3 \text{ reservoir}} \right) \times (T_{\text{eqm}} - T_{\text{sys}}) + \left( \frac{3,319.22 \text{ kJ}}{\text{m}^3 \text{ reservoir}} \right) = \left( \frac{5,6992.5 \text{ kJ}}{\text{m}^3 \text{ reservoir}} \right)$$

$$(T_{\text{eqm}} - T_{\text{sys}}) = 19.09 \text{ K}$$


---

The example shows that if such hydrates are further than 19 K from the phase boundary, it will never be economical to recover the hydrated methane to use for energy. This subcooling is greater than almost all of the recovered hydrate samples shown in [Figure 7.7](#).

#### 7.4.2 Seismic Velocity Techniques and Bottom Simulating Reflections

Seismic velocity techniques for hydrate detection have two components: (1) translation of seismic signals to velocity and (2) translation between velocity and detection of hydrates. The first component is beyond the scope of this monograph. However, a brief consideration will be given to advances in translating velocity to the detection of hydrates.

For hydrates in ocean sediments, the technology for detecting the BSR was determined in 1953 with the development of a precision ocean depth recorder (Hamblin, 1985, p. 11). In this technique a sonic wave penetrates (and is reflected from) the ocean floor, with the time recorded for the return of the reflected wave to the source. Velocity contrasts beneath the ocean floor mark a change in material density, such as would be obtained by hydrate-filled sediments overlying a gas. BSRs related to hydrates are normally taken as indications of velocity contrasts between velocity in hydrated sediments and a gas, marked by a sharp decrease in sonic compressional velocity ( $V_p$ ) and a sharp increase in shear velocity ( $V_s$ ) (Ecker et al., 1996).

Hyndman and Spence (1992) indicated that about one-third of the pore space should be filled with hydrate to give a BSR impedance contrast at the Cascadia

Margin; the sediments contain 15–20% (volume) hydrate. This 33% of the total might be taken as a maximum for the hydrate indicated by a BSR. Hyndman and Davis (1992) indicated that the  $V_p$  decrease (1) suggested a gradational boundary with the thickest hydrate at the BSR and lesser hydrate concentrations above the BSR and (2) that the BSR did not require a gas layer beneath the hydrate.

Andreassen (1995) used the amplitude versus offset (AVO) technique to determine the phases at the BSR interface. The classical AVO technique, as stated by Ostrander (1984), measures the angle-dependent P-wave ratio amplitude (reflected to incident). Andreassen and coworkers determined that usually gas is just below the hydrate layer.

While the AVO technique can be used to determine the phases at the BSR interface, Nur and coworkers (Dvorkin and Nur, 1992; Ecker et al., 1996) used AVO to determine that hydrates were usually located away from grain contacts, only partially filling the pore space. That is, in theory, hydrates typically do not cement the grains of unconsolidated sediment, when reflections are weak and permeability is low.

[Figure 7.12a](#) shows the most famous BSR related to hydrates, in the Blake-Bahama Ridge. Sediments associated with this reflector have been drilled on two ODP voyages, the more recent (Leg 164) in December 1995. [Figure 7.12b](#) illustrates velocity of the wave in the sediment (at the arrow in [7.12a](#)) as a function of depth. [Table 7.8](#) shows the areal extent of many of the BSR's cited in the hydrate locations of [Table 7.4](#).

Ginsburg and Soloviev (1998, pp. 150–151) state that the BSR is the most widely used indirect indication of gas hydrates. “The most important evidence of the hydrate caused nature of the BSR is the coincidence of temperature and pressure calculated at it's depth with the equilibrium temperatures and pressure of gas hydrate stability . . . . The association with the base of the hydrate stability zone is beyond question.”

Paull et al. (1996) summarized requirements for a BSR as the following:

1. Subbottom depths that parallel the ocean floor, varying with water depth in accordance with the phase diagram.
2. Anomalously high seismic velocities ( $V_p > 2.0$  km/s) directly above the BSR.
3. Polarity reversals at the BSR, lower velocities than seawater (<1500 m/s) beneath the BSR perhaps indicating free gas.
4. Blanking or transparent zone above the BSR with a very low impedance contrast.
5. High reflectivity in a zone as much as several hundred meters beneath the BSR.

While the BSR was originally considered as a means of obtaining the areal extent of hydrate, a classic article by Lee et al. (1993) provided a method to determine the amount of hydrate, assuming that the porosity of the sediment is known. Waveform inversion techniques proposed by Minshull and coworkers

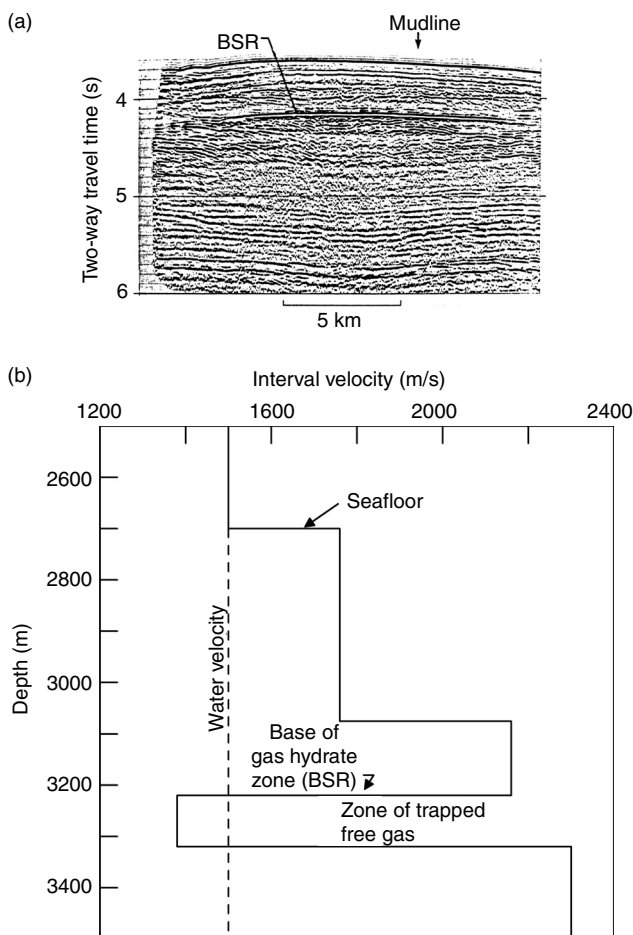


**FIGURE 7.12** (a) Bottom simulating reflector for hydrate deposit in Blake-Bahama Ridge. (b) Velocity analysis at location of arrow of BSR in (a). (Reproduced courtesy of U.S. Geological Survey, Dillon and Paull, 1983.)

(1994, 1996), Singh and Minshull, 1994), Hyndman and coworkers (1996) and Yuan et al. (1996) represent significant improvements. All models are reviewed and compared by Lee et al. (1996) who proposed a new, weighted equation to determine the hydrate amount. It should be noted that BSRs are also useful in determining heat flows through sediments, as shown by Yamano and Uyeda (1990) for the Peru BSR and by Hyndman et al. (1992) for the Cascadia Margin BSR.

Table 7.8 suggests that hydrates are commonly found in the oceans, yet care must be exercised, because BSRs are not reliable as sole indicators of hydrates. For example, Finley and Krason (1986a) indicate Sites 490, 498, 565, and 570 on DSDP Leg 84 in the MAT where hydrates were recovered without BSRs present. Conversely, BSRs existed beneath Sites 496 and 569, yet no hydrates were

**TABLE 7.8**  
**Ocean Gas Hydrate Bottom Simulating Reflector (BSR) Extent**

Number in Figure 7.2 and Table 7.4	Location	Extent and reference area/depth
P1	Pacific Ocean off Panama	4,500 km <sup>2</sup> poor BSR data 250–550 m subbottom depth Krason and Ciesnik (1986a)
P2 and P3	MAT off Costa Rica and Nicaragua	14,000 km <sup>2</sup> variable quality BSR data 600 m subbottom depth Finley and Krason (1986a)
P4	MAT off Guatemala	23,000 km <sup>2</sup> variable quality BSR data 0–450 m depth Finley and Krason (1986a)
P5	MAT off Mexico	19,000 km <sup>2</sup> variable quality BSR data 0–640 m subbottom depth Finley and Krason (1986a)
P7	Eel River Basin off California	3,000 km <sup>2</sup> 200 m subbottom depth Krason and Ciesnik (1986b)
P31	Peru–Chile Trench off Peru	Areal BSR extent not available 350–570 m subbottom depth
A6	Colombia Basin off Panama and Colombia	30,000 km <sup>2</sup> 60–200 m subbottom depth Finley and Krason (1986b)
A7	W. Gulf of Mexico off Mexico	8,000 km <sup>2</sup> good BSR data 100–600 m subbottom depth Krason et al. (1985)
A9	Blake outer Ridge off SE USA	31,000 km <sup>2</sup> good BSR data 22,000 km <sup>2</sup> acceptable BSR data 245 m subbottom depth at Site (533) Krason and Ridley (1985a)
A11	Baltimore Canyon off E. USA	12,600 km <sup>2</sup> good BSR data 19,150 km <sup>2</sup> acceptable BSR 450–600 m subbottom depth Krason and Ridley (1985b)
A12	Labrador Shelf off Newfoundland	<100 km <sup>2</sup> poor BSR data 20–600 m subbottom depth Krason and Rudloff (1985)
N1	Beaufort Sea off Alaska	Areal BSR extent not available 100–800 m subbottom depth Grantz et al. (1976)
A13	Continent Slope off W. Norway	Not available
I1	Makran Margin, Gulf of Oman	Undetermined area 350–700 m subbottom depth White (1979)

**TABLE 7.8**  
**Continued**

Number in Figure 7.2 and Table 7.4	Location	Extent and reference area/depth
P9	Cascadia Margin off Vancouver	30 km wide band, 300 m subbottom Hyndman and Spence (1992); Yuan et al. (1996)
P8	Cascadia Margin off Oregon	73 m subbottom depth; undefined area Westbrook et al. (1994)

recovered by coring to within 200 m (vertical) of the BSR. Similarly at Site 994 of Leg 164, hydrates were recovered without a BSR indication. Since 1998 we have come to realize that the BSR absence may be caused in places where methane supply limits hydrate formation (Xu and Ruppel, 1999) or by localized hydrates along a channel or diapir such as in the Gulf of Mexico (Paull et al., 2005).

However, as indicated by Kleinberg (2006) there is the need for a much better prospecting tool than the BSR, due to reliability issues. First, very little gas is required to produce a strong seismic reflector (Domenico, 1977). Second, an apparently continuous reflector does not imply a continuous gas-saturated zone. It is now well established by high resolution seismic techniques that BSRs that appear continuous in conventional marine seismic can actually be because of discontinuous patches of gas (Wood et al., 2002; and Dai et al., 2004). As a final example, the recent drilling of a BSR off the west coast of India failed because the BSR was caused by a carbonate deposit, rather than hydrates (Collett, T., Personal Communication, November 6, 2006).

In addition to BSRs and the intersections of the geothermal gradients with the hydrate phase boundary, the transport and kinetic tools discussed in the Section 7.2 [e.g., Xu and Ruppel (1999), Davie and Buffett (2001, 2003) or most recently Klauda and Sandler (2005)] can be used as first-order predictions of where hydrates exist.

Johnson (Personal Communication, March 6, 2006) suggests that hydrate indications by BSRs have been superseded by other, more reliable geological factors, “The key elements of commercial gas hydrate prospects are (1) reservoir quality sands, (2) sufficient gas flux, and (3) the GHSZ. Where all three are together commercial accumulations are likely. If any one is missing, there will be no prospect. A BSR will help identify the phase boundary, but has little other value.”

#### 7.4.3 Methane Solubility Further Limits the Hydrate Occurrence

Since, as indicated by Johnson, the availability of methane may control the stability of hydrates, a second reason that hydrates may not exist at the bottom of the  $P-T$

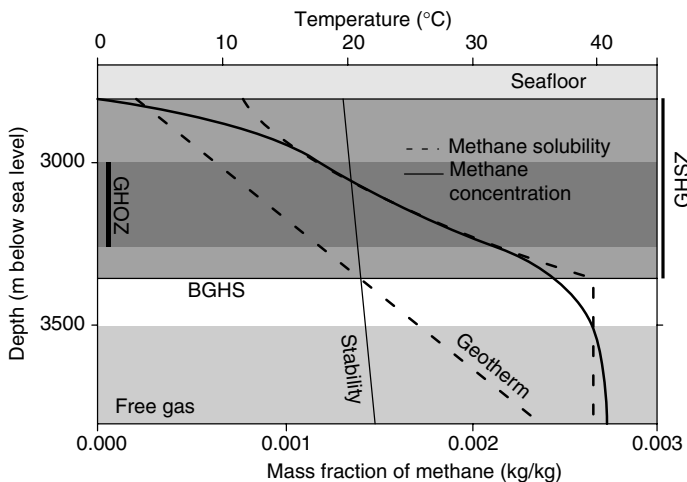


**FIGURE 7.13** Methane solubility imposes a narrower limit than the  $P-T$  stability region for hydrate depth.

stability zone is due to methane solubility. In fact Tréhu et al. (2004a, 2006) suggest that the GHSZ defined by the  $P-T$  field, be considerably narrower, defined by the methane solubility to be the GHOZ.

As shown in Figure 7.13 the pressure and temperature limits to the hydrate stability exists from the seafloor (because hydrates are less dense than seawater) to the intersection of the geotherm (BGHS). The solubility limit, however, imposes a further depth restriction because the methane concentration must equal the solubility limit to be in equilibrium with hydrates. It is assumed that the sediment provides sufficient nucleation sites so that there is no methane metastability, so hydrate forms in the narrow depth region where methane concentration lies atop the methane solubility line. As illustrated in the Leg 311 case study, the GHOZ is always smaller than the GHSZ.

## 7.5 DRILLING LOGS AND/CORING PROVIDE IMPROVED ASSESSMENTS OF HYDRATED GAS AMOUNTS

After the above initial remote assessments, the more expensive methods of drilling and coring enable refinement of estimation of reservoir hydrate content. Logging tools such as caliper, gamma ray, density, resistivity, and neutron porosity determine the hydrate depth, and to some extent the concentration. To this suite of drilling logs, nuclear magnetic resonance (NMR) spectroscopy has recently proved a valuable addition. Secondary tools, such as infrared (IR) temperature sensing, gas evolution from cores, pore water chlorinity decrease, and computed tomography (CT) of cores, provide two important parameters for the extent of hydrates—namely the extent and concentration of the hydrate reservoir. The SMI and methane solubility zone, both notable additions to the core tool suite, enable

estimation of the top hydrate boundary, as discussed in Sections 7.2.2 and 7.4.3, respectively. Third, it has recently proved possible to perform hydrate assessments at the seafloor, using Raman spectroscopy for assessing hydrate amounts and concentrations. Let us consider the three types of assessment tools.

### 7.5.1 Open Hole Well Logs

The most recent well log summaries for hydrates is that by Anderson et al. (2005) and the log summary in the Mallik 2002 case study by Collett et al. (2005). While a brief overview is presented below and exemplified in the Mallik 2002 case study, the reader interested in details is encouraged to review the above two documents for a thorough exposition of hydrate open hole well logging.

Collett (1983) and Collett and Ehlig-Economides (1983) studied the logs of 125 wells in the Prudhoe Bay region, to find 102 hydrate occurrences in 32 wells. The analyses of other permafrost wells were based upon the logs of a known hydrate well, the Northwest Eileen State Well Number Two, in which ARCO/Exxon recovered hydrate cores in 1972. Other studies on the effects of hydrates in wells and logs in the permafrost are by Weaver and Stewart (1982), Collett et al. (1984), Kamath and Godbole (1987), Mathews (1986), Collett (1992), Prensky (1995), with the most recent review of hydrate well logs in by Anderson et al. (2005).

In general, all studies indicated difficulty in distinguishing hydrates based on single logs, particularly within the permafrost interval. It is difficult to distinguish hydrates from ice based upon well logs and thus hydrates within permafrost depth boundaries are seldom assessed. To have some confidence in hydrate determination, it is necessary to consider a suite of logs. Figure 7.14 shows that the simultaneous log responses corroborate hydrate interpretations. Table 7.9 provides a summary of the individual responses of well logs to the presence of hydrates, again illustrating the fact that hydrates are difficult to distinguish from ice. The drilling mud log is the most responsive to hydrates, but its response may not be very different from a log for free gas. NMR logs, the most exciting new log development, is discussed briefly below.

Nuclear magnetic resonance logging presents a new and efficient means of hydrate detection. Dallimore and Collett (2005, p. 21) summarize the NMR method as follows:

Kleinberg et al. (2005) and Takayama et al. (2005) show that NMR-log measurement of sediment porosity, combined with density-log measurement of porosity, is the simplest and possibly the most reliable means of obtaining accurate gas hydrate saturations. Because of the short NMR relaxation times of the water molecules in gas hydrate, they are not discriminated by the NMR logging tool, and the *in situ* gas hydrates would be assumed to be part of the solid matrix. Thus the NMR-calculated “porosity” in a gas-hydrate-bearing sediment is apparently lower than the actual porosity. With an independent source of accurate *in situ* porosities, such as the density-log measurements, it is possible to accurately estimate gas hydrates saturations by comparing the apparent NMR-derived porosities with the actual reservoir porosities . . . . Collett and Lee (2005) conclude that at relatively low gas

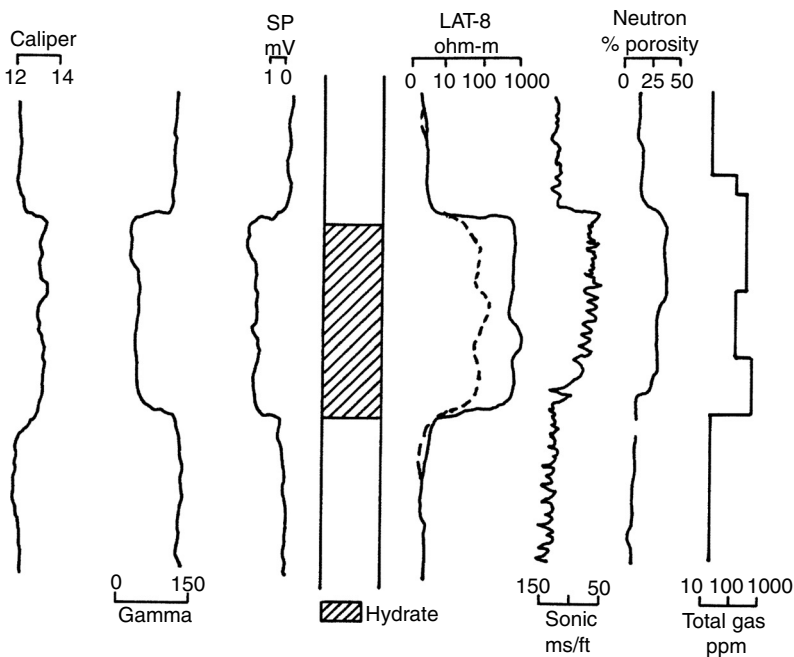


**FIGURE 7.14** Typical well log responses to hydrates in permafrost. (Reproduced from Collett, T.S., *Detection and Evaluation of Natural Gas Hydrates from Well Logs*, Prudhoe Bay, U. Alaska, Anchorage (1983). With permission.)

hydrate saturations in shale-bearing sections, the electrical-resistivity derived gas hydrate saturations are sometimes greater than the NMR-density derived gas hydrate saturations. The cause of this difference is unclear at this time.

The Mallik case study (Figures 7.36 and 7.37) provides the best example of well logs in a permafrost hydrate reservoir, followed closely by the Leg 204 (Figures 7.26 and 7.27) example for ocean hydrates. All four of the case studies for field hydrates have associated logs.

### 7.5.2 Evidence of Hydrates in Cores

There are two types of cores—pressurized, as in the HYACE coring tool developed by Amman et al. (1996) and extended by Schulteiss et al. (2006) to HYACINTH, and the unpressurized coring tools that are more typical of ocean-field experiments. It is important to note the distinction because, while pressurized cores frequently fail due to pressure incontinence, when they function well, they preserve the hydrated core in a much better state than nonpressurized cores, which give unambiguous results only for nonvolatile components such as chloride and sulfates.

When a nonpressurized core is obtained, the trip frequently requires more than 45 min, between the original cored position and the recovery site on the

**TABLE 7.9**  
**Summary of Well Log Responses to Hydrates**

Type of log	Response to hydrates
Mud log	The dissociation of hydrates causes a significant increase of gas in the drilling mud, which is encountered at the top of the well. Cold or dense drilling fluids may suppress dissociation resulting in lower gas
Dual induction	In the shallow penetration log, a higher resistivity is obtained relative to a free gas zone due to hydrate dissociation. This is a very tricky interpretation problem with $R_w$ changing, and gas and hydrate both being insulators. The deep induction log shows high resistivity and mimics an ice-bearing reservoir. However, this log is confounded by $R_w$ changing, and by gas and hydrate both being insulators
Spontaneous potential	Compared to a free gas bearing zone, the spontaneous potential log is less negative, but similar to that of ice
Caliper log	An oversized drill hole is indicated by hydrate dissociation. This may also occur with ice in the permafrost. However, as noted by Kleinberg (Personal Communication, July 20, 2006) "In some circumstances, hydrates can be a good cement (until it dissociates), and strengthen the unconsolidated host sediment"
Acoustic transit time	The acoustic wave time decreases relative to either water or free gas; however, the acoustic transit time for hydrates is like ice-bearing sediments. See <a href="#">Section 7.4.2</a> for BSR and AVO in ocean applications
Neutron porosity	For the neutron log, the hydrate response is nearly the same as liquid water. Hydrate is 6% higher than fresh water, somewhat more than that for salt water. Both differences are swamped by the clay effect
Density	The density decrease apparent in hydrates is very small but may be distinguished from the density of water but not from ice density. However, this is a fine difference, and it should be used with the suite of other logs
NMR	The NMR tool senses porosity including water; the porosity without water is determined by another tool (e.g., density), so the amount of hydrates is obtained by difference. See discussion in paragraph starting 'NMR logging ...'
Drilling rate	The drilling rate also decreases in the hydrate region relative to that in a fluid-saturated sediment, but not significantly different from that of ice

*Source:* Modified from Collett (1983).

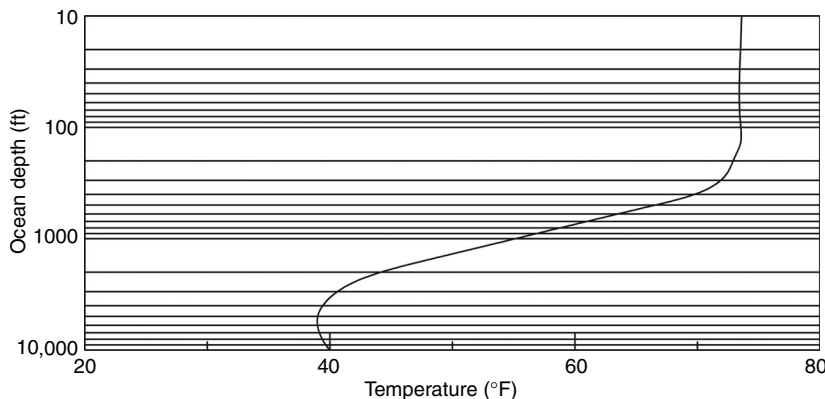


**FIGURE 7.15** Gulf of Mexico ocean temperature vs. depth. (From Churgin J., Halmiski, S.J., *Key to Oceanographic Records Documentation #2, Gulf of Mexico*, Natl Oceanographic Data Center, Washington, DC, 1974. With permission.)

ship or drill site. During this trip time, hydrate dissociates and gas evolves from the nonpressurized core as the core is removed through warmer waters. A typical ocean thermal gradient in the Gulf of Mexico is shown in Figure 7.15, indicating that at most ocean depths below 4000 ft, the water temperature is approximately 40°F, while the ocean-air surface temperature is considerably warmer.

Even when the nonpressurized core is at the surface or aboard the ship, hydrates continue to dissociate, and gas evolves, requiring the drilling of holes in the core liner to relieve the pressure for safety considerations, as shown in Figure 7.16. Because hydrates dissociate in nonpressurized cores, the endothermic heat of dissociation (Chapter 4) causes low temperatures (typically  $-1.5^{\circ}\text{C}$ ) in the cores, which is used as an IR signal of dissociated hydrates in cores. Even with the low temperatures, however, because gas has evolved during the trip to the surface, many dispersed hydrates will completely dissociate before arriving at the surface.

Consequently, gas evolution at the surface cannot be reliably measured for hydrate dissociation. However, it is possible to predict nonpressurized core hydrate dissociation during this trip (Davies and Sloan, 2006) as a function of the depth–temperature–time profile during the coring. The model for nonpressurized core dissociation is modified from CSMPlug (in the book's endpapers) for hydrate plug dissociation in flowlines.

The above discussion suggests two of the common ways of quantifying hydrates in cores: (1) low core temperatures as sensed by IR imaging (Ford et al., 2003) and (2) gas evolution from pressurized core sampling systems (Pettigrew, 1992). A third method of sensing hydrates is by the use of chlorinity, which may be reliable because unlike the previous two methods, it does not depend upon the volatility of gas evolution from nonpressurized cores, nor the time–temperature history of the water surrounding the core.

Recall from Chapter 2 that hydrates exclude all ions on formation. The ions form strong Coulombic bonds with water resulting in effective radii that cause



**FIGURE 7.16** Shipboard drilling of gas pressure relief holes in hydrate nonpressurized core liner to accommodate gas hydrate dissociation. (Courtesy F. Rack, May 5, 2004.)

them to be both too large and too polar for hydrate cage guests; in addition, ions provide competition with clathrates for the available water molecules. Therefore, hydrates formed in salt water are depleted in chloride ions, while the water around recently formed hydrates is enriched in salt concentration.

When hydrates dissociate on core retrieval, the melting hydrates provide water that is lower in chlorinity than the surrounding seawater. *In situ* hydrates content can be determined by measuring the degree of prewater dilution relative to a baseline assumed to represent the *in situ* pore water Cl<sup>-</sup> concentration prior to gas hydrate dissociation (Hesse and Harrison, 1981; Egeberg and Dickens, 1999).

In the following southern Hydrate Ridge Leg 204 case study, Tréhu et al. (2004) compared estimates of hydrate fractions by the three methods, relative to the hydrate fractions estimated by resistivity at bit (RAB) logs. All four results consistently indicate that, at depths greater than the crest of the ridge, the average gas hydrate content is generally <2% of the pore space. Such numbers are typical of oceanic hydrates.

As in Section 7.4.3, Tréhu et al. (2004a) distinguish between the GHSZ and the GHOZ with the former always greater than the latter. The difference between these two values implies that the BSR and thermodynamic stability region are necessary for the GHSZ, but not sufficient for hydrate determinations in the GHOZ, which may be limited by methane availability, stratigraphy, or other factors.

A fourth rapidly evolving hydrated core method that is just coming into use is that of portable CT scanning, which applies x-ray imaging techniques to hydrate cores at the surface. This method was developed and calibrated by Freifeld et al. (2002) at the USA Lawrence Berkeley National Laboratory; it is evolving into frequent use to determine the hydrate content of cores.

When cores are obtained, after shipboard measurements they are preserved in liquid nitrogen (Tulk et al., 1999) and transported to laboratories, where they

are thoroughly studied using diffraction (Eaton et al., 2005), scanning electron microscopy (Genov et al., 2004; Stern et al., 2005; McGrail et al., 2005), and Raman and NMR spectroscopy (Ripmeester et al., 2005) with the last two being a comprehensive reference.

### 7.5.3 Combining Laboratory and Field Experiments

The above experimental work is bifurcated into those in the field and the laboratory. This bifurcation requires resolving the question of how the laboratory experimental results are representative of hydrates in nature. In resolving this question, the work of Brewer, Paull, Peltzer, Ussler, and colleagues at the Monterey Bay Aquarium Research Institute (MBARI) has been exemplary. MBARI has both the goal and resources to perform high quality laboratory experiments subsea, so that core retrieval and possible damage (for example) is not a concern. Their work has been notable for generating ocean scientific knowledge and educating the public about the ocean. In particular, MBARI excels in areas of subsea use of hydrate NMR and Raman spectroscopy (Kleinberg et al., 2003; Hester et al., 2005, respectively), methane and CO<sub>2</sub> hydrate formation and storage (Rehder et al., 2003), and ocean geochemistry (Paull et al., 2005). It is clear that MBARI's efforts are moving ocean science towards quantification.

The above suite of hydrate sensing tools (thermodynamics, geothermal gradients, kinetics, BSRs, lithology and fluid flow, logging and coring tools, and subsea tools) has enabled an assessment of where hydrates may exist worldwide. On the basis of the data provided by these tools, hydrate formation models such as that of Klauda and Sandler (2005) enable our prediction of hydrate formation sites in nature—notably the *a priori* prediction of 68 of the 71 sites at which hydrates have been indicated.

Currently in the state-of-the art, hydrate experiments and modeling are synergistic partners, with the experiments serving as a calibration for models, and the model suggesting new experiments. After reliable models are generated, the models are always more cost effective than laboratory and field experiments.

In the first principle in this chapter, it was indicated that the state-of-the-art was moving away from *in situ* hydrate assessment, to hydrate production. In the next section we turn to hydrate production models, which are calibrated by a number of costly field and laboratory experiments.

Most natural hydrates are in the ocean environment. As a state-of-the-art summary of ocean hydrates, Tréhu et al. (2006) list six major lessons learned during the decade from 1996 to 2006:

1. Lithology may exercise a primary control of hydrate deposition, resulting from permeability, faults, and traps.
2. Gas hydrate is distributed heterogeneously and can fill pore space between sediments grains, or displace grains to form lenses and nodules. Hydrates form preferentially in coarse-grained sands.

3. New remote sensing tools are needed to supplement a BSR indication of hydrates. Gas hydrates can form without a BSR indication.
4. Multiple proxies are required to determine hydrate distributions. Of particular note are the new tools for laboratory imaging (IR, CT, and x-ray), logging while drilling, pressure coring and physical testing under pressure.
5. There are two end-members of hydrates, FHF and DLF. Although it is possible to typify hydrate deposits as predominately one end-member, most deposits contain elements of both end-members.
6. Acceptable geological assessment of hydrates require integration of information from several fields of geology, geophysics, and geochemistry.

## 7.6 HYDRATE RESERVOIR MODELS INDICATE KEY VARIABLES FOR METHANE PRODUCTION

Experiments, both in the field and laboratory, are very expensive. Models of methane production from hydrate can save substantial expense of time, effort, and capital. This section of Chapter 7 gives guidelines from the models for hydrate dissociation.

One might consider the rationale for models, as one of three analogs of the real hydrated reservoir situation:

1. A field test, such as the Mallik 2002 case study, is perhaps the best analog of hydrate dissociation in a reservoir. However, the Mallik 2002 project cost many man years and approximately US\$22,000,000. Even with such a large cost, there was still concern about the data obtained, and how representative the transient data would be for long-term production.
2. A laboratory experiment typically requires months to plan and costs approximately US\$50,000–300,000. There is less certainty here than in the field tests, but also less expense.
3. A mathematical model of the hydrate reservoir typically requires several minutes to days to execute and costs typically US\$10–100. Even with these low costs, unless the model is based upon extensive laboratory and field data, the model will have the weakest link of the three methods to physical reality.

Progressing from each of the above levels to the next saves 2–3 orders of magnitude in financial and time expense. So, for example, if one wished to perform a sensitivity study of methane production rate response to reservoir permeability or hydrate saturation, it is many orders of magnitude easier to do so via a model, than via a field test.

Before summarizing the models, however, consider as background the three common means of hydrate dissociation from Makogon (1997), shown in

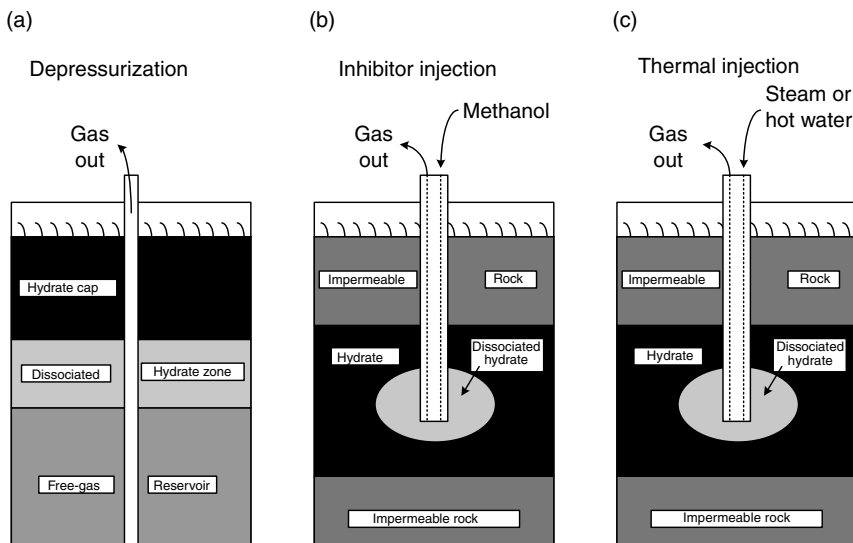


**FIGURE 7.17** The three common means of hydrate dissociation. (From Makogon, Y.F., *Hydrates of Hydrocarbons*, PennWell Publishing Co., Tulsa, 1997. With permission.)

Figure 7.17. In Figure 7.17a, the depressurization method shows that drilling through an overlying hydrate reservoir into free gas allows normal production of gas to depressurize the gas reservoir, which is replenished by gas from dissociating hydrates; this method is illustrated in the Messoyakha case study at the end of the chapter. In Figure 7.17b, the inhibitor injection method is shown to dissociate hydrates via injecting methanol or brine into the wellhead; this was used for a short time at Messoyakha, but quickly abandoned due to the short-lived results. In Figure 7.17c, the thermal stimulation method is shown to increase the temperature of the hydrate reservoir to dissociate the hydrates; the thermal stimulation method is illustrated, combined with the pressure reduction method, in the Mallik 2002 case study.

Relative to our phase equilibrium study in [Chapters 4](#) and [5](#), the above three techniques are illustrated on the phase diagram of [Figure 7.18](#), as  $\Delta T = 0$ ,  $\Delta P = 0$ , and 10% methanol, for depressurization, thermal stimulation, and inhibitor injection, respectively. Additional explanation is given in the figure caption.

The above discussion demonstrates two principles for hydrate dissociation: (1) hydrates will not occur outside the thermodynamic restrictions of the phase equilibria, that is, hydrates require the appropriate temperature, pressure, as shown in the area to the left of the lines in [Figure 7.18](#), as well as methane and water and (2) when hydrates are dissociated, even at constant temperature as shown in [Figure 7.18](#), heat must flow from the surrounding media to the hydrates, causing a cooling. This last point is also intuitive, because gas and water molecules from dissociated hydrates have more energy than they do in nondissociated hydrates. Thus energy must flow to the hydrate surface in order to dissociate it.

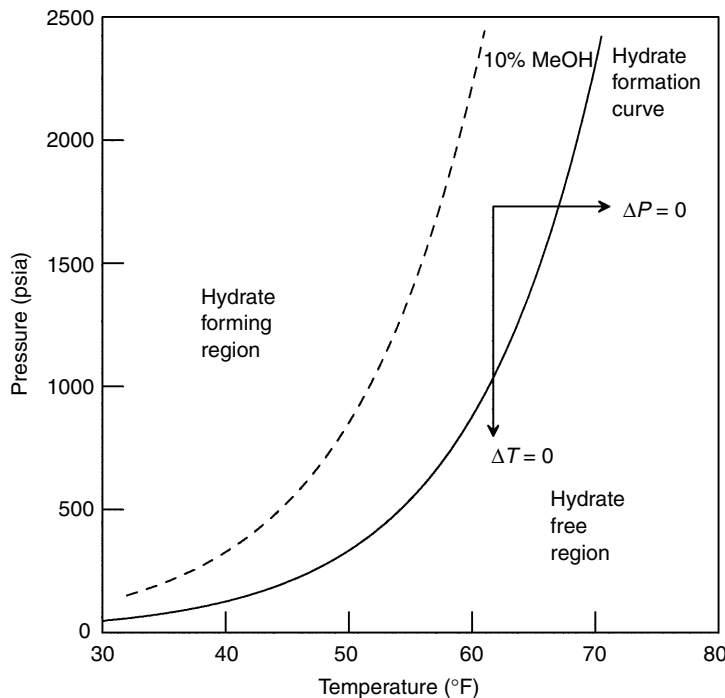


**FIGURE 7.18** A phase diagram showing the three common hydrate dissociation techniques, relative to the initial sample condition (intersection of horizontal and vertical arrows). Depressurization is shown as  $\Delta T = 0$ ; thermal stimulation as  $\Delta P = 0$ ; inhibitor injection is represented by displacing the solid hydrate formation curve to the dashed curve, via injection of 10 wt% methanol in the free water phase.

As additional background for modeling hydrate dissociation, it should be noted that there are three commonly cited classes of hydrate reservoirs in the permafrost, following the definition of Moridis and Collett (2004):

Class 1—hydrate layer underlain by two-phase zone of mobile gas and water

Class 2—hydrate layer underlain by one-phase zone of mobile water

Class 3—hydrate layer with absence of underlying zones of mobile fluids

In every hydrate dissociation process, three phenomena exist: (1) heat transfer to the hydrate–fluid interface, (2) the kinetic dissociation of hydrates, and (3) the flow of fluids (gas and water) away from the hydrate interface. The models are classified according to each of these three phenomena in [Table 7.10](#), modified from a recent review of hydrate models, by the laboratory of Pooladi-Darvish (Hong, 2003).

**TABLE 7.10**  
**Summary of Hydrate Dissociation Models Since 1982**

Model	Heat transfer		Fluid flow		Solution	
	Conduction	Convection	Gas	Water	Kinetics	Method
Holder and Angert (1982)	X		X			Numerical
Burshears et al. (1986)	X		X	X		Numerical
Jamaludin et al. (1989)	X				X	Numerical
Selim and Sloan (1989)	X	X	X			Analytical
Yousif and Sloan (1991)			X	X	X	Numerical
Makogon (1997)	X	X	X	X		Analytical
Tsyplkin (2000)	X	X	X	X		Analytical
Masuda et al. (2002)	X	X	X	X	X	Numerical
Moridis et al. (2002)	X	X	X	X	X	Numerical
Pooladi-Darvish et al. (2003)	X	X	X	X	X	Numerical

As indicated in Table 7.10, only in the last decade have models considered all three phenomena of heat transfer, fluid flow, and hydrate dissociation kinetics. The rightmost column in Table 7.10 indicates whether the model has an exact solution (analytical) or an approximate (numerical) solution. Analytic models can be used to show the mechanisms for dissociation. For example, a thorough analytical study (Hong and Pooladi-Darvish, 2005) suggested that (1) convective heat transfer was not important, (2) in order for kinetics to be important, the kinetic rate constant would have to be reduced by more than 2–3 orders of magnitude, and (3) fluid flow will almost never control hydrate dissociation rates. Instead conductive heat flow controls hydrate dissociation.

Numerical models such as the one by Moridis et al. (2005) are more sophisticated, and are subject to space- and time-discretization errors; so numerical models must be compared to some standard, such as a physical measurement, or perhaps an analytical model.

While economy of space prevents detailing the various models here, it is worthwhile to provide outcomes, based upon the model sensitivity studies. These results summarize the recent work by Pooladi-Darvish and coworkers (2005) and Moridis and coworkers (2005), and the economic studies by Howe et al. (2004) and by Hancock et al. (2005a,b):

1. Of the three common means to dissociate hydrates, depressurization is the most economical.
2. Most economical for dissociation by depressurization is the sub-permafrost reservoir in which hydrates overly a free gas, with impermeable boundaries both at the top of the hydrate layer, and at the bottom of the free gas layer.
3. The sediment setting will control the target to some degree. Hydrate deposits in sandy ocean sediments (e.g., the Gulf of Mexico) likely

contain larger hydrate amounts relative to the silty/clay sediments characteristic of the majority of hydrate reservoirs (e.g., the Blake Bahama Ridge).

4. Proximity to the phase boundary, and the need to supply energy to dissociate the hydrates, will control the rate of dissociation and thus the economics. Because conductive heat transfer controls hydrate dissociation, hydrates closer (in temperature and pressure) to the phase boundary will be most economical to dissociate. Heat transfer limitations indicate that high surface areas (thin layers) are most economical.
5. High hydrate concentrations can lead to drastic reductions in effective permeability, thus limiting the areal extent of depressurization.
6. Pore size is not important until pores are small, less than 100 nm, but salt concentration has a major effect.
7. More data are needed on which to base the models. In the field, long-term production tests are needed to eliminate transient phenomena for validation of the reservoir models. In the laboratory more data are needed for permeability, conductivity, hydrate kinetics, and for determining the transition between heat-, mass-, and kinetic-controlled dissociation.
8. The models for the above reservoir conditions indicate that economical hydrate production can be achieved at a gas cost of US\$9 per MMBTUs in 2005 economics.

## 7.7 FUTURE HYDRATED GAS PRODUCTION TRENDS ARE FROM THE PERMAFROST TO THE OCEAN

The discussion in Section 7.6 is not intended to imply that the three methods of depressurization, thermal stimulation, and inhibitor injection are the only means of hydrate dissociation. Because the hydrate science is available as indicated in the earlier chapters of this book, the application of that science to recovery from hydrates is an exercise for the innovative engineer. Novel ideas such as fire flooding (Halleck et al., 1982), burial of nuclear wastes (Malone, 1985, p. 27), and the use of electromagnetic heating (Islam, 1994) are only three innovative ways of dissociating hydrates, but none have been tried. However, in this portion of the chapter, it is intended to describe trends for dissociating hydrates in several kinds of reservoirs, as an indication of the future.

The state-of-the-art for hydrated energy is in transition—moving from assessment of the location and extent of hydrate concentrations, to the proof of concept for long-term production, first from the permafrost, and then from the ocean. One projection of the way forward in hydrated energy recovery is the following:

1. The 2002 Mallik well provided an indisputable proof of the concept—namely, it is possible to in transient testing to recover energy from permafrost hydrates upon dissociation.
2. Other permafrost-associated hydrate wells should be drilled in 2007–2008 to move beyond the proof of concept, to a proof of long-term

production, eliminating the transient phenomena in the 2002 Mallik three-day tests. Many suggest the Messoyakha Field provided proof of long-term production (Makogon, 1988), but while all agree that hydrates played a part at Messoyakha, the exact role of hydrates is under some scientific dispute (Collett and Ginsburg, 1998).

3. The technology developed in the Mallik production test should be transferred to recover hydrates from the “sweet spots” of high concentrations in the ocean, such as at Barkley Canyon or the Gulf of Mexico.
4. An engineering breakthrough is required for the final step—recovery of hydrates in dispersed concentration (usually around 3.5 vol% in 30% porosity) in the deep ocean (>500 m water depth), which may prove problematic.

Consider the above four steps in some detail:

1. The 2002 Mallik well provided a proof of the concept—namely, that it is possible to recover energy from permafrost hydrates upon dissociation.

This important work was a major advance in technology—moving the state-of-the-art from the identification of hydrate reserves, to the recovery of energy from those reserves. The 2002 Mallik proof of concept (see case study 4) is a cornerstone upon which future energy recovery from hydrates will be built. In addition, the work is validated by a wide diversity of credible scientific organizations and is scientifically established beyond doubt in the Geological Survey of Canada (GSC) Bulletin 585 (Dallimore and Collett, Eds. 2005), which includes more than 65 reviewed, technical publications on Mallik 2002. In essence, a gas flare was generated over a short period to prove the concept of energy evolution from hydrates, combining depressurization and thermal stimulation.

2. Other permafrost-associated hydrate wells should be drilled in 2007–2008, to move beyond the proof of concept, to a proof of production, eliminating the transient phenomena in the 2002 Mallik three-day tests.

Because field tests are so expensive it is important to validate prediction models to obviate future tests, with a minimum of reliable data. However, the three-day Mallik 2002 test contained too many transient phenomena to be modeled accurately. Instead a new 3–6 month production test that eliminates transients should be carried out at a site such as Mallik 2002, to enable modeling of production via state-of-the-art work such as Moridis’ LBNL model for energy production from hydrates. Once the model is refined by production data, cost savings of several orders of magnitude can be realized, to reliably predict the outcome of future tests.

3. The technology developed in the Mallik production test should be transferred to recover hydrates from the “sweet spots” of high concentrations in the ocean, such as at Barkley Canyon or the Gulf of Mexico.

The amount of ocean-hydrated energy is so large that the likely error in its estimate, is greater than all of the hydrated energy in the permafrost. Thus, because of its size, the ocean hydrated energy will be the ultimate target. However, it is not possible to produce oceanic hydrates initially because they are generally too

dispersed—typically less than 3.5% of pore volume, in sediments that have less than 30% porosity.

Leg 204 at Hydrate Ridge (Tréhu et al., 2004b) and the following IODP Leg 311 showed that it is possible to access “sweet spots” in the ocean for the potential recovery of hydrates, such as those close to the surface at the crest of Hydrate Ridge. These higher concentrations will be the first ocean targets for hydrate recovery. Similarly, in the Gulf of Mexico, sandy sediments provide higher porosities, and the sandy sediment pore volume filling can be much higher than the 3.5% cited for a worldwide average.

It can be argued that, if it is not possible to recover oceanic hydrates at high concentrations, it will be impossible to recover hydrates at lower concentrations in the ocean. Thus, success in the Gulf of Mexico, at Hydrate Ridge, or in a similar setting is vital to the energy recovery from more dispersed, deeper hydrates.

4. An engineering breakthrough is required for the final step—recovery of hydrates in dispersed concentration (typically 3.5 vol% in 30% porosity) in the deep ocean (>500 m water depth) to use science and engineering, but most importantly previous experience, to produce hydrates efficiently from very dispersed resources in sediments. Probably not much new science will be needed for this step; rather an engineering breakthrough will be necessary.

This area of hydrated gas recovery is of very active international interest, due to its energy impact. However, because of thermodynamic and practical constraints (Moridis and Sloan, 2006) recovery of energy from low concentration (3% of pore volume) may be problematic. Clearly energy is a major driver of technology, and technology in turn is largely responsible for national economic success (Economides and Oligney, 2000; Bernstein, 2004; Sachs, 2005).

## 7.8 HYDRATES PLAY A PART IN CLIMATE CHANGE AND GEOHAZARDS

Because hydrates are so widely distributed in most of the world’s ocean continental shelves, it seems logical to inquire how hydrates may have impacted the other components in the earth—for example, the climate. Dickens et al. (1995), Dickens (2003) and Kaiho et al. (1996) indicate that an ancient, massive ocean methane hydrate dissociation explains a 4–8°C temperature rise over a brief geologic time interval ( $10^3$  years) called the Late Paleocene Thermal Maximum (LPTM) that occurred 55.5 million years ago. This is documented in deep ocean drilling samples as a prominent negative carbon isotope excursion ( $\delta^{13}\text{C}$  of  $-2.5\text{\textperthousand}$ ) in all ocean sediments, in fossil tooth enamel, and in carbonates and organic sediments in terrestrial sequences. This  $\delta^{13}\text{C}$  reduction in the ocean and the recovery over the ensuing  $200 \times 10^3$  years (see Figure 7.19a) is consistent with pronounced dissolution of calcium carbonate in the deep sea sediment deposited during the LPTM, shown in Figure 7.19b.

The evolution of a large amount ( $1.12 \times 10^{18}$  g of  $\text{CH}_4$ ) of methane from hydrates is the only plausible hypothesis that has been offered to explain this environmental perturbation. The abnormal  $\delta^{13}\text{C}$  isotope indicates that source

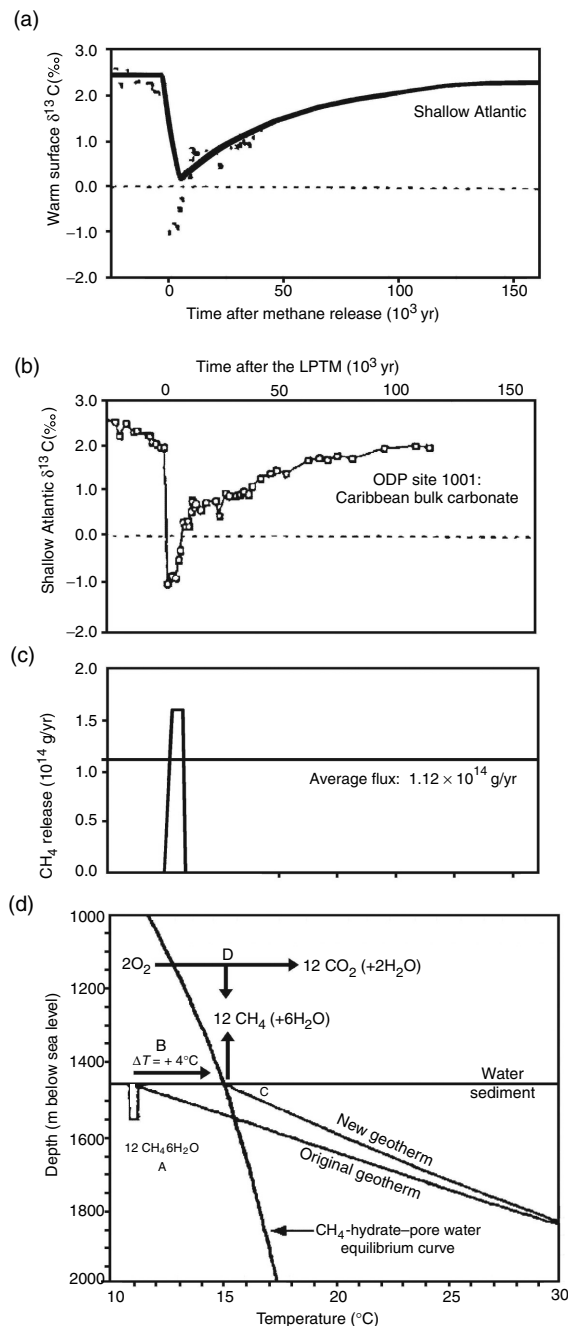


**FIGURE 7.19** Temperature (a) bulk carbonate (b), methane release (c), and change in geotherm (d) with time and temperature associated with the LPTM. (Reproduced from Dickens, G.R., *Nature*, **401**, 752 (1999). Copyright with permission from Macmillan Publishers Ltd.)

was external to the normal ocean-atmospheric-biomass carbon pool. [Figure 7.19c](#) shows a rapid evolution of methane from hydrates, which is hypothesized to be oxidized to CO<sub>2</sub> greatly enriched in  $\delta^{13}\text{C}$  (Dickens et al., 1995; Thomas and Shackleton, 1996).

Figure 7.19d shows the hydrate equilibrium curve as a function of depth and temperature in the ocean. Hydrates are only stable between equilibrium line and the original geotherm to the left of the curved line, at depths below the sediment surface, shown by the small vertical rectangle at A. If the ocean were warmed by 4°C, the hydrates between the original geotherm and the equilibrium curve would melt, as the new geotherm was established. The warming from the original to the new geotherm would result in methane expulsion to the environment, where it would be oxidized to CO<sub>2</sub>, resulting in significant further warming. It was hypothesized that the resulting CO<sub>2</sub> was reabsorbed by the ocean over the ensuing  $200 \times 10^3$  years.

Dickens (1999) cautions that in modern times a similar reoccurrence is prevented by deeper oceans than in ancient times. However, the importance of the LPTM perturbation is that it is the only analog available in the geological record for understanding how the global carbon cycle and other systems is related to a rapid, massive input of fossil fuel such as that which may be occurring in modern industrial times.

A monograph by Kennett et al. (2003) thoroughly documents evidence for Late Quaternary climate change by hydrates, commonly called “The Hydrate Gun Hypothesis.” The concept is that, as little as 15,000 years ago, methane from hydrates caused significant global warming. The data and summary in the monograph by Kennett et al. is the most thorough source for extending the theory to more modern times (the Late Quaternary). However, there is a considerable controversy concerning the validity of the hypothesis, and Kennett et al. (2005) appeal for more data to validate their hypothesis.

In a review of the Kennett et al. monograph, Dickens (2003) generally concurs with the hypothesis, but criticizes it on the grounds that the monograph “perpetuates the common-misconception that present-day methane hydrates are stable. These systems may be in a steady state, but they must be viewed as dynamic with large . . . carbon fluxes to and from the ocean, even at present day.” The question of climate change is the current focus of much research, for example, in the Hydrate Ridge case study by Boetius and Suess (2004), who conclude that location may not be contributing much methane to climate change.

In closing the discussion on hydrate-related climate change, it should be noted that seafloor hydrate dissociation is also directly related to slumping of sediments on the seafloor. Significant ocean hydrated sediment slumps can jeopardize the foundation of subsea structures such as platforms, manifolds, and pipelines. The single incident off the Carolina coast shown in [Figure 7.20](#) occurred about 15,000 years ago (Dillon, et al., 2001) and increased the extant earth’s atmospheric methane as much as 4%. The interested reader is referred to the recent monograph by Paull and Dillon (2001) on this topic. It should be noted that subsea subsidence was the major focus of a U.S. Department of Energy, Joint Industry Project in 2005 in the Gulf of Mexico (Boswell, 2006).

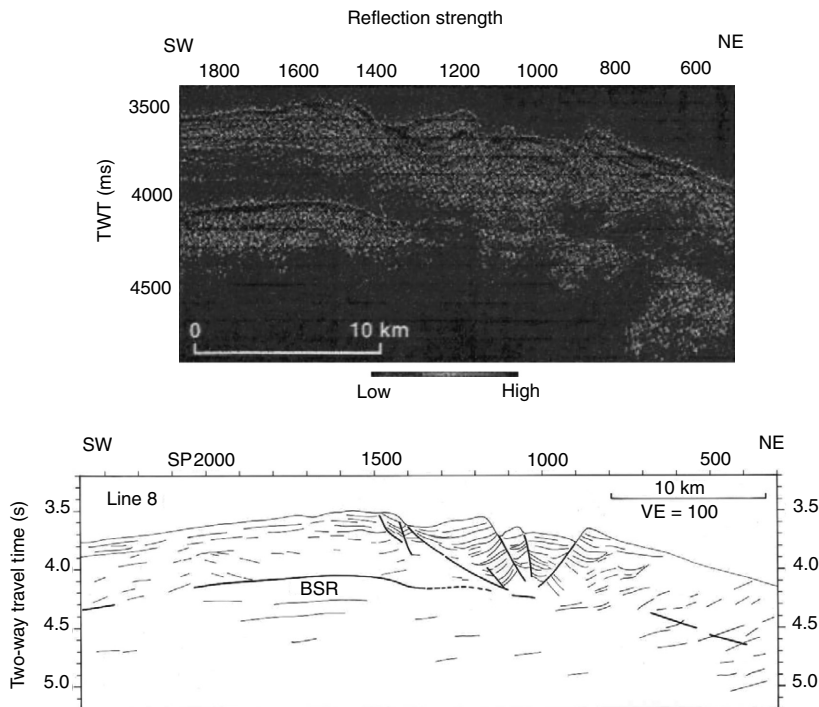


**FIGURE 7.20** (See color insert following page 390.) Seafloor slump in the Blake-Bahama Ridge shown in both seismic (top) and cartoon (bottom) relief. (From Dillon, W.P., Nealon, J.W., Taylor, M.H., Lee, M.W., Drury, R.M., Anton, C.H., *Natural Gas Hydrates: Occurrence, Distribution, and Detection*, (Paull, C.K., Dillon, W.P., eds.) American Geophysical Union Monograph, 124, p. 41, Washington DC (2001). With permission.) Note the bottom simulating reflector parallel to the ocean bottom, except in the middle section where it appears a seafloor eruption has occurred.

This chapter's preceding eight principles of hydrates in nature find application in the following four field case studies. The first two (Blake-Bahama Ridge and Hydrate Ridge) illustrate the geoscience fundamentals of locating and assessing hydrate formation in ocean deposits. The final two case studies (Messoyakha and Mallik 2002) deal with production of energy from permafrost hydrate reservoirs, which are a necessary prelude to recovery of energy from ocean hydrates.

### 7.8.1 Case Study 1: Leg 164 in the Blake-Bahama Ridge (Hydrate Assessment)

The discussion in this section is excerpted from Leg 164 Scientific Party Report. The Ocean Drilling Program (ODP) Leg 164, represented a drilling effort in late

1995 to understand the amounts of gas associated with the famous Blake-Bahama Ridge BSR (see Figures 7.12a,b) that was known since the late 1960s (Markl et al., 1970). Samples indicating the presence of hydrates were obtained earlier in this BSR vicinity at Deep Sea Drilling Project (DSDP) Leg 11, Site 102, 103 (Ewing and Hollister, 1972) and Leg 76, Site 553 (Kvenvolden and Barnard, 1983). Figure 7.21a gives the location of earlier sites, as well as those of Leg 164 (Sites 991 through 997).

On ODP Leg 164, three sites were drilled below the base of hydrate stability over a short distance (9.6 km) in the same stratigraphic interval. Figure 7.21b shows the three Leg 164 holes: Site 994 without a BSR, Site 995 with a weak BSR, and

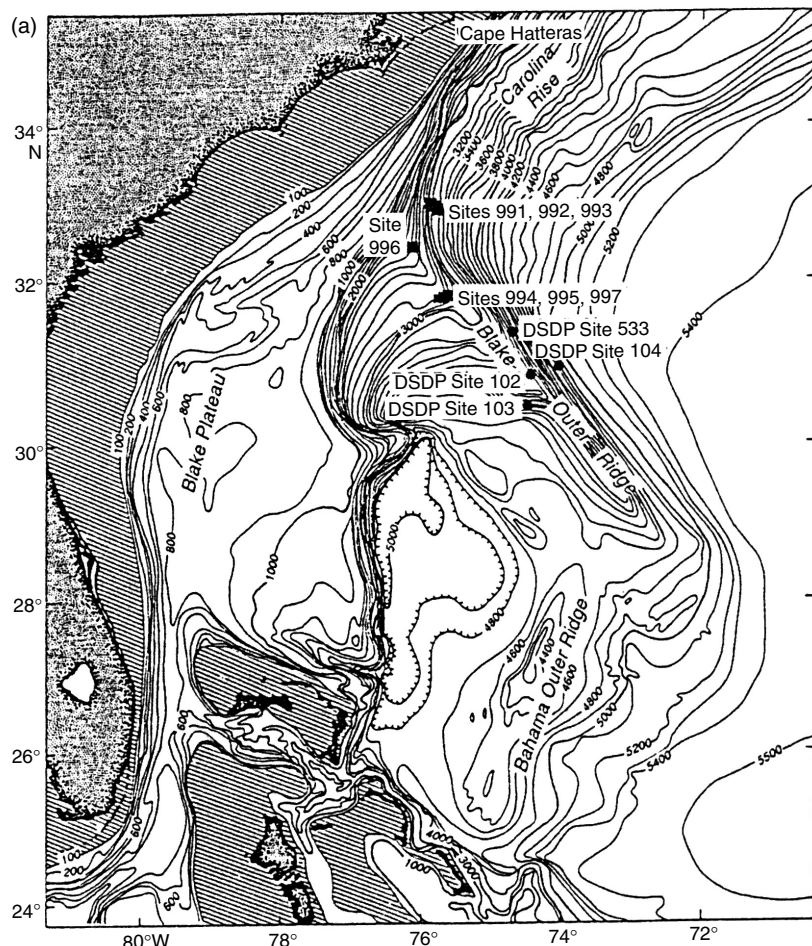


**FIGURE 7.21a** Map showing the location of Leg 164 in the Blake-Bahama Ridge (Sites 991 through 997). (Paull et al., 1996.)

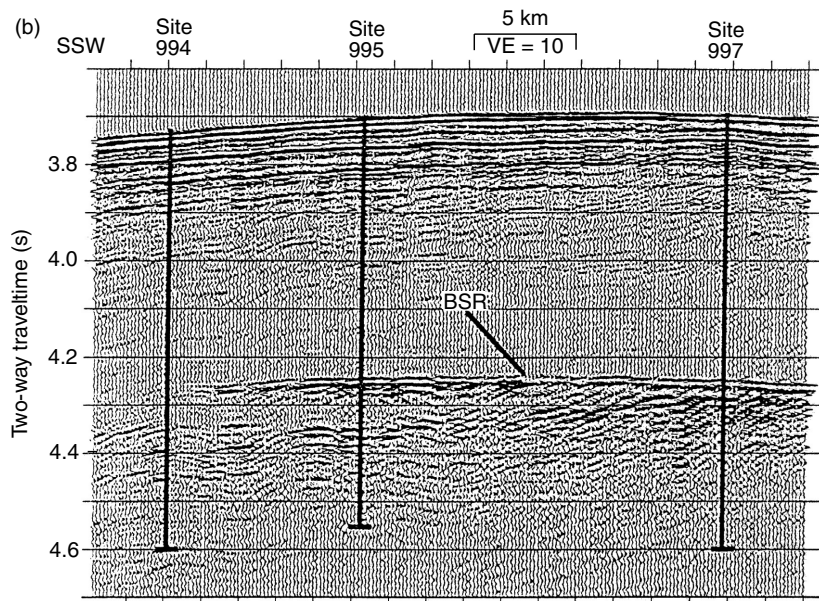


**FIGURE 7.21b** Bottom simulating reflector for the Three Leg 164 Holes at Blake-Bahama Ridge. (Paull C.K., et al., Leg 164 Scientific Party, in *Gas Hydrates—Relevance to World Margin Stability and Climatic Change*, The Geological Society, London, Special Publication, 1998. With permission.)

Site 997 with a strong BSR on the ridge crest. Site 996 was drilled some distance away from the BSR, to investigate migration in a fault zone where methane was leaking from the rise.

### 7.8.1.1 Site 994

Hydrates were indicated by both direct evidence [nodules at 259 m below seafloor (mbsf) in 994C, and a piece  $<1\text{ cm}^3$  in 994D at 261 mbsf] and indirect evidence (low chloride values and logs that show dramatic changes in P-wave velocity and electrical resistivity). As shown in Figure 7.22a the chloride anomalies and the electrical resistivity and sonic velocity logs indicate significant changes just below 220 mbsf where the hydrate samples were recovered, and at the base of the BSR, 420 mbsf.

The hydrate recovered consisted of methane ( $\sim 99\%$ ), with minor to trace amounts of carbon dioxide (1.22%), ethane (86 ppmv), propane (2 ppmv), with a volumetric ratio of methane to water of 154. The chlorinity concentration (57.2 mM) of water collected indicated that the sample was a mixture of 10% pore water and 90% freshwater. The gas:water ratio exceeded 170, higher than any previously reported for *in situ* hydrates. The  $C_1/C_2$  ratio was 11,500, compared to a headspace value three times lower; however, both gas ratios indicate biogenic gas.

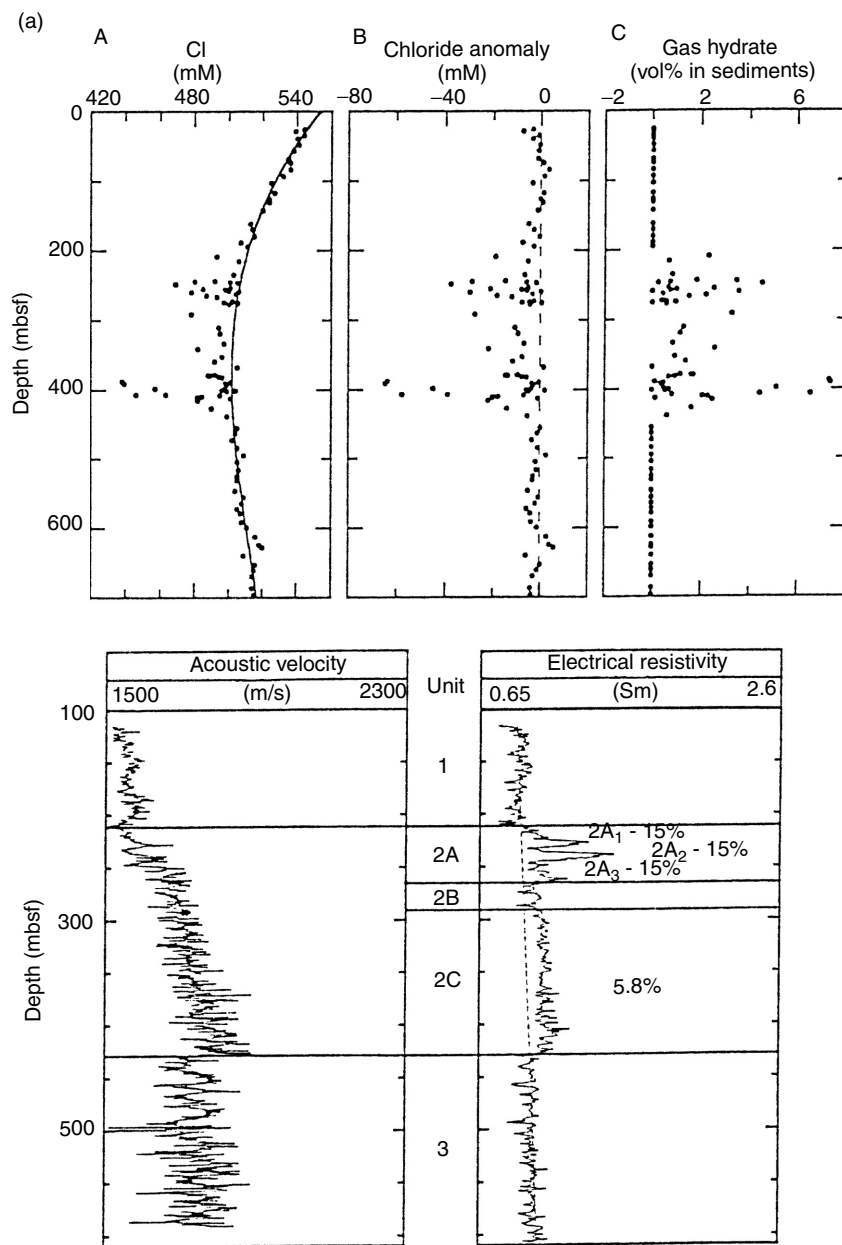


**FIGURE 7.22a** Chloride anomalies and acoustic and resistivity logs for Blake-Bahama Ridge site 994. (Paul et al., 1996. With permission.)

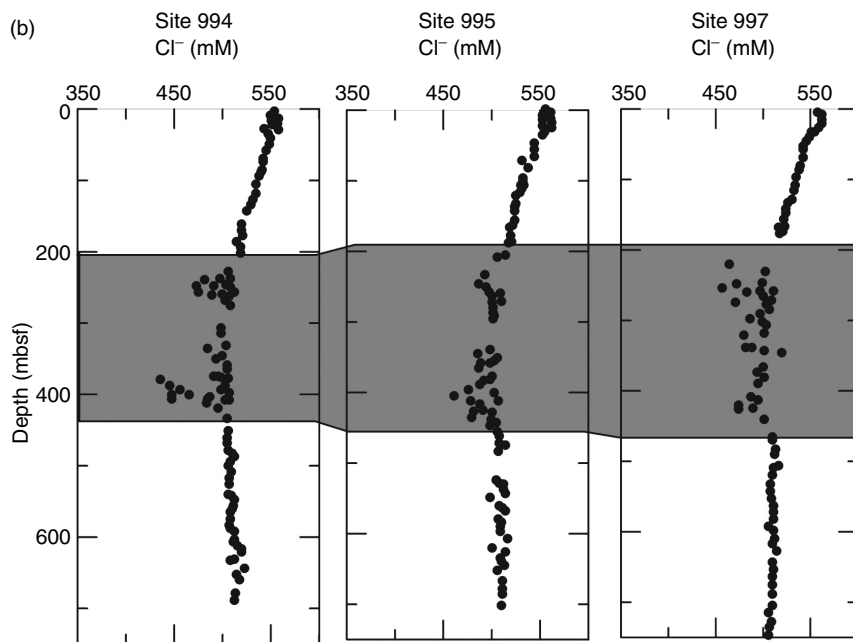


**FIGURE 7.22b** Similar chlorinity anomalies for Blake Bahama Ridge Sites 994, 995, and 997. (From Paull, C.K., Lorenson, T.D., Borowowski, W.S., Ussler, W., Olsen, K., Rodriguez, N.M., Wehner, H., in *Proc. Ocean Drilling Program, Scientific Results*, **164**, 67 (1996). With permission.)

In addition at Site 994 recovered cores were very gassy, and recovery below 190 mbsf was poor, as a result of vigorous degassing. The average geothermal gradient ( $35.4^{\circ}\text{C}/\text{km}$ ) intersected the hydrate stability phase line about 50 m below the other hydrate indicators. The reason for this discrepancy is unclear, but it should be noted that a similar discrepancy was noted at the Cascadia Margin in ODP Leg 146 (Hovland et al., 1995). Some possible reasons for this discrepancy are considered after the Site 997 discussion.

Core temperatures upon recovery on the catwalk were variable. Small areas of low temperatures ( $6\text{--}8^{\circ}\text{C}$  versus other parts of the core at  $11\text{--}13^{\circ}\text{C}$ ) were interpreted as indicating areas where endothermic hydrate decomposition decreased the core temperature. Cores evolved large amounts of gas, which was considered responsible for low core recovery—from a norm of  $>80\%$  to 20–60% in the hydrate region.

The estimated amount of hydrate by chloride anomalies had a mean value of  $1.3 \pm 1.8$  vol%, ranging to as high as 7%; however, these values may be minimum because the baseline may have been lower than the actual interstitial water chlorinities. The logging tools indicate the presence of as much as 2.9 vol% hydrate, ranging as high as 9.5%. Recovered pieces of hydrate were concentrated in zones from 2 to 10 cm thick. However, most of the hydrate was disseminated

as fine-grained crystals in clay and claystone pore spaces. All inferred hydrates occurred well above the phase-equilibria base of the hydrate zone.

### 7.8.1.2 Site 995

Although a strong BSR occurred at  $440 \pm 10$  mbsf, at Site 995 samples of hydrate were not recovered. Instead a suite of chemical, thermal, and log indicators suggested that hydrate was present in a significant section, but hydrate was so fine-grained that it had dissociated prior to inspection. The sediment physical properties at Site 995 were coincident with those at Site 994, without differences that could account for changes in the strength of the BSR between the two sites.

The logs at Site 995 indicate a material of increased resistivity and acoustic velocity, but similar density. The 450 mbsf boundary depth detected by logs coincides with the BSR. A zone of anomalously low chloride values (as low as 466 mM between 195 and 440 mbsf) was coincident with that found at Site 994, indicating that sites 3 km apart possessed similar vertical distributions of hydrate.

Low chlorinity zones were coincident with zones of anomalously low recovered core temperatures on the ship catwalk. For example, while some of the background core temperatures were at 10–12°C, cores in suspected hydrate regions had temperatures as low as 1°C, perhaps caused by endothermic dissociation of hydrate. The extrapolated geothermal gradient of 33.5°C/km yielded a temperature of 18.3°C at the BSR (440 mbsf), well within the temperature stability field of methane hydrate.

The concentrations of gases in the core voids were measured, with C<sub>1</sub>/C<sub>2</sub> ratios from approximately 1,200 to 39,000 indicating biogenic sources. Concentrations of propane through heptane were usually below 10 ppmv, and the concentration of carbon dioxide varied widely from 0% to 20% of the free gas.

Hydrate inferred at Site 995 existed as fine-grain, pore-filling accumulations that were widely dispersed in host sediments rather than as concentrated nodules large enough to survive the coring/recovery process. Gas voids and expansions were noted in several core samples, and the amount of methane recovered exceeded that expected from methane saturation of the interstitial waters at *in situ* pressures.

Although no hydrate was recovered from Site 995, the interstitial-water chlorinity anomalies, anomalously cold temperature in recovered cores, and log data all indicate that gas hydrates occurred between 1 and 4 vol% in sediments from 195 to 450 mbsf, with some intervals containing as much as 10 vol% hydrate. However, Paull et al. (1998) noted that these are probably minimum values because the baseline chlorinity might be lower than actual *in situ* interstitial water chlorinities.

In Site 995, as in Site 994, there is a discrepancy between the inferred lowest hydrate level (450 mbsf) and the experimentally predicted base of the stability zone (541–577 mbsf). Possible reasons for this discrepancy are discussed after the Site 997 discussion.

### 7.8.1.3 Site 997

Site 997 was drilled at the crest of the Blake-Bahama Ridge (where the strongest BSR occurs) at 450 mbsf. One large solid piece of gas hydrate was recovered from approximately 331 mbsf at a suspected small fault plane. However, the presence of more disseminated hydrates was inferred over a zone from approximately 180 to 450 mbsf. It was indicated that gas hydrate development may be extensive at this location, possibly acting as a means of sealing with permeability and porosity reduction.

Hydrate was inferred by low temperature observations, interstitial-water low chloride values, and velocity and resistivity logs. Most of the indirect indicators were very similar to those in the earlier Sites 994 and 995. Increases in resistivity (by 0.2  $\Omega\text{m}$ ) and acoustic velocity (by 0.2 km/s) were marked in the hydrate region. In some cases, the temperature ( $-2.1^\circ\text{C}$ ) was less than the ice point due to endothermic hydrate dissociation.

The hydrate produced gas of 98.43%  $\text{CH}_4$  and 1.57%  $\text{CO}_2$ . Ethane and propane were at 196 and 3.8 ppmv, respectively, and the  $\text{C}_1/\text{C}_2$  ratio (4936) was between the ratios of gas in the headspace (1880) and free gas (6748). All above indicators suggested the gas was biogenic. However, microscopically visible oil occurred from approximately 500–620 mbsf, which suggested migration of some oil and gas, when coupled with the occurrence of higher molecular weight hydrocarbons.

Similar to Sites 994 and 995, six indicators of hydrate were present: (1) large gas exsolution from cores, (2) high methane sediment concentration, (3) BSRs, (4) low interstitial-water chlorinity, (5) low core temperatures (although IR technology was introduced just after this hydrate leg), and (6) P-wave velocity logs and resistivity logs. As in Sites 994 and 995, there was a discrepancy between the indicated base of the inferred hydrate zone (452 mbsf) and the phase-equilibria stability zone (491 to 524 mbsf).

The estimated volume of hydrate via chlorinity had a mean value of  $2.4 \pm 2.7$  vol% ranging as high as 13.6 vol%; again these are minimum values, perhaps caused by a low baseline. Logging tools indicated that hydrate occupied approximately 4 vol% of bulk sediments, ranging as high as approximately 11 vol%.

### 7.8.1.4 Common features

At all three sites, the six indirect indicators were found as listed in the Site 997 discussion. The similarity of the indicators in the three sites is exemplified by the chlorinity anomalies in the hydrate regions of [Figure 7.22b](#). There is a minimum of approximately 1.4 vol%, 1.7% and 2.1% gas hydrate at Sites 994, 995, and 997, respectively assuming a low chlorinity baseline, and a sediment porosity of 50%. The amount of gas hydrate appears to increase from the ridge flank (Site 994) to the ridge crest (Site 997) with various indicators shown in [Table 7.11](#).

At all three sites many direct and indirect evidences indicated the base of the hydrate to be at  $450 \pm 10$  mbsf. However, there was a discrepancy between hydrate signals and the phase boundary. The temperature gradient indicated

**TABLE 7.11**  
**Fraction of Bulk Sediment as Hydrates at**  
**Leg 164 Sites**

Detection means	Bulk hydrate volume
Chlorinity	1–2% (minimum) as high as 12%
Log suite	8%
Acoustic VSP	6–7%

that the boundary should have been significantly lower (at 490–570 m) than observed.

Paull et al. (1998) cited four possible reasons for the above discrepancy:

1. The inferred base is a fossil depth reflecting conditions during a previous sea level stand or bottom water temperature regime.
2. Experimental ( $P$ – $T$ ) data do not adequately characterize hydrates, particularly in fine-grained sediments. Clennell et al. (1999) used surface effects to explain this discrepancy. Inhibition by localized salt could also explain this discrepancy.
3. Gas hydrate existed below  $450 \pm 10$  mbsf, but was undetected.
4. The hydrate depth is limited by the gas supply as suggested by Xu and Ruppel (1999).

In all samples there was a large (10 vol%) amount of gas below the hydrates and as much as 50% water, so three phases were present in all cases. However, most of the hydrates were recovered in disseminated form—that is, they had decomposed by the time the core barrel reached the deck. In two instances (Sites 994 and 997) samples of hydrates were recovered.

### 7.8.2 Case Study 2: Hydrate Ridge (Hydrate Assessment)

Hydrate Ridge is one of the best-studied convergent ocean margin with intense fluid flow and large-scale gas hydrate deposits. Due to the significant amount of hydrate found both at the seafloor surface and in deeper sediments, this site has provided an effective ocean laboratory to study hydrates in a marine environment. The following four research groups have performed extensive studies of the hydrate environment at Hydrate Ridge:

1. Geomar studied the habitat of hydrates and chemosynthetic communities for over two decades (see the review by Boetius and Suess, 2004).
2. The ODP devoted ODP Leg 204 to the study of hydrates (Milkov et al., 2003; Torres et al., 2004; Tréhu et al., 2004a,b; Claypool et al., 2006).

IODP Expedition 311 was also at this site, but articles are just being published as this book goes to press.

3. Scripps Institute of Oceanography and others laid the groundwork for Leg 204 through hydrate work in Sites 889 and 892 on ODP Leg 146 (Kastner et al., 1995, ODP Leg 146 Scientific Party). Controlled source electromagnetics at Hydrate Ridge was done by a different Scripps group (Weitemeyer et al., 2006).
4. The MBARI (Brewer, Paull, Peltzer, Ussler, and colleagues) have pioneered subsea science using remote operated vehicles (ROVs)—particularly the use of spectroscopic equipment to quantify hydrate measurements, especially with Raman subsea deployment at southern Hydrate Ridge (Hester et al., 2005), to supplement the NMR spectroscopy with MBARI (Kleinberg et al., 2003) in Monterey Canyon waters.

From the above studies has come a composite picture of hydrate formation at Hydrate Ridge, with particular emphasis on the southern summit. While a composite picture is attempted in the following few pages, the interested reader will turn to the above review articles for a detailed expansion.

Hydrate Ridge is located 80 km west of Newport, Oregon on the second accretionary ridge of the Cascadia subduction of the Juan de Fuca Plate and the North American Plate. The northern summit is in 600 m of water depth with an area of 0.4 km<sup>2</sup>, while the southern peak is in 800 m of water with an area of 0.8 km<sup>2</sup>.

The methane from hydrates has a stable isotopic signature of  $-65\text{\textperthousand}$   $\delta^{13}\text{C}$ , showing its biogenic origin, although infrequently there is as much as 10% contribution from thermogenic gas (Claypool et al., 2006). Boetius and Suess (2004) estimated the amount of methane in hydrates at North and South Hydrate Ridge at 0.5 and  $1.7 \times 10^{10}$  mol CH<sub>4</sub> respectively. They assumed that (1) 50% of summit has hydrates in 10% of sediment volume down to the bottom of the stability zone and (2) methane hydrates occupy 50% of pore space, to obtain an average hydrate content of 2.5% of the pore volume in the GHSZ. Tréhu et al. (2004b) estimated that the average hydrate content is less than 2% of pore volume within the GHSZ. However, Tréhu comments (Personal Communication, January 8, 2006) that there is a large amount of heterogeneity, so that a single average number can be misleading.

In this summary, we will concentrate on the southern Hydrate Ridge summit, which appears to be the most interesting due to the higher concentrations of hydrates. In Leg 204 (Tréhu et al., 2004b) southern Hydrate Ridge sites were chosen to complement ODP Site 892 on Leg 146, where there was an anomalously shallow BSR (Kastner et al., 1995). At the southern summit, there are three strong reflections, resulting from gas-charged, coarse-grained sediments. There are three groupings of nine Leg 204 sites drilled on southern Hydrate Ridge as shown in Figure 7.23:

1. Sites 1244–1247 characterize the flank
2. Sites 1248–1250 characterize the ridge crest with active venting

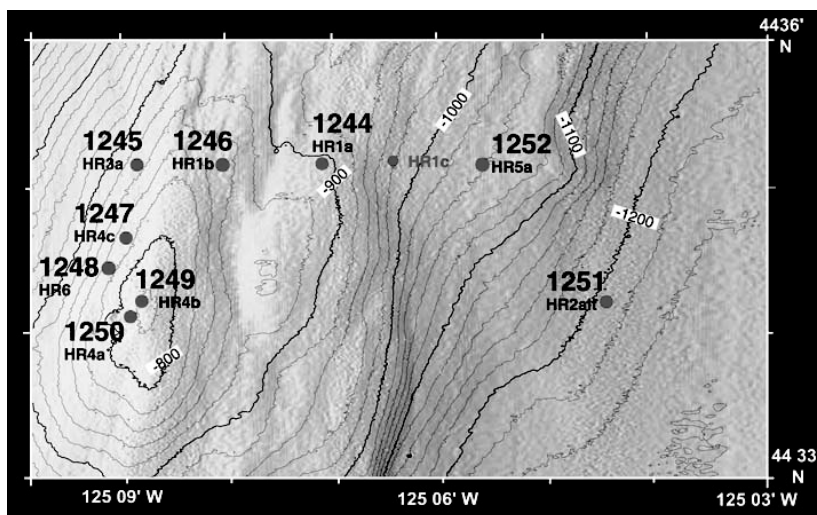


**FIGURE 7.23** The location of the Leg 204 drilling sites on southern Hydrate Ridge. Note that sites 1249 and 1250 are at the summit. (From Tréhu, A.M., Long, P.E., Torres, M.E., Bohrmann, G., Rack, F.R., Collett, T.S., Goldberg, D.S., et al., *Earth Planet. Sci. Lett.*, **222**, 845 (2004b). With permission from Elsevier.)

3. Sites 1251 and 1252 deal with the slope basin to the east with rapid sedimentation

At the southern Hydrate Ridge summit, hydrate is deposited in two regions: (1) the first region with hydrates in 30–40% of the pore volume, extends from the surface to approximately 25 m below the seafloor and (2) a deeper region with much less hydrate (averaging less than 2–4% of pore volume) beginning approximately 25 mbsf to the BSR at a depth of approximately 115 mbsf.

Both Tréhu et al. (2004b) and Boetius and Suess (2004) suggest that emission of methane bubbles is much more effective at producing the observed phenomena than flow of dissolved methane through sediment–water interface. Most of the dissolved methane is consumed in the sediments by methanotropic communities. Torres et al. show that a free gas phase is required to produce the high hydrate concentration and high salinities observed at shallow depth near the summit. Tréhu (2004a) provides a mechanism to feed gas at saturation, that overtakes the amount of water locally available to form hydrates. Milkov and Xu (2005) have suggested alternative, salinity-based models for free gas migration. Torres et al. (2004) provide a rebuttal to Milkov and Xu’s critique, but the details of how gas gets from the base of the stability zone to the seafloor remain poorly constrained.

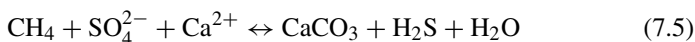
#### 7.8.2.1 Near surface hydrates: the chemosynthetic community and chemoherms

As a case study of rapid gas fluxes with hydrate formation, the work of Geomar [reviewed by Boetius and Suess (2004)] has provided an understanding of the

intertwined life of the chemosynthetic communities and gas hydrates. Over two decades this work has effectively provided insight into the nature of cold gas seeps, with surface microorganisms effectively acting as markers of hydrates.

The study of Hydrate Ridge by multiple teams of scientists, both at Geomar, and in ODP Legs 146 and 204 (Torres et al., 2004; Tréhu et al., 2004b), provide an illustration that has analogs in other parts of the world, for example, the Gulf of Mexico, intensively studied by Sassen and MacDonald (1994, 1997a,b) and Sassen et al. (2004). At Hydrate Ridge, cold seeps have enabled determination of the reaction sequence of anaerobic oxidation of methane (AOM), with visual determination of hydrates near the seafloor surface.

It is well known that the AOM process involves a transfer of electrons from methane to sulfate, producing bicarbonate and sulfide in equimolar amounts, which in-turn react with hydronium and calcium ions in the water, to produce the overall reaction:



The first product ( $\text{CaCO}_3$ ) of reaction (7.5) produces chemoherms, or chimney-like carbonate structures, up to 40 m high on the seafloor. However, understanding the interactive role of  $\text{H}_2\text{S}$ , the second reaction product, with the microorganisms mediating AOM was more recent, awaiting the joint participation of microbiologists, geochemists, and geologists studying cold seeps and gas hydrate deposits.

In Figure 7.24, structure I hydrates underlie bacterial mats of giant sulfide-oxidizing bacteria (*Beggiatoa*) and fields of *Calyptogena* clams that have sulfide oxidizing bacteria in their gills. Both the sulfide concentration and rate of sulfide flux determines the species present and the location close to the hydrate deposits. Distribution is mainly related to sulfide fluxes regulated by the supply of methane (electron donor) from below and sulfate (electron acceptor) from above, for the AOM, mediated by consortia of methanotrophic archaea, and sulfate reducing bacteria.

Sahling et al. (2002) indicate that the diffusive sulfide fluxes limit the growths that are classified into:

1. *Beggiatoa* at the mudline with a sulfide flux of  $23 \pm 13 \text{ mol/m}^2\text{yr}$
2. *Calyptogena* clams at the mudline with a sulfide flux of  $6.6 \pm 2.4 \text{ mol/m}^2\text{yr}$
3. *Acharax* at 5 to  $-30 \text{ cm}$  below seafloor, with a sulfide flux of  $0.05 \pm 0.05 \text{ mol/m}^2\text{yr}$

These different settings have fluid flow rates varying over four orders of magnitude.

Boetius and Suess (2004) note that clams, mussels, and tubeworms have distinct adaptations to obtain oxygen from the seawater and sulfide from the sediments. If fluid flow is reduced so that sulfide does not reach the seafloor, these communities are replaced by specially adapted faunas, such as *Acharax*, that are

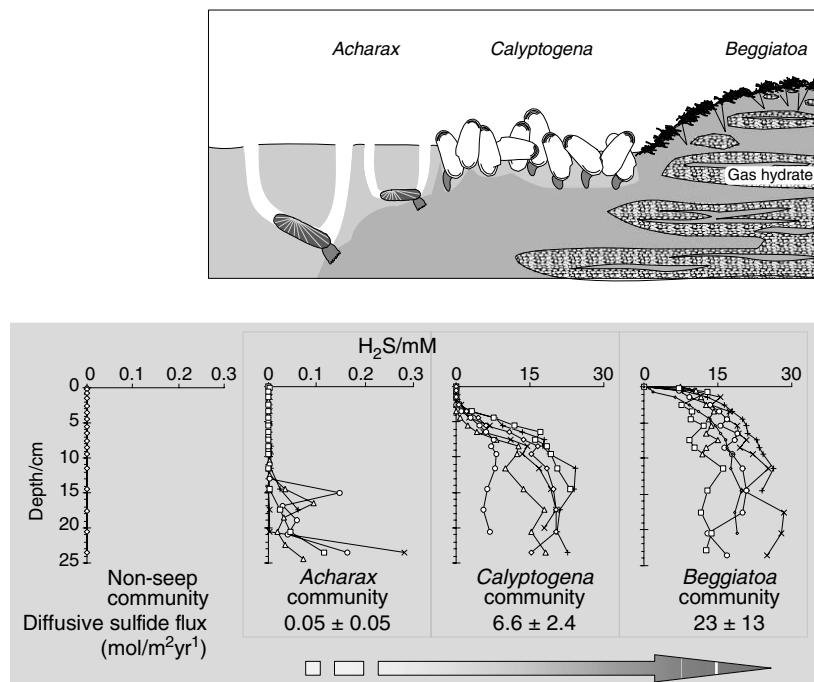


**FIGURE 7.24** Chemo-synthetic species above their  $\text{H}_2\text{S}$  concentrations and fluxes. Note that *Beggiaatoa* and *Calyptogena* overlie the hydrate deposits. (From Sahling, H., et al., *Marine Ecol. Prog. Ser.*, **231**, 121 (2002). With permission.)

able to burrow more deeply into the sediments to obtain sulfide. Members of the deep-sea community invade seeps to use the seep fauna, or seep structures as a habitat, as in the case of ice worms (Fisher et al., 2000).

The biologically active surface (to 10 cm depth) has a methane flux that varies between 1 and 100  $\text{mmC}/\text{m}^2$  per day. The hydrate results from free gas and gas dissolved in water. Two types of hydrate fabric result: (1) porous hydrates, from accumulation of bubbles of free gas and (2) massive hydrates, with twice the density of porous hydrates (0.9 g/L versus 0.4 g/L). In the recent Raman spectroscopy, southern Hydrate Ridge experiments by the MBARI (Hester et al., 2005), the near-surface hydrate Raman spectra contained significant amounts of free gas as well as hydrates, with only a trace of hydrogen sulfide in the methane gas.

Another way of considering the hydrates at Hydrate Ridge relates to the SMI concept of Paull, indicated in Section 7.2.2. At Hydrate Ridge, hydrates near the surface (up to a few meters) are related to rapid methane flux from below, perhaps with contributions from dissociated hydrates. While these hydrates relate to the SMI, as indicated in reaction (7.5), the methane comes from below, and the

near-surface methane hydrate concentration is not indicative of the entire Hydrate Ridge reserve.

Below the SMI to a submudline level ten times the depth of the SMI, hydrates are not found because the methane concentration is too low to produce hydrates. It should be noted that this Rule of 10 is perhaps related to methane solubility limit in the liquid phase. Even though the deeper hydrate layers have a lesser concentration, due to the larger volume, the deeper hydrate amounts represent the largest in the reservoir, and cause the total reservoir concentration to be estimated at 2.5% of pore volume.

### 7.8.2.2 Deeper hydrates at Southern Hydrate Ridge: characterization and assessment

Even with the high concentrations of the near-surface hydrates, the deeper (>20 m) hydrate deposits contain most of the gas in the hydrated reservoir. This deeper hydrated gas is mostly biogenic, with anecdotal incidents of 10% thermogenic gas.

Figure 7.25 shows the position of five Leg 204 drill sites. The off-summit Site 1245 intersects an unusual horizon marked "A" extending from about 1600 to 1400 m (although not shown here, this fault does extend to the summit). This silty sand horizon is important because its porosity and permeability allows for rapid

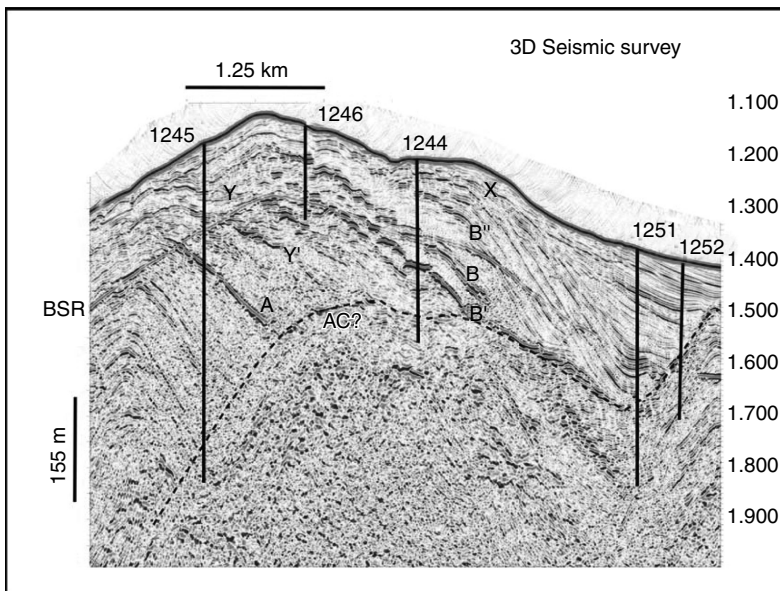


**FIGURE 7.25** The position of five off-summit drill sites at southern Hydrate Ridge. Note the under-thrust sediments of the accretionary complex labeled AC. The reflections labeled A, B, and B' result from gas-charged, coarse-grained sediments. (From Tréhu, A.M., et al., *Earth Planet Sci. Lett.*, **222**, 845 (2004b). With permission from Elsevier.)

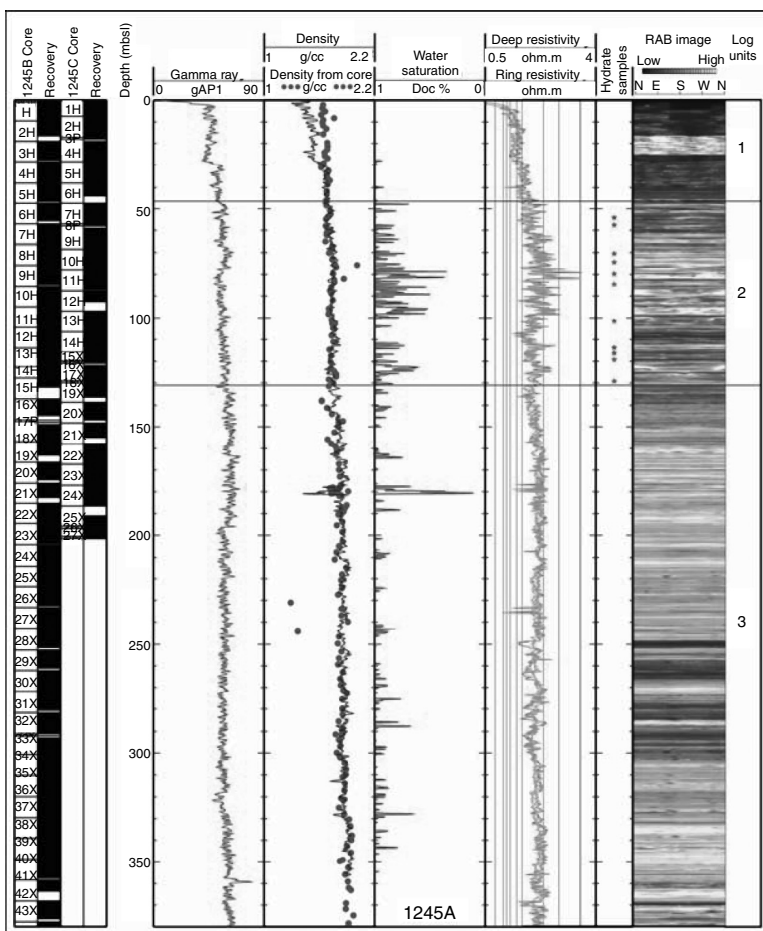


**FIGURE 7.26** (See color insert following page 390.) Site 1245A southern Hydrate Ridge Flank logs (gamma ray, density, Resistivity at Bit, and Archie water saturation). (T.S. Collett, Personal Communication, November 18, 2005, Leg 204, Scientific Party, 2005)

migration of free gas and methane-saturated fluids from depth. Horizon A acts as a restricted pipeline to transport lighter fluids from depth to the summit.

Sediment stratigraphy controls the hydrate distribution at Hydrate Ridge. The methane-rich migration pathway of Horizon A provides enriched hydrate formation relative to other sediments. In Figure 7.26, the remote sensing logs (gamma ray, density, RAB, and Archie water saturation) are most sensitive to hydrates.

### 7.8.2.3 Logs and remote sensing

In the well logs of Figure 7.26 for Site 1245A note the log responses (e.g., the high water content indicated by the resistivity) indicative of hydrates between the two

black horizontal lines where the hydrate saturation ranges between 10% and 80% of pore volume. The high water content means low hydrate saturation. Hydrate saturation is typically around 10–15%. The maximum concentration is 60%, and then only at two spikes. Around 70 m a fine-clay porosity restricts the hydrate saturation to 10–20% of pore volume, while further down at around 175 m, the more porous/permeable silt (associated with Horizon A in Figure 7.25) provides for hydrate occupation of up to 60–80% of pore volume.

The subtleties of the well logs for hydrate detection at Site 1245A for the southern Hydrate Ridge flank can be contrasted with the more prominent hydrate indications at Hydrate Ridge crest, through the well logs data of Figure 7.27. In the figure, note particularly the region between 20 and 50 mbsf, where three logs

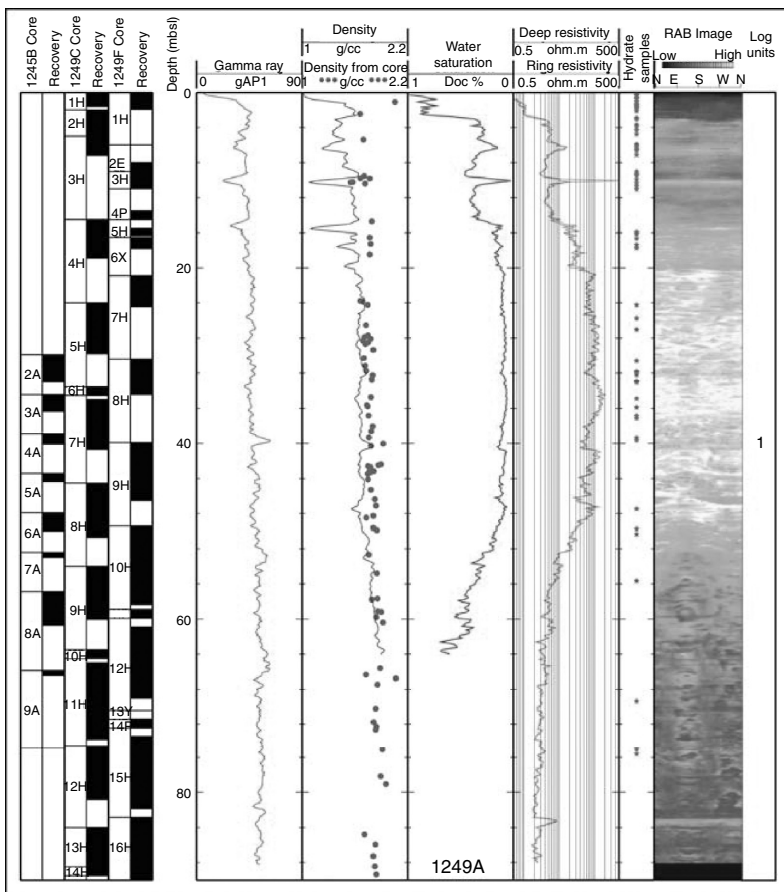


**FIGURE 7.27** (See color insert following page 390.) Site 1249A southern Hydrate Ridge crest remote sensing logs (gamma ray, density, RAB, and Archie water saturation). (T.S. Collett, Personal Communication, November 18, 2005, Leg 204 Scientific Party, 2005.)

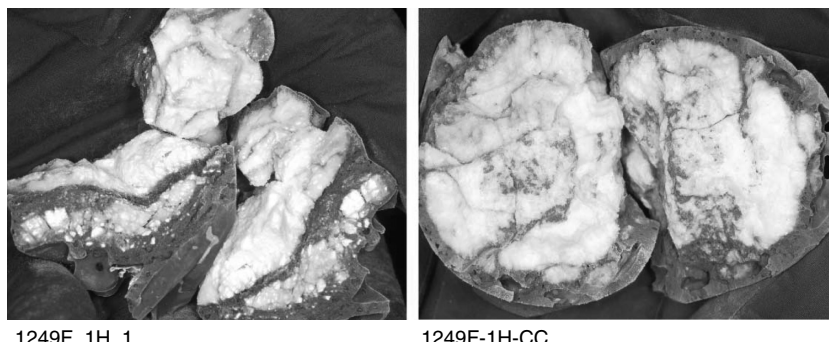


**FIGURE 7.28** Site 1249F southern Hydrate Ridge crest recovered hydrate cores. (T.S. Collett, Personal Communication, November 18, 2005, Leg 204 Scientific Party, 2005.)

(water saturation, resistivity, and the lighter sections of RAB) provide a combined remote sensing image of hydrate occurrence. Visual evidence of massive recovered hydrates at the same Site 1249F, are shown in Figure 7.28 confirming the log.

In combination, these logs give further evidence of gas migration from the ridge flank (in Figure 7.26 of Site 1245A, at 70 and 175 mbsf) to the ridge summit (in Figure 7.27 of Site 1249A at 20–50 mbsf).

#### 7.8.2.4 Coring and direct evidence

Tréhu et al. (2004b) compared hydrate estimates from RAB such as those shown in Figures 7.26 and 7.27, with more direct hydrate evidence from cores of the following three types:

1. Infrared (IR) sensing of the cores gave reduced temperatures ( $\Delta T$ ) as a result of endothermic heats of hydrate dissociation. These temperature indications were taken as linearly related to the amounts of hydrate present.
2. Hydrated-methane evolution from the pressure core sampler (PCS) was far beyond the normal gas solubility in the core waters, and provided an estimate of hydrate amounts.
3. Reduction in chlorinity resulted from hydrate dissociation upon retrieval, and the amount of the reduction can be used to estimate hydrate amount (Torres et al., 2004). It should be noted that an accurate method was determined for the chlorinity baseline decrease, due to the deposit of ions within the shale, and the expulsion of fresh water from the shale, due to overpressure.

Tréhu et al. (2004b) distinguish between the GHSZ defined as the region from the BSR to the mudline, and the GHOZ, a thinner zone, defined as the region

**TABLE 7.12****Hydrate Amount Estimates (% Pore Volume) Via Four Techniques**

Estimated method→ Site/BSR(m)↓	RAB					Overall GHOZ/GHSZ
	ΔT GHOZ/GHSZ	PCS GHOZ/GHSZ	Chlorinity GHOZ/GHSZ	GHOZ/GHSZ Hole A at site		
1245B/134	3.8/1.9	NA	3.0/2.0	3.1/1.9	2.74/1.74	
1247B/130	1.9/1.5	2.6/1.3	1.5/0.8	2.0/1.6	2.74/1.74	
1250C/114	2.6	0.7	4.3	26/5	NA	
1251B/200	9.4	1.6/1.2	0.5/0.5	1.2/1.0	2.48/2.00	

from the BSR and the shallowest occurrence of hydrate based on one of the three indicators above.

Table 7.12 compares the hydrate amounts (as percent of pore space) estimated by the above three techniques, to that from the RAB for the GHOZ and GHSZ. Below the surficial hydrates mentioned earlier, for a few tens of meters below the mudline, the methane concentration is not sufficient for hydrate formation. One possible reason for the discrepancy in the values of GHOZ and GHSZ is “Paull’s Rule of 10,” which relates hydrate depth to ten times the SMI, as discussed in Section 7.2.2. As mentioned this Rule of 10 may be related to methane solubility.

In the formation model of the above hydrate concentrations, Torres et al. (2004) indicate that the pressure of hydrate crystallization can exceed the overburden pressure. This can occur at shallow subseafloor depth, to cause massive hydrate deposits such as those shown in Figure 7.28, if hydrates do not promptly cement the grains. This finding is similar to that observed by Sassen and coworkers in the Gulf of Mexico (Personal Communication, November 10, 2005). Torres and coworkers also suggest that methane dissolved in water alone is insufficient to cause the noted hydrate concentrations—there must be additional free gas present.

Linke et al. (2005) provide macroscopic evidence of free gas in recovered cores, but it might be argued that such gas could evolve from dissociated hydrates. However, in recent MBARI ROV Raman spectroscopy deployment at the crest of southern Hydrate Ridge, Hester et al. (2005) presents spectroscopic evidence for free gas associated with hydrates at the seafloor. An earlier paper by Bohrmann et al. (2002) suggested hydrates act as an enclosure to free gas, as does the observations of bubble streaming from the seafloor (Heeschen et al., 2003). This “Bubble-wrap” mechanism finds an analogy in hydrate formation in pipelines, shown in Chapter 8, and some cross-technology applications.

### 7.8.2.5 The lessons of Hydrate Ridge

Because this site is one of the most extensively studied in the world, the lessons from it are important to summarize for future seafloor hydrate exploration:

1. The cold seeps of methane migration along the geologic faults or permeable stratigraphic horizons provide concentrations in excess of

methane solubility, resulting in two types of hydrate communities:

- (a) Surface hydrates have an evolved synergism between hydrates, chemoherms, and chemosynthetic communities. These communities provide visual hydrate prospecting tools for high (30–40% of pore volume) surface hydrate amounts. In these communities the free gas affects hydrate fabric and morphology.
  - (b) Deeper hydrates extend from 20 to 200 mbsf, in which the pressure of crystallization may exceed that on the seafloor to provide massive amounts of hydrates. The concentration of these deeper hydrates is less than 2% of pore volume, but the overall hydrate amounts in the deep deposits far exceed the surficial hydrates.
2. Well logs from Hydrate Ridge indicated acceptably consistent estimates of hydrate occurrence, particularly water saturation, and RAB. Hydrate concentration data from logging tools have been confirmed and quantified by more direct core methods of IR sensing of temperature, gas evolution, and chlorinity decrease.
  3. There are deeper zones of stratigraphically controlled hydrates that can contain up to 20% of pore space, when averaged over zones 10 m thick.
  4. The cold seeps at Hydrate Ridge, cause this site to be labeled a “sweet spot” of high hydrate concentration, relative to others such as the Blake-Bahama Ridge (ODP Leg 164) example that may be more representative of hydrate deposits in the world. Tréhu et al. (2004a) estimate  $1.5\text{--}2 \times 10^8 \text{ m}^3(\text{STP})$  of methane for the summit deposit, on the basis of the drilling and seismic data, which also define the limits of the deposit. Tréhu (Personal Communication, January 8, 2006) indicated that this amount is comparable to a small gas field, not economical unless facilities are already in place.

### 7.8.3 Case Study 3: Messoyakha (Hydrate Production in Permafrost)

The Messoyakha gas hydrate field is the first exemplar for gas production from hydrate in the permafrost. Hydrates were produced from this field semicontinuously for over 17 years. The field is located in the northeast of western Siberia, close to the junction of the Messoyakha River and the Yenisei River, 250 km west of the town of Norilsk, as shown in [Figure 7.29](#).

Figure 7.30 provides a cross section of the field, showing the hydrate deposit overlying the free gas zone. The depth–temperature plot of Figure 7.31 from Sheshukov (1972) shows the hydrate layer to extend to the intersection of the 281 K geotherm, later determined to be closer to 283 K by Makogon (1988). The gas in the hydrate zone is both in the free and in the hydrated state. Makogon (1988) provided summary information regarding the properties of the field, as tabulated in [Table 7.13](#). Krason and Finley (1992) provided an additional summary.

A suite of well logs from Well Number 136 of the Messoyakha field is presented in [Figure 7.32](#) by Sapir et al. (1973). The Soviet work indicated the need to use a

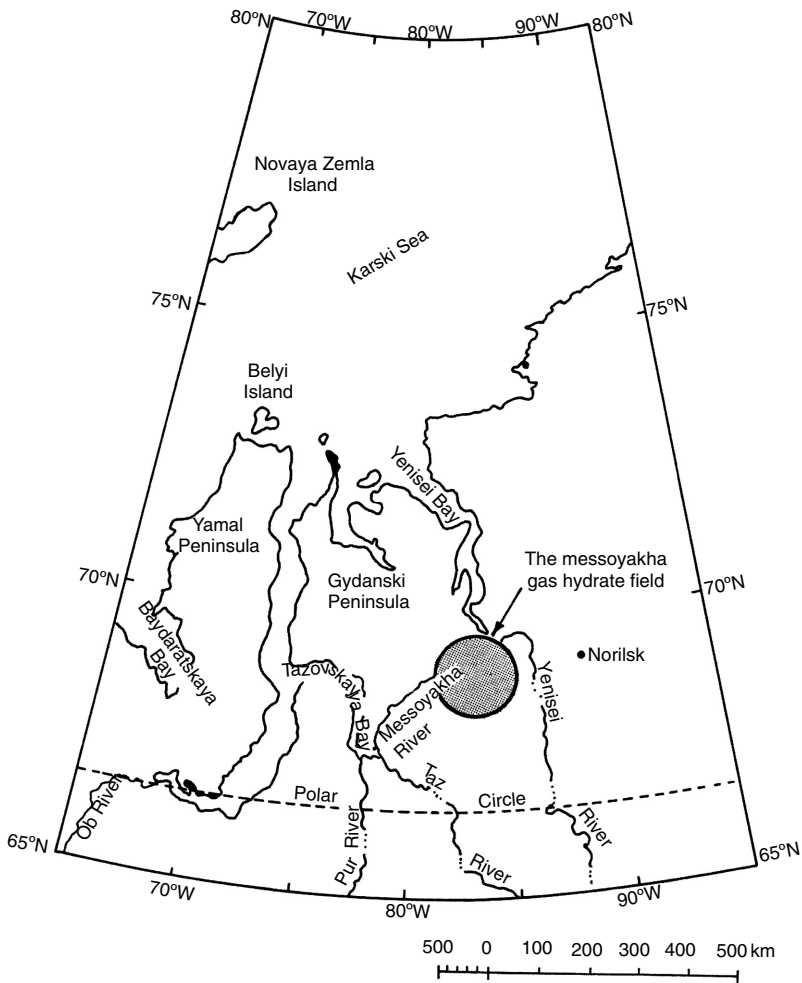


**FIGURE 7.29** Location of Messoyakha gas hydrate field. (Reproduced courtesy of U.S. Dept. of Energy (Krason and Ciesnik, 1985).)

suite of well logs rather than a single log to indicate hydrates, similar to the later findings in the Western hemisphere as previously discussed in Section 7.5.

The Messoyakha field has been produced through both inhibitor injection and depressurization, as well as combinations of the two. The inhibitor injection tests, presented in Table 7.14 from the combined results by Sumetz (1974) and Makogon (1981, p. 174), frequently gave dramatic short-term increases in production rates, due to hydrate dissociation in the vicinity of each injected well bore. In the table, methanol and mixtures of methanol and calcium chloride were injected under pressure, using a “cement aggregate.” For long-term dissociation of hydrates, depressurization was used.

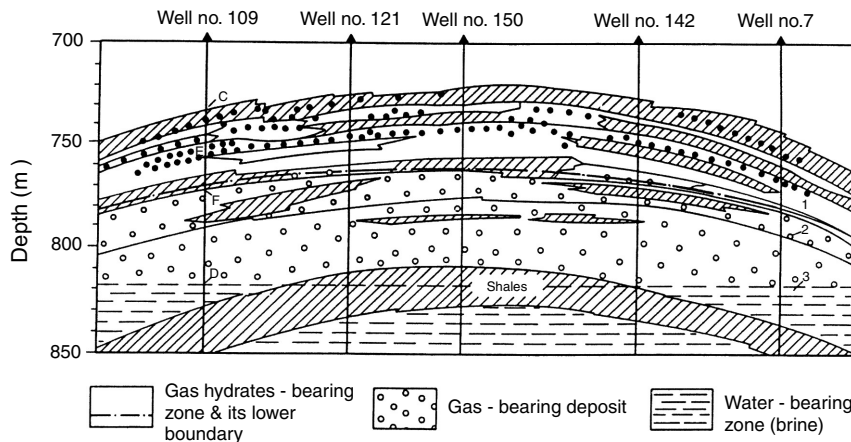


**FIGURE 7.30** Cross section of Messoyakha field with hydrates overlying gas. (Reproduced from Makogon, Y.F., "Natural Gas Hydrates: The State of Study in the USSR and Perspectives for Its Use," paper presented at the *Third Chemical Congress of North America*, Toronto, Canada, June 5–10 (1988). With Permission.)

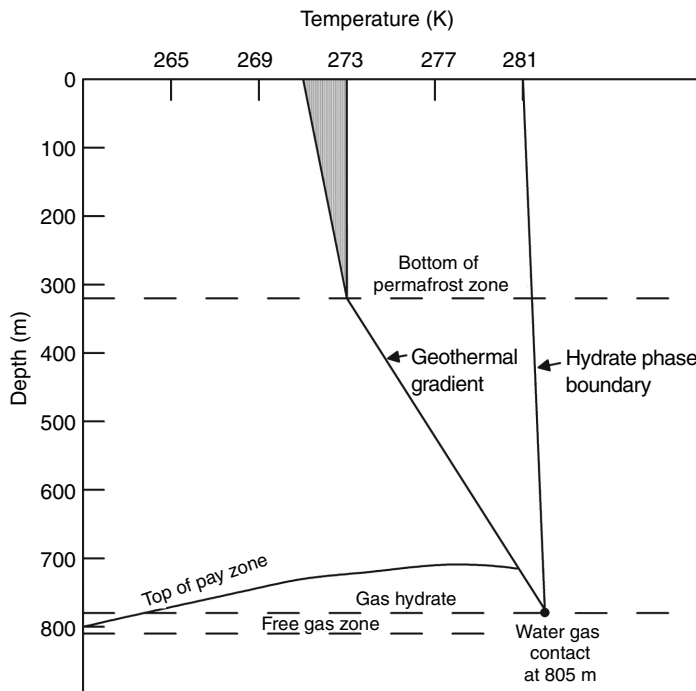


**FIGURE 7.31** Gas hydrate stability envelope at Messoyakha. (Reproduced courtesy of U.S. Dept. of Energy (Sheshukov, 1972).)

**TABLE 7.13**  
**Properties of Messoyakha Gas Hydrate Field**

Area of the pay zone	12.5 km
Thickness of the pay zone	84 m
Open porosity	16–38% (average 25%)
Residual water saturation	29–50% (average 40%)
Initial reservoir pressure	7.8 MPa
Reservoir temperature range	281–285 K
Reservoir water salinity	<1.5 wt%
Water-free gas composition	98.6% CH <sub>4</sub>
	0.1% C <sub>2</sub> H <sub>6</sub>
	0.1% C <sub>3</sub> H <sub>8</sub> <sup>+</sup>
	0.5% CO <sub>2</sub>
	0.7% N <sub>2</sub>

*Source:* After Makogon, Y.F., "Natural Gas Hydrates: The State of Study in the USSR and Perspectives for Its Use," paper presented at the *Third Chemical Congress of North America*, Toronto, Canada, 1988. With permission.

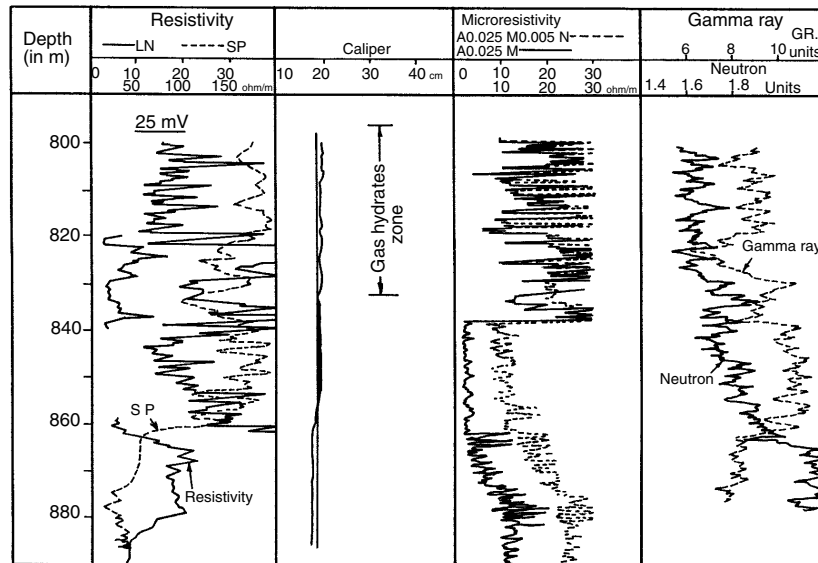


**FIGURE 7.32** Well Logs from Well Number 136 at Messoyakha. (Reproduced Courtesy of U.S. Dept. of Energy (Sapir, et al., 1973).)

**TABLE 7.14**  
**Test Results from Inhibitor Injection in the Messoyakha Field**

Well no.	Type of inhibitor	Volume of inhibitor m <sup>3</sup>	Gas flow before treatment	Gas flow after treatment
			1000 m <sup>3</sup> /day	1000 m <sup>3</sup> /day
2	96 wt% methanol	3.5	Expected results not achieved	
129	96 wt% methanol	3.5	30	150
131	96 wt% methanol	3.0	175	275
133	Methanol	Unknown	25	50
			50	50
			100	150
			150	200
138	Mixture 10% MeOH 90 vol% of 30 wt% CaCl <sub>2</sub>	4.8	200	300
139	Mix of Well 138	2.8		
141	Mix of Well 138	4.8	150	200
142	Methanol	Unknown	5	50
			10	100
			25	150
			50	200

Source: From Sumetz, V.I., *Gaz. Prom.*, 2, 24, 1974 and Makogon, Y.F., *Hydrates of Natural Gas*, Moscow, Nedra, Izdatelstro, (1974 in Russian) Transl. J. Cieslesicz, PennWell Books, Tulsa, Oklahoma, 237pp., 1981. With permission.

Makogon (1988) indicates that of all the complex studies obtained during the 19 years of the production life of the Messoyakha field, the most informative results came from an analysis of the reservoir pressure change as a function of the gas withdrawal rate. A diagram showing pressure and gas production as a function of time is shown in Figure 7.33, with the accompanying pressure–temperature relationship in Figures 7.34a,b. While Figure 7.34a may represent the measured pressure–temperature values (Makogon, 1988) far away from the hydrate, Poettmann (Personal Communication, July 20, 1988) suggested that the values in the neighborhood of the hydrate interface are better represented by Figure 7.34b, for reasons given below. The combination of these three figures represents a classic study in slow depressurization, done via the production of the free gas reservoir over a period of years.

In Figure 7.34 the following initial points are used (with C,D,E,F corresponding to letters on Well No. 109 in the reservoir diagram of Figure 7.30): AB = hydrate equilibrium line; C = temperature at the top of the pay zone; D = temperature at a level of gas and water contact; E average gas–hydrate temperature; F = temperature at boundary surface between gas and gas–hydrate reserves; H = beginning dissociation pressure for gas hydrates.

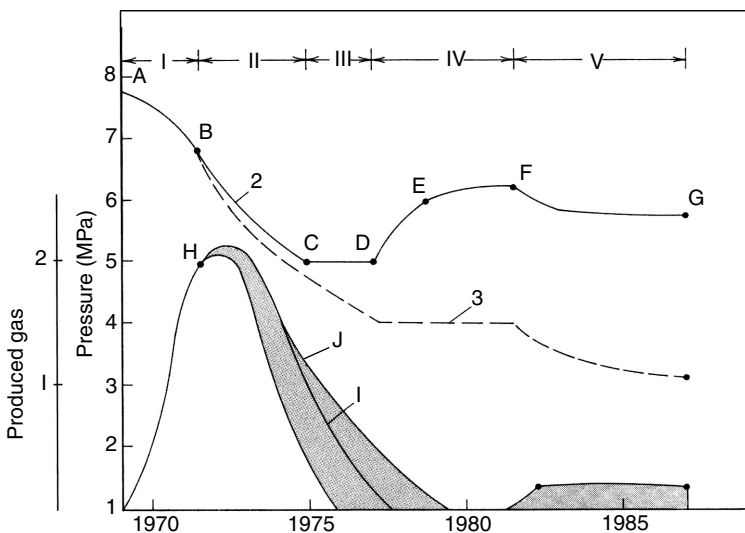


**FIGURE 7.33** Pressure (upper curves) without hydrates (dashed) and with hydrates (solid) as a function of time; Produced gas (lower curves) both with and without hydrates. See text for labels. (Reproduced from Makogon, Y.F., “Natural Gas Hydrates: The State of Study in the USSR and Perspectives for Its Use,” paper presented at the *Third Chemical Congress of North America*, Toronto, Canada, June 5–10 (1988). With Permission.)

As the production of the field was begun from 1969 to mid-1971, the pressure decreased from E to just above the hydrate dissociation point at H in Figures 7.33 and 7.34a,b. During this period, only free gas was produced because the pressure was above the hydrate equilibrium value.

When the pressure reached the hydrate equilibrium value at point H, the hydrates began to dissociate, adding the shaded portion to the gas production curve at the lower half of Figure 7.33. The top half of Figure 7.33 shows the reservoir pressure was maintained at a higher value (solid line 2) than the expected pressure (dashed line 3) due to the addition of gas to the reservoir by the hydrates. After point H in Figure 7.34a, Makogon (1988) indicated that the pressure away from the hydrate decreased below the equilibrium value, with a slight decrease in temperature. The pressure at the hydrate interface in Figure 7.34b, however, should not deviate from the equilibrium line, unless all of the hydrates were dissociated. Consequently, the pressure and temperature at the hydrate interface decreased along the equilibrium curve as the reservoir was depressurized. Between the third and sixth year of the field development there was probably a pressure drop between the hydrate interface, from H to L in Figure 7.34b, and the measured pressure from H to L in Figure 7.34a, due to the flow of gas in porous media.

As the Messoyakha reservoir attained the pressure at point L, the average pressure stabilized for 2 years to point M, indicating that the volume of gas recovered was replenished by the gas liberated from the hydrate. The difference between

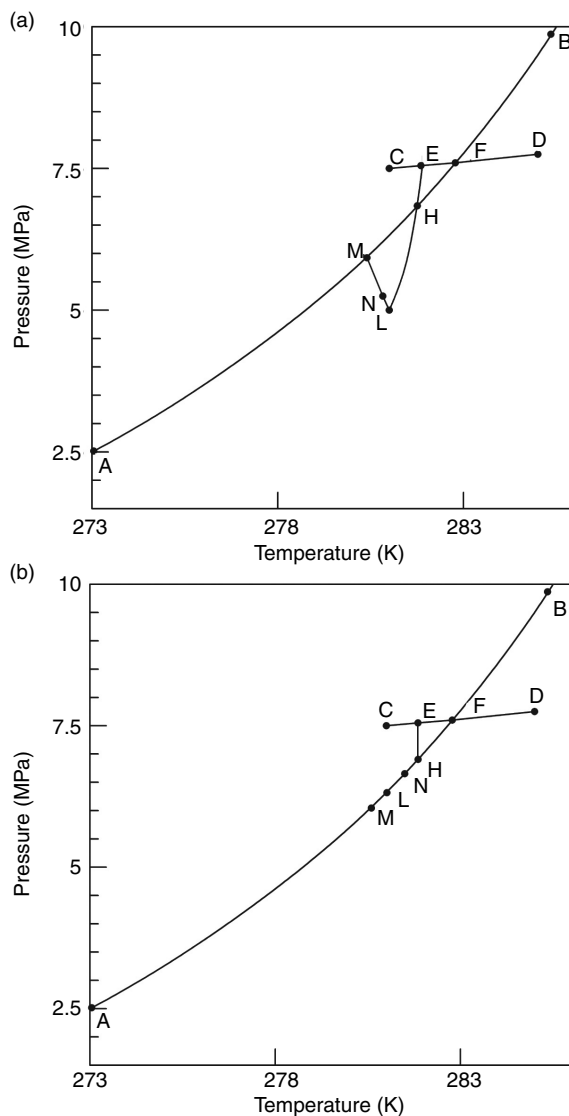


**FIGURE 7.34** Messoyakha pressure and temperature with hydrate production (top) away from hydrate face (Makogon, 1988), (bottom) hypothesized at hydrate face (Poettmann, Personal Communication, July 20, 1988).

curves I and J in Figure 7.33 indicates that the total gas produced (curve I) was slightly less than the gas liberated (curve J) by the hydrates. During this period, from the seventh to the eighth year of the life of the reservoir, the pressure away from the hydrate face in Figure 7.34a rose slightly ( $L \rightarrow M$ ), compensated by a corresponding pressure decrease at the hydrate face in Figure 7.34b.

At point M, the reservoir was shut in, while other higher pressure reservoirs were produced (Makogon, 1988). During that period, the average pressure of the reservoir began to rise from point M to point N in [Figure 7.34b](#). The difference between curves I and J in [Figure 7.33](#) indicates that gas continued to be liberated by the hydrate until the reservoir pressure was uniform in mid-1981. As the average gas pressure approached the equilibrium value, the amount of gas produced decreased exponentially. Makogon indicated that the temperature of the reservoir tended to be restored to its original value, after a period of time. The equilibrium pressure itself rose slightly as the high reservoir heat capacity increased the temperature of the hydrate mass.

Since 1982 there has only been a modest production of the Messoyakha reservoir. The amount of gas withdrawn has been equivalent to the amount of gas liberated from the hydrate. The total amount of gas liberated from hydrates thus far has amounted to 36% of the total gas withdrawn from the field. It is noted further that the position of the gas–water interface did not change over the 17-year period of the production of the field.

#### 7.8.4 Case Study 4: Mallik 2002 (Hydrate Production in Permafrost)

For readers who wish more Mallik 2002 details than the present, a brief overview is referred to the 63-paper compilation in the GSC Bulletin 585 (Dallimore and Collett, 2005) that includes a CD of manuscripts, an interactive-data viewer CD, and expanded charts and maps.

While the Messoyakhan well was an engineering production application from hydrates, the Mallik 2002 well provided the first scientifically documented evidence that gas could be produced from hydrates. It may be suggested that this concept had been shown before at Messoyakha (Makogon, 1988), however, while there is widespread agreement that hydrates did play some part in Messoyakhan production, some authors (e.g., Collett and Ginsburg, 1998) have suggested that a detailed understanding of the role of hydrates in Messoyakhan production is unclear.

Another perspective relating Messoyakha to Mallik 2002 is that applications drive research, as suggested in the preface. That is, the engineering production of hydrates in the Messoyakha field over the decade of the 1970s provided an impetus for further research with scientifically enhanced tests at Mallik 2002, which were not feasible at the time of Messoyakhan production. Consider only three differences of many:

1. At Messoyakha, production from gas hydrates began substantially about 2 years after the initial depressurization of the gas reservoir underlying hydrates, as shown in [Figure 7.33](#). As indicated below, the Mallik 5L-38 site was chosen because the presence of hydrates had been validated there twice before (Mallik L-38 in 1972 and Mallik 2L-38 in 1998). Yet the Mallik site had no BSR because only a few meters of free gas underlay the hydrates, making Messoyakha-like depressurization problematic. However, in any short-term production testing, it is

impractical to wait for 2 years before obtaining results from hydrate dissociation by depressurization

2. Many scientists were involved to document the Mallik effort. In contrast to a relatively small number of engineers at Messoyakha, the Mallik 2002 well had 265 scientists and engineers who participated from six different entities [Japan National Oil Corporation (JNOC), GSC, BP–Chevron–Burlington joint-venture, the International Continental Scientific Drilling Program (ICDP) based at GFZ (GeoForschungsZentrum-Potsdam), the Indian National Gas Hydrate Program (NGHP), and the United States (Department of Energy and United States Geological Survey)].

3. Many modern scientific tools were applied to Mallik that were not available at the time of Messoyakha. For example, well logs had advanced substantially so that it was possible to determine, for example, the porosity, permeability, and hydrate saturation of the sediments at Mallik, which were not available at Messoyakha. In addition, reservoir models for hydrate production could be based upon well-constrained Mallik 2002 production data, such as pressure stimulation tests over constrained well intervals or thermal stimulation tests.

After the differences between the two production sites, it is important to list the two major accomplishments of Mallik 2002:

1. Gas was immediately produced from hydrates via controlled depressurization and thermal stimulation tests, without question regarding the gas source.
2. Data were obtained to calibrate well logs and gas hydrate production simulators.

The above two accomplishments are milestones in the knowledge development of hydrates in nature. It is now beyond question that gas can be produced from hydrates, and that data from such production can be accurately modeled. However, because only a few days were spent proving the concept, the transient results prevented the unambiguous long-term modeling of hydrate production, as shown in the sections that follow. As one result of this work, it appears to be important to provide a longer production test, to enable the long-term projection of gas production from hydrates.

#### 7.8.4.1 Background of the Mallik 2002 well

In the Mallik L-38 (ca. 69°27' latitude, 134°40' longitude) well drilled in 1972, Bily and Dick (1974) provided one of the first permafrost hydrate descriptions, from a MacKenzie Delta well site on Richard's Island bordering the Beaufort Sea in Canada. In 1998 the JAPEX/JNOC/GSC 2L-38 well at the same site found core and well-log evidence for hydrates from 900 to 1100 m with *in situ* porosities of 35% and hydrate concentrations often in excess of 80% of the pore volume. The documentation of the 2L-38 well is provided in a compilation of 31 technical papers in GSC Bulletin 544 (Dallimore et al., 1999).

#### 7.8.4.2 Overview of the Mallik 2002 well

When in 2002, the Japanese National Hydrate Program wanted evidence of the conceptual production of gas from hydrates, they chose the proven Mallik site, so it was natural to join with the Canadian Geological Survey. Over the course of the project, a team of 265 scientists/engineers joined the effort, with six major sponsoring entities, as indicated in the introduction.

The Mallik 2002 drilling program was conducted from December 25, 2001 until March 14, 2002, with the completion of two observation wells (3L-38 and 4L-38) drilled to 1188 m depth, coplanar with the 5L-38 main well, drilled to 1166 m. Well logs were obtained from 885 to 1151 m in 5L-38 (Collett et al., 2005). Forty-eight wireline cores were obtained (Dallimore and Collett, p. 82, 2005), three successful pressure stimulation tests (Hancock et al., 2005a) were performed over 0.5 m intervals, and a thermal stimulation test (Hancock et al., 2005b) was done over a 13 m reservoir interval.

In three zones 110 m of gas hydrate bearing strata were observed: (1) 892–930 m in which thermal stimulation was done for hydrate dissociation; (2) 942–993 m in which two successful pressure stimulation tests were performed over a 0.5 m interval, and (3) 1070–1107 m also with a successful pressure stimulation test. The average porosity was 29.3% over the hydrate interval and the average hydrate saturation was 47% of pore volume, with a bimodal distribution of hydrate saturations within the GHSZ. The lateral continuity in the area of the three historical wells (L-38, 2L-38, and 5L-38) indicated there is  $5.39 \times 10^7 \text{ m}^3$  of hydrated gas in place over an area of 10,000 m<sup>2</sup>.

While a number of important results (e.g., well logs, coring methods, etc.) were determined in the Mallik 2002 test for future hydrate applications, this overview will concentrate on two major outcomes in the test itself: (1) proving the concept of gas production from hydrates and (2) modeling the gas production. The gas was principally of thermogenic origin, migrating from deeper in the earth, with low number of methanogens in the sediment (Colwell et al., 2005). In the cores, hydrates averaged about 40–50% of core volume, mostly in a pore-filling habit, as shown by sonic velocities and the new technique of magnetic resonance logging (Kleinberg, et al., 2005). The frozen mechanical strength of the cores at –30°C was 22 MPa, decreasing to 6 MPa at 5°C. The sediments of the three hydrate zones of are briefly characterized as follows:

*The Zone A* (892–930 m) sand had uniform porosity of 32–38% with hydrates preferentially occupying the larger sediment pores and visible hydrate coatings on sand grains. The permeability of hydrate-free sand ranged from 100 to 1000 mD, but with hydrates present the permeability became as low as 0.1 mD. This region had very high hydrate saturations, frequently attaining values of 80% of pore volume.

*Zone B* (942–993 m) had interbedded silt and sand, with porosities between 30% and 40%, and hydrates occupying 40–80% of pore volumes. Without hydrates, the clay permeability was as high as 1 mD but with hydrates the sand permeability reduced to 0.01–0.1 mD.

*Zone C* (1070–1107 m) consisted of sandy silt of 30–40% porosities and hydrate saturations of 80–90% of pore volumes. With hydrates in sand, the permeability ranged from 0.01 to 0.1 mD, becoming less than 0.1 mD in silt.

The depths of the pressure stimulation and thermal stimulation experiments are superimposed on the methane phase equilibria—geothermal gradient diagram shown in Figure 7.35 (Wright et al., 2005). Without a BSR, the geothermal gradient

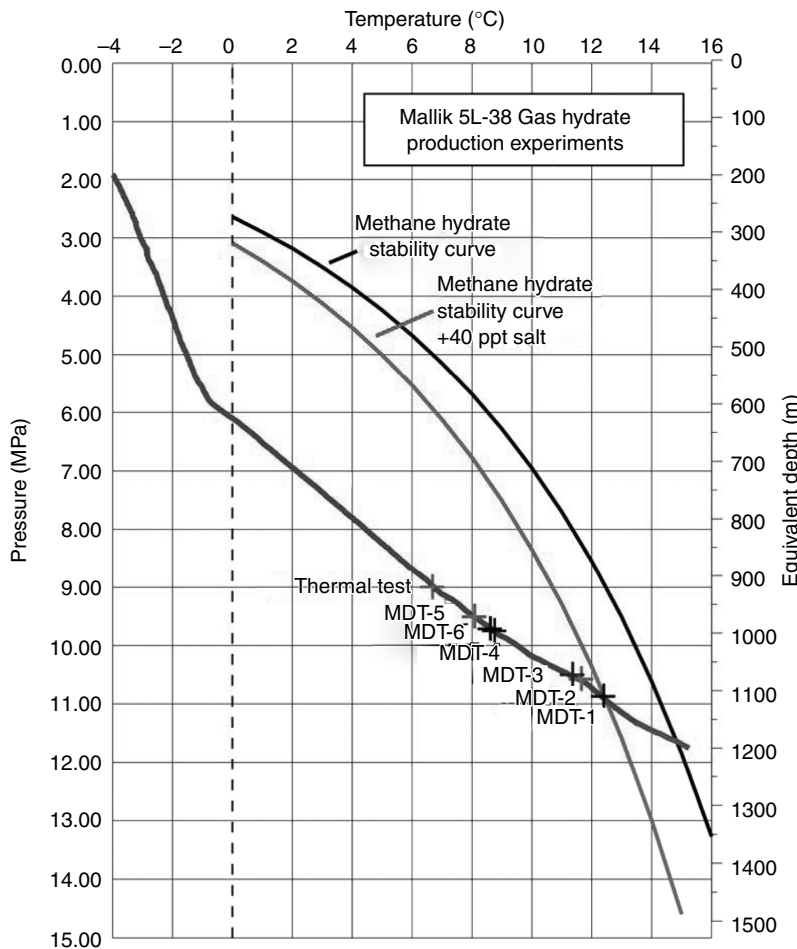


**FIGURE 7.35** Mallik 2002 geothermal gradient and hydrate stability curve for pure water and water containing 40 ppt salt. Note the depths of the thermal stimulation test and the six pressure stimulation (MCT) tests. (From Wright, J.F., et al., in *Scientific Results from the Mallik 2002 Gas Hydrate Production Research Well Program*, Mackenzie Delta, Northwest Territories, Canada, Geological Survey of Canada Bulletin 585, including CD (2005). With permission.)

must be combined with the phase equilibrium line. Equilibrium data in [Figure 7.35](#) are in [Chapter 6](#), with prediction methods of [Chapter 5](#) and the prediction methods of CSMGem on the disk in the Appendix of this book. These results confirm the suggestion of Wright et al. (2005) that when hydrates increase the salt in the remaining reservoir water, the sharp phase equilibrium boundary becomes displaced over a region from 0 to 45 ppt of salt concentration.

#### 7.8.4.3 Well logs in Mallik 2002

[Figure 7.36](#) shows the common well logs in the Mallik test Well 2L-38. Note the suite of wells confirming hydrates in the shaded region from about 900 to 1100 m, provide reinforcing evidence of gas hydrates.

In addition to the above suite of well logs, the newest type of log was obtained via NMR (here called CMR) as shown in [Figure 7.37](#). In this new method, the capillary, clay-bound, and free water (on the right) as determined by the NMR log, are subtracted from the total porosity as determined by the density tool (not shown) to obtain the hydrate saturation in the middle column.

#### 7.8.4.4 Pressure stimulation tests in the 5L-38 well

There were three successful Modular Formation Dynamics Tester (MDT) tests that provided two important pieces of information: (1) evidence of hydrates through the reservoir response to pressure simulation and (2) geomechanical/geothermal measurements at pressure production interval.

To illustrate the hydrate dissociation pressure response, consider the evidence for hydrates from one pressure stimulation test (MDT-2) at 1090 m depth in hydrate Zone C. [Figure 7.38](#) (Hancock et al., 2005b). In this test 0.5 m of wells were temporarily sealed at the top and bottom of the section, before the well was perforated. In the figure three pressure stimulation tests were performed over the first 8 h, with pressure responses shown by the lower line:

1. About 30 min into the test, gas was removed for 8 min to reduce the pressure, then for 25 min the pressure increased as reservoir hydrates dissociated, flowing gas into the well.
2. Similarly at 1.2 h the pressure was drawn down for 37 min, and dissociating hydrates replenished the pressure over the next 69 min. The response time for the pressures can be modeled as indications of reservoir permeability, determined to range from 0.001 to 0.1 mD.
3. Just before 3 h into the test, the pressure was drawn down for 16 min, and gas from dissociating hydrates replenished the pressure over the next 190 min, until about 6.25 h into the test.

Between 7 and 8 h into the test, the flow was reversed and well fluids were pumped into the reservoir to cause three microfracture sequences. Finally just before 9 h in [Figure 7.38](#), the interval was flowed for 21 min, and the pressure

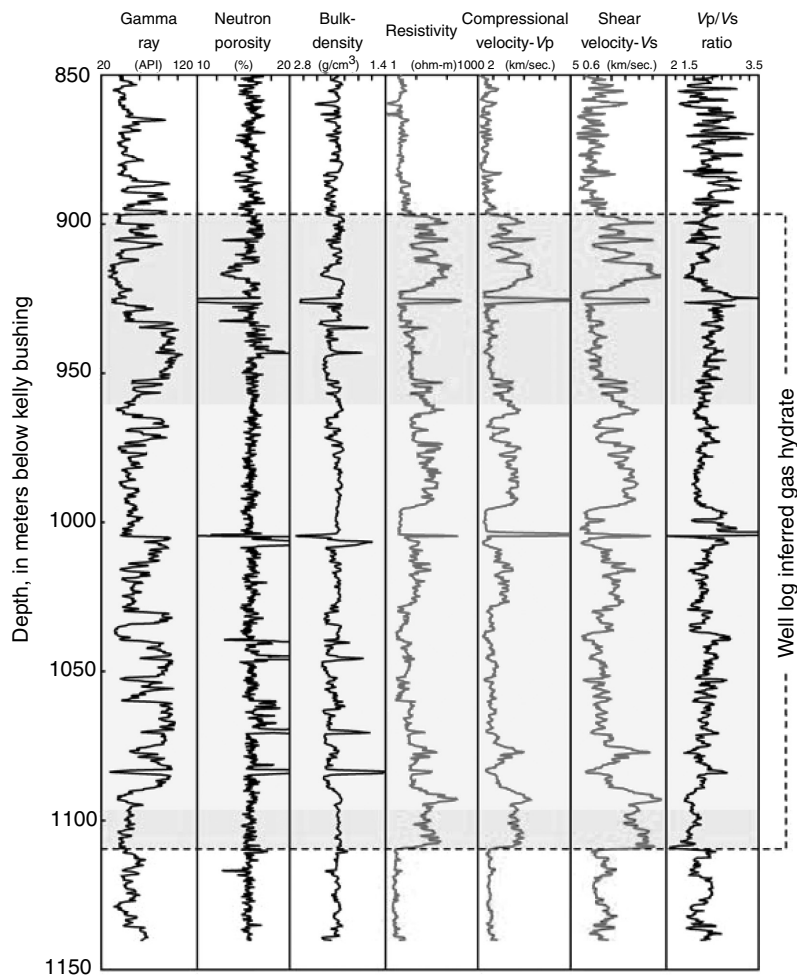


**FIGURE 7.36** Well logs from Mallik 2L-38 showing inferred gas hydrates. (From Collett, T.S., et al., in *Scientific Results from the Mallik 2002 Gas Hydrate Production Research Well Program*, Mackenzie Delta, Northwest Territories, Canada, Geological Survey of Canada Bulletin 585, including CD (2005). With permission.)

rebuilt over the next 76 min, to determine the permeability increase due to the previous microfractures.

#### 7.8.4.5 The Thermal stimulation test in Mallik 5L-38

A thermal stimulation test was performed on hydrates in Zone A, with well flow blockers above and below the interval between 907 and 920 m depth. The well was perforated over the 13 m length and hot brine was pumped down the circulation

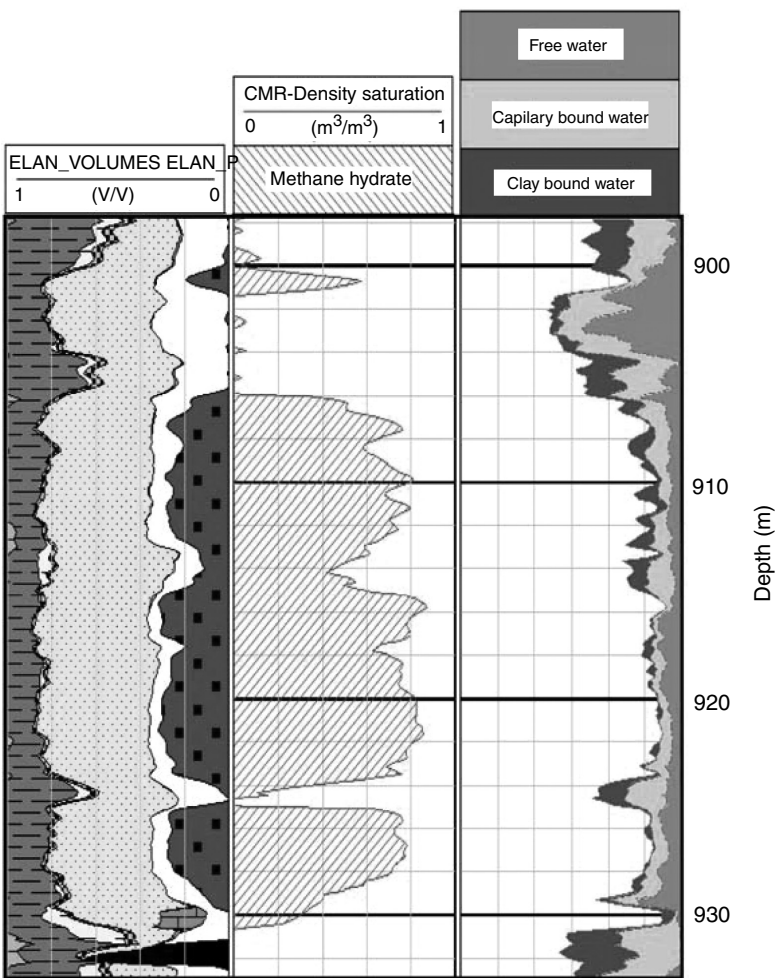


**FIGURE 7.37** (See color insert following page 390.) 5L-38 CMR logs showing hydrate extent at depths between 900 and 930 m. Note that hydrates are obtained by the difference (middle column) between the total porosity as determined by density (not shown), and the capillary, clay-bound and free water determined by NMR.

string, returning in the outer tubing. In this way the 13 m of the reservoir was increased to above 50°C, as shown in Figure 7.39 (Hancock et al., 2005b). The resulting gas was handled at the wellhead by the process shown in Figure 7.40 (Hancock et al., 2005b) and sent to flare.

Over the interval of the test, the gas saturation averaged about 70% of pore volume, as shown in Figure 7.41 (Hancock et al., 2005b), and the permeability average was about 0.1 mD, indicated in Figure 7.42 (Hancock et al., 2005b). The Mallik Scientific Party (Dallimore and Collett, 2005) emphasized that the test was not designed as a conventional industrial-style test, but one to show the

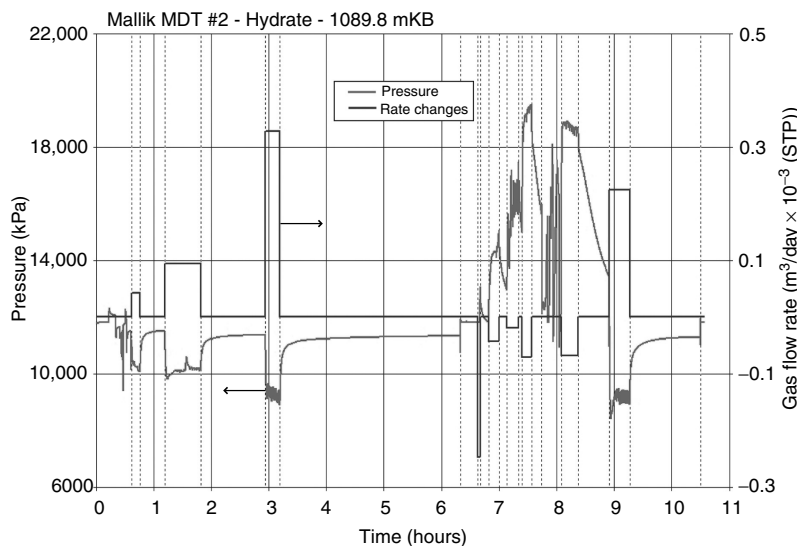


**FIGURE 7.38** Mallik 2002 pressure stimulation test 2 at 1090 m, showing the initial three flow and shut-in sequences, 3 fractures sequences, and a final flow and shut in sequence. (From Hancock, S.H., et al., in *Scientific Results from the Mallik 2002 Gas Hydrate Production Research Well Program*, Mackenzie Delta, Northwest Territories, Canada, Geological Survey of Canada Bulletin 585, including CD (2005b). With permission.)

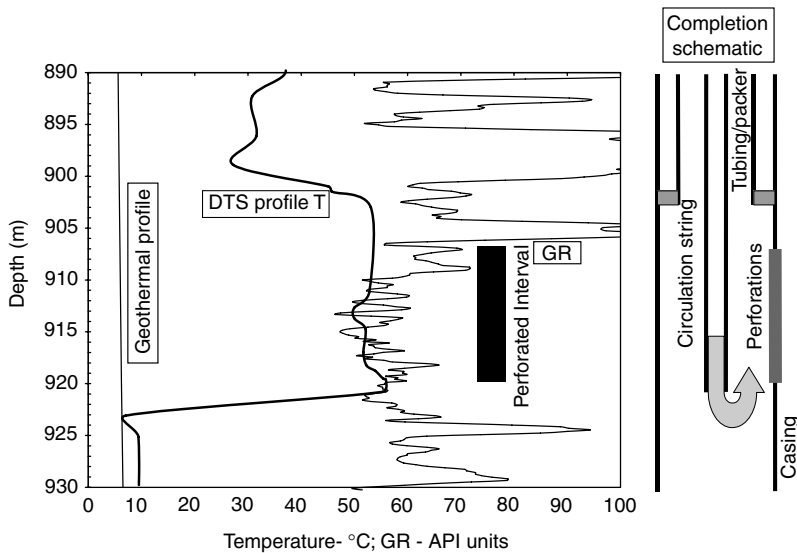


**FIGURE 7.39** The Mallik 5L-38 thermal stimulation test. Note the geothermal profile (leftmost line) and reservoir temperature profile (middle line). (From Hancock, S.H., et al., in *Scientific Results from the Mallik 2002 Gas Hydrate Production Research Well Program*, Mackenzie Delta, Northwest Territories, Canada, Geological Survey of Canada Bulletin 585, including CD (2005b). With permission.)

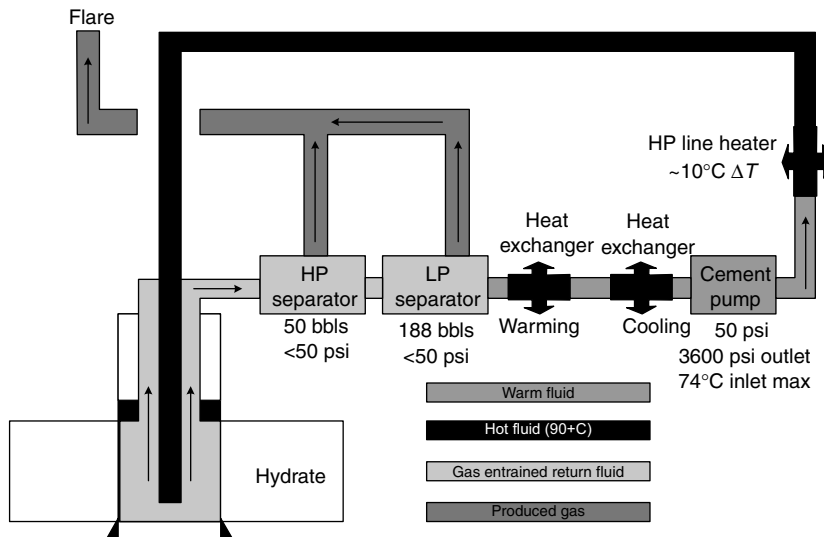


**FIGURE 7.40** Mallik 5L-38 process flow diagram for well-head handling of gases and recirculating brine during thermal test. (From Hancock, S.H., et al., in *Scientific Results from the Mallik 2002 Gas Hydrate Production Research Well Program*, Mackenzie Delta, Northwest Territories, Canada, Geological Survey of Canada Bulletin 585, including CD (2005b). With permission.)

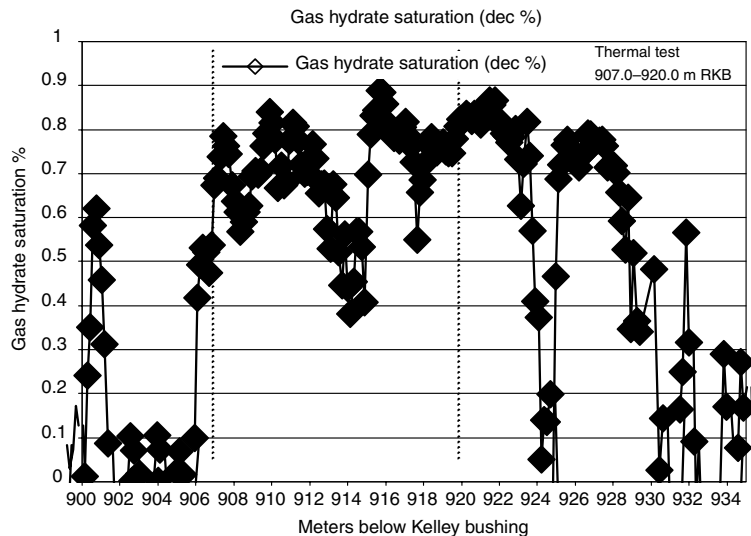


**FIGURE 7.41** Mallik 5L-38 gas hydrate saturations at point of thermal stimulation test. (From Hancock, S.H., et al., in *Scientific Results from the Mallik 2002 Gas Hydrate Production Research Well Program*, Mackenzie Delta, Northwest Territories, Canada, Geological Survey of Canada Bulletin 585, including CD (2005b). With permission.)

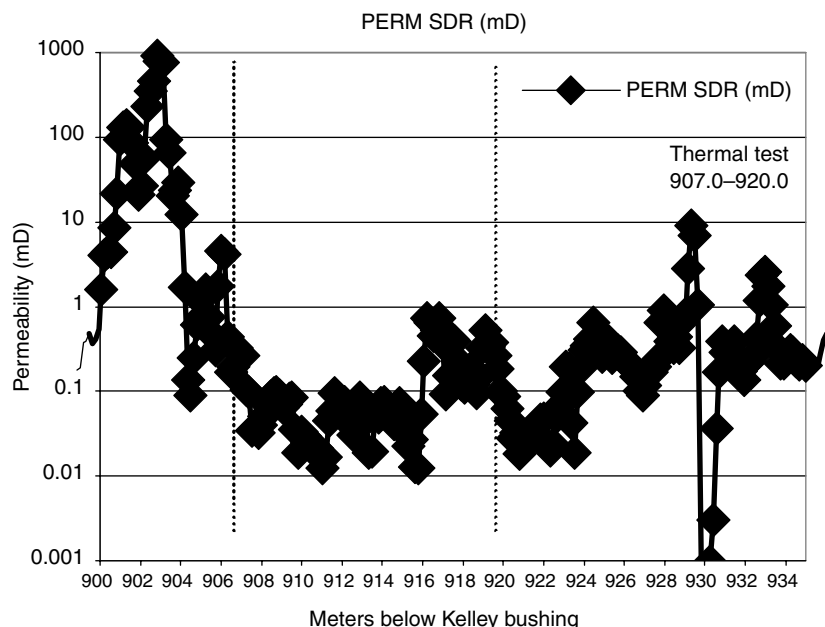


**FIGURE 7.42** Mallik 5L-38 gas hydrate sediment permeability at point of thermal stimulation test. (From Hancock, S.H., et al., in *Scientific Results from the Mallik 2002 Gas Hydrate Production Research Well Program*, Mackenzie Delta, Northwest Territories, Canada, Geological Survey of Canada Bulletin 585, including CD (2005b). With permission.)

concept of producing gas from reservoir hydrates, and to provide calibration data for modeling. Figure 7.43 (Hancock et al., 2005b) shows the gas produced from the thermal stimulation test as a function of time. A total of 468 SCM was produced during the 125 h of the test, with another 48 m<sup>3</sup> produced during the test shutdown. Figure 7.44 (Dallimore and Collett, 2005) is a picture of flared gas from the thermal hydrate production test.

#### 7.8.4.6 Modeling gas production from hydrates

Three models were used to fit the Mallik 2002 production data, and to extrapolate the results for long-term gas production: (1) the Kurihara et al. (2005) model, frequently called the JOE (Japan Oil Engineering Co., Ltd.) model, which was fit to the thermal stimulation and one pressure-stimulation test, (2) the Moridis et al. (2005) model, labeled LBNL (Lawrence Berkeley National Laboratory), which was used to model the thermal stimulation test, and (3) the Hong and Pooladi-Darvish (2005) model, which was used to predict production from first principles, rather than to fit data of the production itself.

In the LBNL model for the thermal test, initially shown as part of Figure 7.43 and repeated here in Figure 7.45 it is shown that heat-transfer-limited hydrate

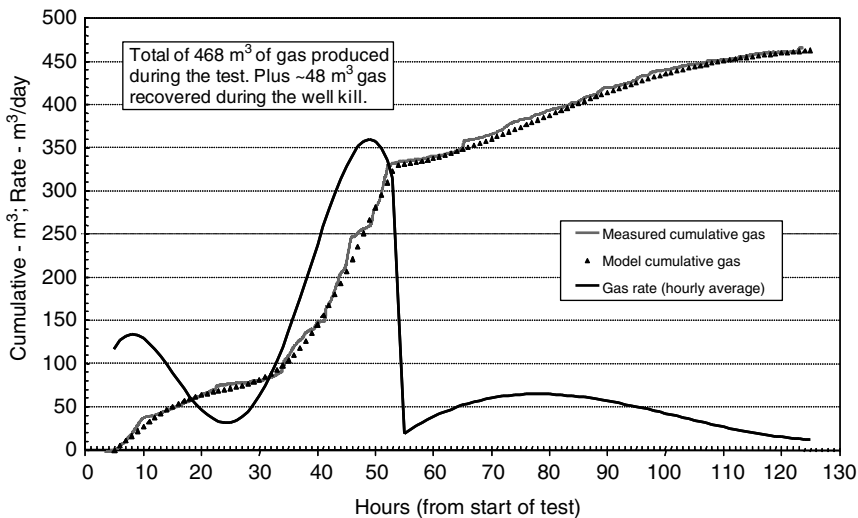


**FIGURE 7.43** Mallik 5L-38 gas production on thermal test. (From Hancock, S.H., et al., in *Scientific Results from the Mallik 2002 Gas Hydrate Production Research Well Program, Mackenzie Delta, Northwest Territories, Canada*, Geological Survey of Canada Bulletin 585, including CD (2005b). With permission.)

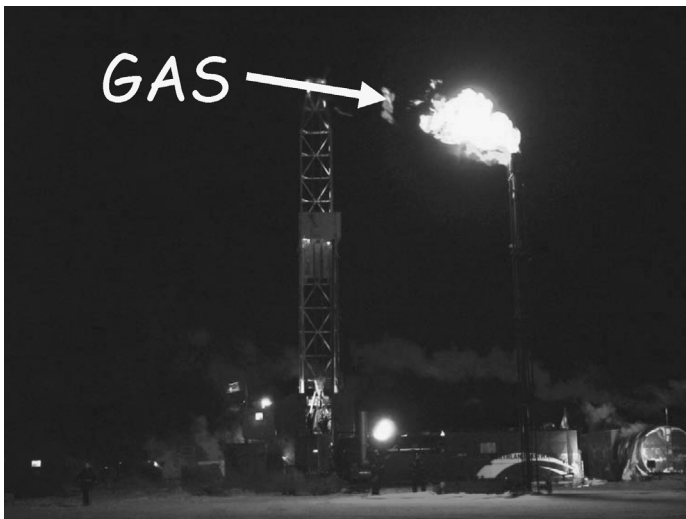


**FIGURE 7.44** Flared gas from Mallik 5L-38 thermal stimulation test.

dissociation (marked “Simulation–Equilibrium” in the figure), rather than the kinetics of hydrate dissociation. The progress of the thermal wave to the hydrate interface was limited by a low hydrate thermal conductivity, so that hydrate kinetics were insignificant. The results of Figure 7.45 appear to match the data equally well,

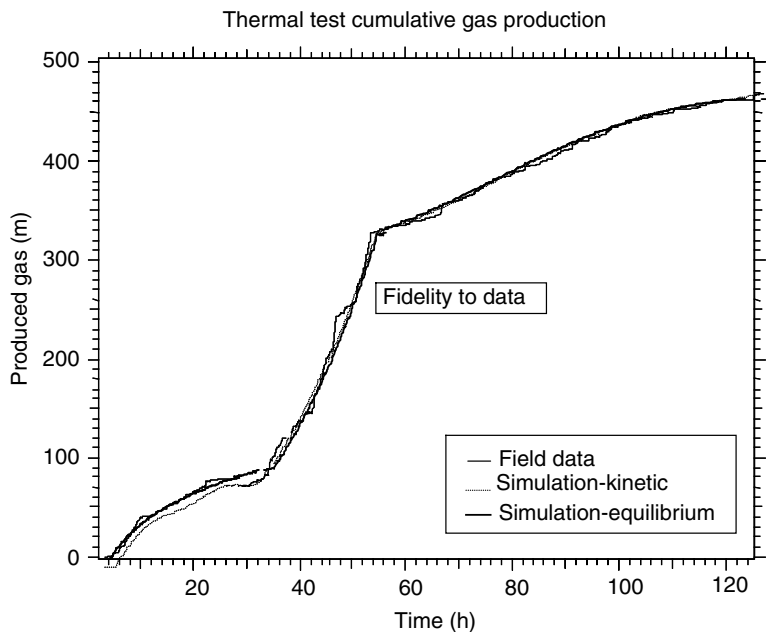


**FIGURE 7.45** Cumulative gas production from Mallik 5L thermal test using LBNL heat transfer limited and kinetic dissociation models (Moridis et al., 2005).

whether hydrate kinetics are included or not. This result is confirmed in Hong's thesis (2003, p. 188) which indicates that the hydrate dissociation rate constant would have to be reduced by five orders of magnitude in order for hydrate kinetics to significantly limit the dissociation rate.

Consider the ten year cumulative gas production prediction of the JOE model shown in Figure 7.46 (note the logarithmic scale of both axes). From the figure it is clear that hot water circulation alone will not be productive for a period after 0.02 years, due to the low thermal conductivity of the hydrates and sediments. However, depressurization does appear to be a favorable production mechanism, comparing favorably to hot water circulation with reduce bottom hole pressure, or partial hot water injection.

Finally, it is important to note that, while both the JOE and LBNL model fit the Mallik production data acceptably, as shown in Table 7.15 both extrapolate to significantly different long-term production values, perhaps due to the short-term and transient nature of the Mallik production test.

Two things should be noted from Table 7.15: (1) while both the JOE and LBNL models fit the short-term Mallik 2002 data, the variation in predicted gas production varies from a factor of 3.7 to 290 and (2) the long-term gas production varies between 0.9 and 325 m<sup>3</sup>/day.

While the above production rates are somewhat encouraging, the variation in the prediction provides impetus for longer-range testing, to eliminate the transient

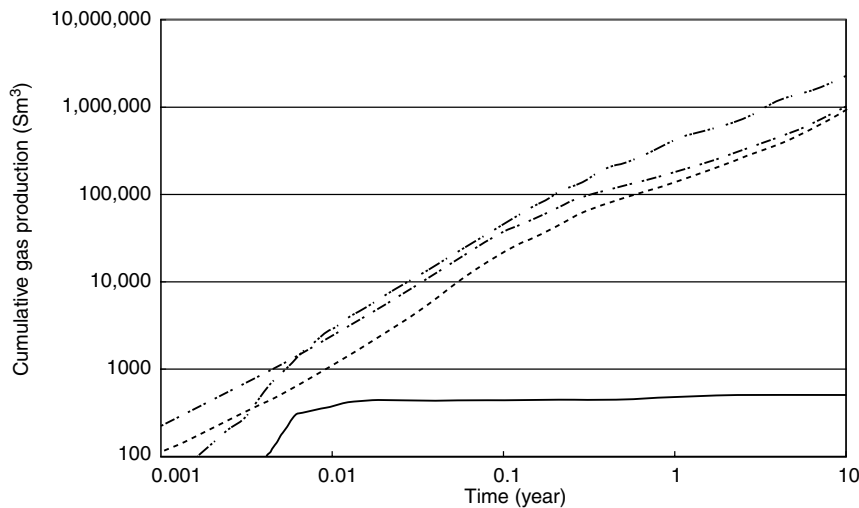


**FIGURE 7.46** Cumulative gas production at Mallik 5L-38. Lowest line: hot water circulation. Second lowest line: depressurization. Third lowest line: hot water circulation with reduced BHP. Top line: partial hot water injection (Kurihara et al., 2005).

---

**TABLE 7.15**  
**Hydrated Gas Production Predictions of JOE and LBNL Models**

Type test/model	Test period	JOE prediction, m <sup>3</sup>	LBNL prediction, m <sup>3</sup>
Depressurization (no heating) with 2.2 Mpa = bottom hole flow pressure	3 years	290,000	1,000
Depressurization with heating	5 days	500	1,850
	3 years	356,000	71,867

---

phenomena inherent in Mallik 2002, and provide a more fundamental basis for modeling.

## 7.9 SUMMARY

The hydrates-in-nature paradigm is currently changing from reservoir assessment to production from the most likely reservoirs. However, most of the methane-containing hydrates are in low concentrations (<3.5 vol%) in the ocean bottom. While production of gas from such lean, deep-lying hydrates is now too expensive, mankind is currently poised to produce hydrates, first from hydrates overlying gas in permafrost, then in the near future we will produce gas from “sweet spots” of high concentrations in the ocean, near where the distribution infrastructure exists.

With the hydrate technology from permafrost and ocean sweet spots in hand, it is likely that one day mankind will need to tap the leaner hydrate fuel source to meet growing energy demands.

## REFERENCES

- Amann, H.-J., et al., ODP Leg 164 Shipboard Scientific Party, Explanatory Notes, in *Proc. Ocean Drilling Programme. Initial Reports*, **164**, 13 (1996).
- Anderson, B.I., Collett, T.S., Lewis, R.E., Dubourg, I., in *Proc. SPWLA 46th Annual Logging Symposium*, New Orleans, LA, June 26–29, 2005.
- Anderson, R., Biderkab, A.-B., Tohidi, B., Clennell, M.B., in *Proc. 63rd European Association of Geoscientist and Engineering Conference and Technical Expedition*, Amsterdam, June 1–15 (2001).
- Andreassen, K., *Seismic Reflections Associated with Submarine Gas Hydrates*, Dr. Scient. Thesis, University of Tromso, Norway (1995).
- Andreassen, K., Hogstad, K., Berteussen, K.A., *First Break*, **8**, 235 (1990).
- Aoki, Y., Tamano, T., Kato, S., *Am. Assoc. Pet. Geol. Memoir*, **34**, 309 (1983).
- Arato, H., Akai, G., Uchiyama, S., Kudo, T., Sekiguchi, K., *BSRs Recognized within the Offshore Chiba Basin*, Abstract, Spring Meeting, Japanese Association for Petroleum Technology (1995).
- Austvik, T., (ed.) in *Proc. 5th International Conference on Natural Gas Hydrates*, (4 volumes and CD) Trondheim, Norway, June 13–16 (2005).
- Ben-Avraham, Z., Smith, G., Reshef, M., Jungslager, E., *Geology*, **30**, 927 (2002).
- Bernard, B.B., Brooks, J.M., Sackett, W.M., *Earth. Planet. Sci. Lett.*, **31**, 48 (1976).
- Bernstein, W., *The Birth of Plenty*, McGraw-Hill Co., New York (2004).
- Besnard, G., Song, K.Y., Hightower, J.W., Kobayashi, R., Elliot, D., Chen, R., in *Proc. 213th ACS National Meeting*, San Francisco, CA, April 13–17, **42**(2), 551 (1997).
- Bily, C., Dick, J.W.L., *Bull. Can. Pet. Geol.*, **22**, 320 (1974).
- Boetius, A., Suess, E., *Chem. Geol.*, **205**, 291 (2004).
- Bohrmann, G., Suess, E., Greinert, J., Teicheret, B., Nahr, T., in *Proc. Fourth International Conference on Gas Hydrates* (Mori, Y.H., ed.), Yokohama, May 19–23, 18 (2002).
- Bolin, B., in *Oceanography: The Present and Future* (P.G. Brewer, ed.), Springer-Verlag, NY, pp. 305–326 (1983).
- Booth, J.S., Rowe, M.M., Fischer, K.M., “*Offshore Gas Hydrate Sample Database*” USGS Open-file Report 96-272, June 1996.
- Bornhold, B.D., Prior, D.B., *GeoMarine Lett.*, **9**, 135 (1989).
- Boswell, R., *An Interagency Roadmap for Methane Hydrate Research and Development*, [http://www.fe.doe.gov/programs/oilgas/publications/methane\\_hydrates/mh\\_inter-agency\\_plan.pdf](http://www.fe.doe.gov/programs/oilgas/publications/methane_hydrates/mh_inter-agency_plan.pdf), July (2006).
- Brewer, P.G., Orr, F.M., Friederich, G., Kvenvolden, Orange, D.L., in *Proc. 213th ACS National Meeting*, San Francisco, CA, April 13–17, **42**(2), 475 (1997).
- Brooks, J.M., Anderson, A.L., Sassen, R., MacDonald, I.R., Kennicutt II, M.C., Guinasso, Jr., N.L., *Ann. N.Y. Acad. Sci.*, **715**, 318 (1994).
- Brooks, J.M., Cox, H.B., Bryant, W.R., Kennicutt, M.C., Mann R.G., McDonald, T.J., *Org. Geochem.*, **10**, 221 (1986).
- Brooks, J.M., Field, M.E., Kennicutt, M.C., *Mar. Geol.*, **96**, 103 (1991).

- Brooks, J.M., Jeffrey, A.W.A., McDonald, T.J., Pflaum, R.C., *Initial Reports of Deep Sea Drilling Project* (von Huene, R., Auboin, J. et al., eds.), Washington, U.S. Govt Printing Office **LXXXIV**, 699 (1985).
- Brooks, J.M., Kennicutt, M.C., Bidigare, R.R., Wade, T.L., Powell, E.N., Denoux, G.J., Fay, R.R., Childress, J.J., Fisher, C.R., Rossman, I., Boland, G., *EOS, Trans. Am. Geophys. Union*, **68**(18), 498 (1987).
- Bugge, T., Befring, S., Belderson, R.H., Eidvin, T., Jansen, E., Kenyon, N.H., Holtedahl, H., Sejrup, H.P., *Geo-Marine Lett.*, **7**, 191 (1987).
- Burshears, M., O'Brien, T.J., Malone, R.D., "A MultiPhase Multi-Dimensional, Variable Composition Simulation of Gas Production from a Conventional Gas Reservoir in Contact with Hydrates," in *Proc. SPE Unconventional Gas Technology Symposium*, SPE 15246, Louisville, KY, May 18–21, (1986).
- Cande, S.C., Leslie, R.B., Parra, J.C., Hobart, M., *J. Geophys. Res.*, **92**(B1), 495 (1987).
- Carlson, P.R., Golan-Bac, M., Karl, H.A., Kvenvolden, K.A., *Am. Assoc. Pet. Geol. Bull.* **69**, 422 (1985).
- Carpenter, G., *Geo-Marine Lett.*, **1**, 29 (1981).
- Charlou, J.L., Donval, J.P., Fouquet, Y., Ondreas, H., Knoery, J., Cochonat, P., Levaché, D., Poirier, Y., Jean-Baptiste, P., Fourré, E., Chazallon, B., and the ZAIROV Leg 2 Scientific Party, *Chem. Geol.*, **205**, 405 (2004).
- Cherskiy, N.V., Tsaarev, V.P., Nikitin, S.P., *Petrol. Geol.*, **21**, 65 (1982).
- Chi, W-C., Reed, D.L., Liu, C-S., Lundberg, N., *Terrestrial, Atmos. Oceanic Sci.*, **9**, 779 (1998).
- Churgin, J., Halimski, S.J., *Key to Oceanographic Records Documentation #2, Gulf of Mexico*, National Oceanographic Data Center, Washington, DC (1974).
- Claypool, G.E., Kaplan, I.R., *Natural Gases in Marine Sediments* (Kaplan, I.R., ed.), Plenum Press, New York, **3**, 99 (1974).
- Claypool, G.E., Kvenvolden, K.A., *Ann. Rev. Earth Planet. Sci.*, **11**, 299 (1983).
- Claypool, G.E., Milkov, A.V., Lee, Y.-J., Torres, M.E., Borowski, W.S., Tomaru, H., in *Proc. ODP Scientific Results Leg 204* (Tréhu, A.M., Bohrmann, G., et al., eds.), College Station, TX, **113** (2006).
- Clemnell, B., Hovland, M., Booth, J.S., Henry, P., Winter, W.J., *J. Geophys. Res.*, **104**(22), 985 (1999).
- Collett, T.S., Detection and Evaluation of Natural Gas Hydrates from Well Longs, Prudhoe Bay, U. Alaska, Anchorage, AL (1983).
- Collett, T.S., *Well Log Evaluation of Natural Gas Hydrates*, USGS Open-File Report 92-381 (1992).
- Collett, T.S., *Am. Assoc. Pet. Geol. Bull.*, **77**, 793 (1993).
- Collett, T.S., *1995 National Assessment of U.S. Oil and Gas Resources* (on CD-ROM) (Gautier, D.L., Goldton, G.L., et al., eds.), USGS (1995).
- Collett, T.S., in *Proc. 2nd International Conference on Natural Gas Hydrates* (Monfort, J.P., ed.), Toulouse, France, June 2–6, 499 (1996).
- Collett, T.S., Bird, K.J., Kvenvolden, K.A., Magoon, L.B., *Geologic Interrelations Relative to Gas Hydrates Within the North Slope of Alaska*, Final Report DE-AI21-83MC20422, U.S. Department of Energy, (1988).
- Collett, T.S., Ehlig-Economides, C., "Detection and Evaluation of the *In-Situ* Natural Gas Hydrates in the North Slope Region, Alaska," SPE 11673, in *Proc. 1983 SPE California Regional Meeting*, March 23–25 (1983).
- Collett, T.S., Ginsburg, G.D., *Int. J. Offshore Polar Eng.*, **8**, 22 (1998).

- Collett, T.S., Godbole, S.P., Ehlig-Economides, C., in *Proc. 35th Annual Meeting of Canadian Institute of Mining*, Calgary, Canada, June 10–12 (1984).
- Collett, T.S., Lee, M.W., in *Scientific Results from the Mallik 2002 Gas Hydrate Production Research Well Program*, Mackenzie Delta, Northwest Territories, Canada (Dallimore, S.R., Collett, T.S., eds.), Geological Survey of Canada Bulletin 585, including CD, p. 112 (2005).
- Collett, T.S., Lewis, R.E., Dallimore, S.R., in *Scientific Results from the Mallik 2002 Gas Hydrate Production Research Well Program*, Mackenzie Delta, Northwest Territories, Canada (Dallimore, S.R., Collett, T.S., eds.), Geological Survey of Canada Bulletin 585, including CD, p. 111 (2005).
- Colwell, F.S., Nunoura, T., Delwiche, M.F., Boyd, S., Bolton, R., Reed, D.W., Takai, K., Lehman, R.M., Horikoshi, K., Dlias, D.A., Phelps, T.J., in *Scientific Results from the Mallik 2002 Gas Hydrate Production Research Well Program*, Mackenzie Delta, Northwest Territories, Canada (Dallimore, S.R., Collett, T.S., eds.), Geological Survey of Canada Bulletin 585, including CD, p. 102 (2005). Dai, J., Xu, H., Snyder, F., Dutta, N., *Leading Edge*, **23**, 60 (2004).
- Dallimore, S.R., Collett, T.S., (eds.), in *Scientific Results from the Mallik 2002 Gas Hydrate Production Research Well Program*, Mackenzie Delta, Northwest Territories, Canada, Geological Survey of Canada Bulletin 585, including CD (2005).
- Dallimore, S.R., Uchida, T., Collett, T.S., *Geol. Sur. Can. Bull.*, **544**, 403 (1999).
- Davidson, D.W., El-Defrawy, M.K., Fuglem, M.O., Judge, A.S., in *Proc. Third International Conference on Permafrost*, **1**, 938, Calgary, Alberta, March 15 (1978).
- Davie, M.K., Buffett, B.A., *J. Geophys. Res.*, **106**, 497 (2001).
- Davie, M.K., Buffett, B.A., *J. Geophys. Res.*, **108**(B10), 2495 (2003).
- Davies, S.R., Sloan, E.D., “Predictions of the Dissociation of Hydrate in Sediment Samples with Numerical Heat Transfer Models Based on Fourier’s Law” presented at the *16th Symposium on Thermophysical Properties* (<http://symp16.boulder.nist.gov/>) Boulder, CO, July 30–August 4 (2006).
- Davis, E.E., Hyndman, R.D., Villinger, H., *J. Geophys. Res.*, **95**(B6), 8869 (1990).
- DeLange, G.J., Brumsack, H.-J., *Gas Hydrates—Relevance to World Margin Stability and Climatic Change* (Henriet, J.-P., Mienert, J., eds.), The Geological Society, London, Special Publication, **137**, p. 167 (1998).
- Dholabhai, P.D., Englezoa, P., Kalogerakis, N., Bishnoi, P.R., *Can. J. Chem. Eng.*, **69**, 800 (1991).
- Diaconescu, C.C., Kieckhefer, R.M., Knapp, J.H., *Mar. Pet. Geol.*, **18**, 209 (2001).
- Dickens, G.R., *Nature*, **401**, 752 (1999).
- Dickens, G.R., *Organ. Geochem.*, **32**, 1179 (2001).
- Dickens, G.R., *Science*, **299**, 1017 (2003).
- Dickens, G.R., O’Neil, J.R., Rea, D.K., Owen, R.M., *Paleoceanography*, **10**, 965 (1995).
- Dillon, W.P., Danforth, W.W., Hutchinson, D.R., Drury, R.M., Taylor, M.H., Booth, J.S., *Gas Hydrates—Relevance to World Margin Stability and Climatic Change* (Henriet, J.-P., Mienert, J., eds.), The Geological Society, London, Special Publication, **137**, p. 293 (1998).
- Dillon, W.P., Fehlhaber, K., Coleman, D.F., Lee, M.W., Hutchinson, D.R., *U.S. Geological Survey, Miscellaneous Field Studies Map, MF 2268*, 2 sheets (1995).
- Dillon, W.P., Hutchinson, D.R., Drury, M., in *Proc. Ocean Drilling Program Initial Reports*, (Paull, C.K., Matsumoto, R., et al., eds.), **164**, p. 47 (1996).

- Dillon, W.P., Lee, M.W., Fehlhaber, K., Coleman, D.G., *The Future of Energy Gases, U.S. Geological Survey, Professional Paper 1570*, pp. 313–330 (1993).
- Dillon, W.P., Max, M.D., *Natural Gas Hydrate in Oceanic and Polar Environments* (Max, M.D., ed.), Kluwer Academic Publishers, Dordrecht, 61 (2000).
- Dillon, W.P., Max, M.D., in *Proc. 33rd Offshore Technical Conference*, Houston, TX, OTC 13034, 30 April–3 May (2001).
- Dillon, W.P., Nealon, J.W., Taylor, M.H., Lee, M.W., Drury, R.M., Anton, C.H., *Natural Gas Hydrates: Occurrence, Distribution and Detection* (Paull, C.K., Dillon, W.P., eds.), Geophysical Monograph 124, American Geophysical Union, Washington, DC, p. 211, (2001).
- Dobrynin, V.M., Korotajev, Yu, P., Plyuschev, D.V., in *Long Term Energy Resources* (Meyer, R.G., ed.), Pitman, Boston, MA, 727 (1981).
- Domenico, S.N., *Geophysics*, **65**, 565 (1977).
- Dvorkin, J., Nur, A., *The Future of Energy Gases USGS Prof. Paper No 1570*, 293 (1992).
- Eaton, M.K., Hester, K.C., Sloan, E.D., in *Scientific Results from the Mallik 2002 Gas Hydrate Production Research Well Program*, Mackenzie Delta, Northwest Territories, Canada (Dallimore, S.R., Collett, T.S., eds.), Geological Survey of Canada Bulletin 585, including CD, p. 107 (2005).
- Ecker, C., Lumley, D., Dvorkin, J., Nur, A., in *Proc. Second International Conference on Natural Gas Hydrates* (Monfort, J.P., ed.), Toulouse, France, June 2–6, 491 (1996).
- Economides, M., Oligney, R., *The Color of Oil*, Round Oak Publishing, Katy, TX (2000).
- Edeberg, P.K., Dickens, G.R., *Chem. Geol.*, **153**, 53 (1999).
- Ewing, J.I., Hollister, C.D., *Initial Rep. Deep Sea Drilling Project*, **11**, 951 (1972).
- Exon, N.F., Dickens, G.R., Auzende, J-M., Lafoy, Y., Symonds, P.A., Van de Beuque, S., *Pet. Explor. Soc. Aust. J.*, **26**, 148 (1998).
- Field, M.E., Kvenvolden, K.A., *Geology*, **13**, 517 (1985).
- Finley, P., Krason, J., *Geological Evolution and Analysis of Confirmed or Suspected Gas Hydrate Localities: Basin Analysis, Formation and Stability of Gas Hydrates in the Middle America Trench*, U.S. Department of Energy, DOE/MC/21181-1950, **9** (1986a).
- Finley, P., Krason, J., *Geological Evolution and Analysis of Confirmed or Suspected Gas Hydrate Localities: Basin Analysis, Formation and Stability of Gas Hydrates of the Colombia Basin*, U.S. Department of Energy, DOE/MC/21181-1950, **7** (1986b).
- Finley, P.D., Krason, J., Dominic, K., *Am. Assoc. Pet. Geol. Bull.*, **71**(5), 555 (1987).
- Fisher, C.R., MacDonald, I.R., Sassen, R., Young, C.M., Macko, S.A., Hourdez, S., Carney, R.S., Joye, S., McMullin E., *Naturwissenschaften*, **87**, 184 (2000).
- Fontana, R.L., Mussemecci, A., in *Proc. First International Conference on Natural Gas Hydrates, Ann. N.Y. Acad. Sci.* (Sloan, E.D., Happel, J., et al., eds.), **715**, 106 (1994).
- Ford, K.H., Naehr, T.H., Skilbeck, C.G., in *Proc. ODP Initial Reports*, Ocean Drilling Program (D'Hondt, S.L., Miller, B.B. et al., eds.), College Station, TX, **201**, 1 (2003).
- Freifeld, B.M., Kneafsey, T.J., Tomutsa, L., Stern, L.A., Kirby, S.H., in *Proc. Fourth International Conference on Gas Hydrates* (Mori, Y.H., ed.), Yokohama, May 19–23, 750 (2002).
- Froelich, P.N., Kvenvolden, K.A., Torres, M.E., Waseda, A., Didyk, B.M., Lorenson, T.D., in *Proc. Ocean Drilling Program, Scientific Results*, **141**, 279 (1995).
- Gas Epoch, *Gas Epoch*, **8**, 18 (1995).

- Genov, G., Kuhs, W.F., Staykova, D.K., Goreshnik, E., Salamatin, A.N., *Am. Mineral.*, **89**(8–9), 1228 (2004).
- Ginsburg, G.D., Guseynov, R.A., Dadashev, A.A., Ivanova, G.A., Kazantsev, S.A., Soloviev, V.A., Telepnev, E.V., Askeri-Nasirov, P. Ye., Yesikov, A.A., Mal'tseva, V.I., Mashirov, G. Yu., Shabayeva, I. Yu., *Int. Geol. Rev.*, **43**, 765 (1992).
- Ginsburg, G.D., Kremlev, A.N., Grigor'ev, M.N., Larkin, G.V., Pavlenkin, A.D., Saltykova, N.A., *Geologiya I Geofizika*, **31**(3), 10 (1990).
- Ginsburg, G.D., Milkov, A.V., Soloviev, V.A., Egorov, A.V., Cherdashev, G.A., Vogt, P.R., Crane K., Lorenson, T.D., Khutorskoy, M.D., *Geo-Marine Lett.*, **19**, 57 (1999).
- Ginsburg, G.D., Soloviev, V.A., *Bull. Geol. Soc. Denmark*, Copenhagen, **41**, 95 (1994).
- Ginsburg, G.D., Soloviev, V.A., in *Proc. 27th Annual Offshore Technology Conference*, Houston, OTC 7693, May 1–4, 513 (1995).
- Ginsburg, G.D., Soloviev, V.A., *Mar. Geol.*, **137**, 49 (1997).
- Ginsburg, G.D., Soloviev, V.A., *Submarine Gas Hydrates*, VNIIOkeangeologgia, St. Petersburg (1998).
- Ginsburg, G.D., Soloviev, V.A., Cranston, R.E., Lorenson, T.D., Kvenvolden, K.A., *Geo-Marine Lett.*, **13**, 41 (1993).
- Gornitz, V., Fung, I., *Global Biogeochem. Cycles*, **8**, 335 (1994).
- Grantz, A., Boucher, G., Whitney, O.T., *U.S. Geol. Surv. Circ.* **733**, 17 (1976).
- Grantz, A., Dinter, D.A., *Oil Gas J.* **78**(18), 304 (1980).
- Gudmundsson, J.-S., Parlaktuna, M., "Storage of Natural Gas at Refrigerated Conditions," in *AICHE Spring National Meeting*, New Orleans, LA, March 15 (1992).
- Halleck, P.M., Byrer, C.W., McGuire, P.L., Judge, A.S., Corlett, R.C., Barracough, B., in *Proc. Methane Hydrate Workshop*, Morgantown, WV, Mar 29–30, 63 (1982).
- Hamblin, W.K., *The Earth's Dynamic Systems*, Macmillan, New York (1985).
- Hammond, R.D., Gaither, J.R., *Geophysics*, **48**, 590 (1983).
- Hancock, S.H., Dallimore, S.R., Collett, T.S., Carle, D., Weatherill, B., Satoh, T., Inoue, T., in *Scientific Results from the Mallik 2002 Gas Hydrate Production Research Well Program*, Mackenzie Delta, Northwest Territories, Canada (Dallimore, S.R., Collett, T.S., eds.), Geological Survey of Canada Bulletin 585, including CD, p. 134 (2005a).
- Hancock, S.H., Collett, T.S., Dallimore, S.R., Satoh, T., Inoue, T., Huenges, E., Henninges, J., Weatherill, B., in *Scientific Results from the Mallik 2002 Gas Hydrate Production Research Well Program*, Mackenzie Delta, Northwest Territories, Canada (Dallimore, S.R., Collett, T.S., eds.), Geological Survey of Canada Bulletin 585, including CD, p. 135 (2005b).
- Handa, Y.P., *J. Phys. Chem.*, **94**, 2652 (1990).
- Harrison, W.E., Curiale, J.A., *Initial Rep. Deep Sea Drilling Project*, **67**, 591 (1982).
- Harrison, W.E., Hesse, R., Gieskes, J.M., *Initial Rep. Deep Sea Drilling Project*, **67**, 603 (1982).
- Harvey, L.D.D., Huang, Z., *J. Geophys. Res.*, **100**D2, 2905 (1995).
- Heesch, K.U., Tréhu, A.M., Collier, R.W., Suess, E., Rehder, G., *Geophys. Res. Lett.*, **30**(12), 1643 (2003).
- Henriet, J.P., De Mol, B., Pillen, S., Vanneste, M., Van Rooij, D., Versteeg, W., Croker, P.F., Shannon, P.M., Unnithan, V., Bouriak, S., Chachkine, P., and The Porcupine—Beligica 97 Shipboard Party, *Nature*, **391**, 648 (1998).
- Henriet, J.-P., Minert, J., (eds.), *Gas Hydrates: Relevance to World Margin Stability and Climate Change*, Geological Society of London, Special Publication, 137 (1998).

- Hesse, R., *Geosci. Can.*, **14**(3), 165 (1986).
- Hesse, R., Harrison, W.E., *Earth. Plan. Sci. Lett.*, **55**, 453 (1981).
- Hesse, R., Lebel, J., Gieskes, J.M., *Initial Rep. Deep Sea Drilling Project*, **84**, 727 (1985).
- Hester, K.C., White, S.N., Peltzer, E.T., Brewer, P.G., Sloan, E.D., *Mar. Chem.*, **98**, 304 (2005).
- Holbrook, W.S., Hoskins, H., Wood, W.T., Stephen, R.A., Lizarralde, D., and Leg 164 Science Party, *Science*, **273**, 1840 (1996).
- Holder, G.D., Angert, P.F., in *Proc. Soc. Petr. Enq. Meet.*, SPE 11105, New Orleans, LA, September 26–29 (1982).
- Holder, G.D., Bishnoi, P.R., *Gas Hydrates: Challenges for the Future*, *Ann. N.Y. Acad. Sci.*, **912**, (2000).
- Hong, H., *Modeling of Gas Production from Hydrates in Porous Media*, M.Sc. Thesis, University of Calgary, Alberta, Canada, p. 267 (2003).
- Hong, H., Pooladi-Darvish, M., in *Scientific Results from the Mallik 2002 Gas Hydrate Production Research Well Program*, Mackenzie Delta, Northwest Territories, Canada, (Dallimore, S.R., Collett, T.S., eds.), Geological Survey of Canada Bulletin 585, including CD, p. 138 (2005).
- Hong, H., Pooladi-Darvish, M., *J. Can. Pet. Technol.*, **44**(11), 39 (2005).
- Hovland, M., Lysne, D., Whiticar, M., in *Proc. Ocean Drill Program, Leg 146* (Carson, B., Westbrook, G.K., et al., eds.), **146**(1), 151 (1995).
- Howe, S.J., Nanchary, N.R., Patil, S.L., Ogbe, D.O., Chukwu, G.A., Hunter, R.B., Wilson, S.J., in *Proc. Hedberg Conference on Gas Hydrates: Energy Resource Potential and Associated Geologic Hazards*, Vancouver, BC, September 12–16 (2004).
- Hunt, J.M., *Petroleum Geochemistry and Geology*, W.H. Freeman, San Francisco, CA (1979).
- Hutchinson, D.R., Golmshtok, A.J., Scholz, C.A., Moore, T.C., Lee, M.W., Kuzmin, M., *Trans. Am. Geophys. Union*, **72**(17, Supplement), 307 (1991).
- Hutchinson, D.R., Ruppel, C.D., Pohlman, G., Hart, P.E., Dugan, B., Snyder, F., Coffin, R.B., “An integrated geological, geophysical, and geochemical analysis of subsurface gas hydrates in the Northern Gulf of Mexico,” in *Proc. of Gas Hydrates: Energy Resources Potential and Associated Geologic Hazards*, American Association of Petroleum Geologists Hedberg Conference, Sepetmeber 12–16, 2004, Vancouver, Canada, Available at [http://www.searchanddiscovery.net/documents/abstracts/2005hedberg-\\_vancouver/extended/Hutchinson/hutchinson.htm](http://www.searchanddiscovery.net/documents/abstracts/2005hedberg-_vancouver/extended/Hutchinson/hutchinson.htm).
- Hyndman, R.D., Davis, E.E., *J. Geophys. Res.*, **97**(B5), 7025 (1992).
- Hyndman, R.D., Foucher, J.P., Yamano, M., Fisher, A., and Sci Team of ODP leg 131, *Earth Planet Sci. Lett.*, **109**, 289 (1992).
- Hyndman, R.D., Spence, G.D., *J. Geophys. Res.*, **97**(B5), 6683 (1992).
- Hyndman, R.D., Spence, G.D., Yuan, T., Desmons, B., in *Proc. Second International Conference on Natural Gas Hydrates* (Monfort, J.P., ed.), Toulouse, France, June 2–6, 485 (1996).
- Islam, M.R., *J. Pet. Sci. Eng.*, **11**, 267 (1994).
- Jamaluddin, A.K.M., Kalogerakis, N., Bishnoi, P.R., *Pet. Soc. Can. Inst. Mining*, **89**, 5 (1989).
- Jansen, E., Befring, S., Bugge, T., Eidvin, T., Hotedahl, G., Sejrup, H.P., *Mar. Geol.*, **78**, 77 (1987).
- Jenden, P.D., Gieskes, J.M., *Initial Rep. Deep Sea Drilling Project* (Sheridan, R.E., Gradstein, F., et al., eds.), US Government Printing Office, **76**, 453 (1983).

- JNOC press release, Proof of the methane-hydrate-containing layer in the national wildcat, "Nankai Trough," based on the National Domestic Petroleum Exploration Program, Japan National Oil Corporation, January 20 (2000).
- Judge, A.S., in *Proc. Fourth Canadian Permafrost Conference 1981*, 320, Calgary, Alberta, March 15 (1982).
- Kaiho, K., Arinobu, T., Ishiwatari, R., Morgans, H.E.G., Okada, H., Takeda, N., Taxaki, K., Zhou, G., Kajiwara, Y., Matsumoto, R., Hirai, A., Niituma, N., Wada, H., *Paleoceanography*, **11**, 447 (1996).
- Kamath, V.A., Godbole, S.P., *J. Pet. Tech.*, **39**, 1379 (1987).
- Kastner, M., Kvenvolden, K.A., Lorenson, T.D., *Earth Planet. Sci. Lett.*, **156**, 173 (1998).
- Kastner, M., Kvenvolden, K.A., Whiticar, M.J., Camerlenghi, A., Lorenson, T.D., in *Proc. Ocean Drill Program, Leg 146* (Carson, B., Westbrook, G.K., et al., eds.), **146**(1), 175 (1995).
- Katz, H.R., *J. Pet. Geol.*, **3**, 315 (1981).
- Kayen, R.E., Lee, H.J., *Mar. Geotechnol.*, **10**, 125 (1991).
- Kennett, J.P., Cannariato, G., Hendy, I.L., Behl, R.J., *Methane Hydrates in Quaternary Climate Change: The Clathrate Gun Hypothesis*, The American Geophysical Union, Washington, DC, (2003).
- Kennett, J.P., Hill, T.M., Behl, R.J., in *Proc. Fifth International Conference Gas Hydrates*, (Austvik, T., ed.), (paper 3008), 4 volumes and CD, Trondheim, Norway, June 13–15, 759 (2005).
- Klauda, J.B., Sandler, S.I., *Energy and Fuels*, **19**, 469 (2005).
- Kleinberg, R.L., *New Techniques in Sediment Core Analysis*, Geological Society of London, Special Publication (Rothwell, R.G., ed.), **267**, 179 (2006).
- Kleinberg, R.L., Brewer, P.G., Malby, G., Peltzer, E.T., Friederich, G., Yesinowski, J., Flaum, C., *J. Geophys. Res.*, 108:B3, doi:10.1029/2001JB0000919 (2003).
- Kleinberg, R.L., Flaum, C., Collett, T.S., in *Scientific Results from the Mallik 2002 Gas Hydrate Production Research Well Program*, Mackenzie Delta, Northwest Territories, Canada (Dallimore, S.R., Collett, T.S., eds.), Geological Survey of Canada Bulletin 585, including CD, p. 114 (2005).
- Krason, J., Ciesnik, M., *Geological Evolution and Analysis of Confirmed or Suspected Gas Hydrate Localities: Gas Hydrates in the Russian Literature*, U.S. Department of Energy, DOE/MC/21181-1950, **5** (1985).
- Krason, J., Ciesnik, M., *Geological Evolution and Analysis of Confirmed or Suspected Gas Hydrate Localities: Basin Analysis, Formation and Stability of Gas Hydrates in the Panama Basin*, U.S. Department of Energy, DOE/MC/21181-1950, **6** (1986a).
- Krason, J., Ciesnik, M., *Geological Evolution and Analysis of Confirmed or Suspected Gas Hydrate Localities: Basin Analysis,Formation and Stability of Gas Hydrates in the Northern California Offshore*, U.S. Department of Energy, DOE/MC/21181-1950, **8** (1986b).
- Krason, J., Finley, P.D., *Structural Traps VII. (AAPG Treatise Petrol Geol Atlas of Oil and Gas Fields)*, 197 (Beaumont E.A., Foster, N.H., eds.), AAPG, Tulsa, OK (1992).
- Krason, J., Finley, P.D., Rudloff, B., *Geological Evolution and Analysis of Confirmed or Suspected Gas Hydrate Localities: Basin Analysis,Formation and Stability of Gas Hydrates in the Western Gulf of Mexico*, U.S. Department of Energy, DOE/MC/211811950, **3** (1985).
- Krason, J., Ridley, W.I., *Geological Evolution and Analysis of Confirmed or Suspected Gas Hydrate Localities: Blake-Bahama Outer Ridge-U.S. East Coast*, U.S. Department of Energy, DOE/MC/21181-1950, **1** (1985a).

- Krason, J., Ridley, W.I., *Geological Evolution and Analysis of Confirmed or Suspected Gas Hydrate Localities: Baltimore Canyon Trough and Environs U.S. East Coast*, U.S. Department of Energy, DOE/MC/21181-1950, **2** (1985b).
- Krason, J., Rudloff, B., *Geological Evolution and Analysis of Confirmed or Suspected Gas Hydrate Localities: Offshore of Newfoundland and Labrador*, U.S. Department of Energy, DOE/MC/21181-1950, **4** (1985).
- Kumar, P., Turner, D., Sloan, E.D., *J. Geophys. Res.*, **109**, B01207 (2004).
- Kuramoto, S., Okamura, I., *Geol. Surv. Jpn.*, **28** (1995).
- Kurihara, M., Funatsu, K., Kusaka, K., Yasuda, M., Dallimore, S.R., Collett, T.S., Hancock, S.H., in *Scientific Results from the Mallik 2002 Gas Hydrate Production Research Well Program*, Mackenzie Delta, Northwest Territories, Canada (Dallimore, S.R., Collett, T.S., eds.), Geological Survey of Canada Bulletin 585, including CD, p. 139 (2005).
- Kus'min, M.I., Kalmychkov, G.V., Geletii, R.F., Gnilusha, V.A., Goreglyad, A.V., Khakhaev, B.N., Pevzner, L.A., Kawai, T., Yoshida, N., Duchkov, A.D., Ponomarchuk, V.A., Kontorovich, A.E., Abazhin, N.M., Makhov, G.A., Dyadin, Yu. A., Kuznetsov, F.A., Larionov, E.G., Manakov, A.Yu., Smolyakov, B.S., Mandel'baum, M.M., Zheleznyakov, N.K., *Doklady Akademii Nauk*, **362**, 541 (1998) [Translation in *Doklady Earth Sciences*, **362**, 1029 1998].
- Kvenvolden, K.A., *Mar. Pet. Geol.*, **2**, 65 (1985a).
- Kvenvolden, K.A., *Chem. Geol.*, **71**, 41 (1988).
- Kvenvolden, K.A., *Org. Geochem.*, **23**, 997 (1995).
- Kvenvolden, K.A., Barnard, L.A., *Initial Reports DSDP* (Sheridan, R.E., Gradstein, F., et al., eds.), U.S. Government Printing Office, Washington, DC, **76**, 353 (1983).
- Kvenvolden, K.A., Claypool, G.E., in *Proc. Unconventional Gas Recovery: Gas Hydrates Peer Review Session*, Bethesda, MD., April 24–25, (1985).
- Kvenvolden, K.A., Claypool, G.E., *U.S. Geological Survey Open File Report 88-216*, p. 50 (1988).
- Kvenvolden, K.A., Claypool, G.E., Threlkeld, C.N., Sloan, E.D., *Org. Geochem.*, **6**, 703 (1984).
- Kvenvolden, K.A., Golan-Bac, M., McDonald, T.J., Pflaum, R.C., Brooks, J.M., in *Proc. Ocean Drilling Program, Scientific Results*, **104**, 319 (1989).
- Kvenvolden, K.A., Golan-Bac, M., Rapp, J.B., *Circum-Pacific Council on Energy and Mineral Resources, Earth Science Series 5A*, 205 (1987).
- Kvenvolden, K.A. Grantz, A., in *The Geology of North America*, **50**, *The Arctic Ocean Region*, Geological Society of America, 539 (1990).
- Kvenvolden, K.A., Kastner, M., in *Proc. Ocean Drilling Program, Scientific Results*, **112**, 517 (1990).
- Kvenvolden, K.A., Lorenson, T.D., in *Natural Gas Hydrates: Occurrence, Distribution and Detection* (Paull C.K., Dillon, W.P., eds.), Geophysical Monograph 124, American Geophysical Union, Washington, DC, 3 (2001).
- Kvenvolden, K.A., McDonald, T.J., *Initial Rep. Deep Sea Drilling Project*, **84**, 667 (1985).
- Kvenvolden K.A., von Huene, R., *Circum-Pacific Council on Energy and Minerals, Earth Science Series*, **1**, 31 (1985).
- Ladd, J., Westbrook, G., Lewis, S., *Lamont-Doherty Geological Observatory Yearbook 1981–1982*, **8**, 17, Columbia University Thesis, NY (1982).
- Ladd, J.W., Truchan, M., Talwani, M., Stoffa, P.L., Buhl, P., Houtz, R., Mauffret, A., Westbrook, G., in *The Geological Society of America Memoir 162* (Bonini W.E., Hargraves, R.B., et al., eds.), 153, Geol. Soc of America, Washington, DC (1984).

- Lee, M.W., Hutchinson, D.R., Collett, T.S., Dillon, W.P., *J. Geophys. Res.*, **101B9**(20), 347 (1996).
- Lee, M.W., Hutchinson, D.R., Dillon, W.P., Miller, J.J., Agena, W.F., Swift, B.A., *Mar. Pet. Geol.*, **10**, 493 (1993).
- Linke, P., Wallmann, K., Suess, E., Hensen, C., Rehder, G., *Earth Plan. Sci. Lett.*, **235**, 79 (2005).
- Lodolo, E., Camerlenghi, A., Brancolini, G., *Antarctic Sci.*, **5**, 207 (1993).
- Lonsdale, M.J., in *Proc. Ocean Drilling Program, Scientific Results*, **113**, 27 (1990).
- Lonsdale P., *Am. Assoc. Pet. Geol. Bull.*, **69**, 1160 (1985).
- Lorenson, T.D., Collett, T.S., in *Proc. Ocean Drilling Program, Scientific Results*, **164**, 37 (1999).
- MacDonald, G.J., *Climatic Changes*, **16**, 247 (1990).
- Makogon, Y.F., *Gazov. Promst.*, **5**, 14 (1965).
- Makogon, Y.F., *Hydrates of Natural Gas*, Moscow, Nedra, Izadatelstro, (1974 in Russian) Transl. J. Cieslesicz, PennWell Books, Tulsa, Oklahoma, p. 237 (1981).
- Makogon, Y.F., "Natural Gas Hydrates: The State of Study in the USSR and Perspectives for Its Use," paper presented at the *Third Chemical Congress of North America*, Toronto, Canada, June 5–10 (1988).
- Makogon, Y.F., *Hydrates of Hydrocarbons*, PennWell Publishing Co., Tulsa, OK, p. 482 (1997).
- Makogon, Yu. F., Trebin, F.A., Trofimuk, A.A., Tsarev, V.P., Cherskiy, N.V., *Doklady Akademii Nauk SSSR*, **196**, 203 (1971) [Translation in *Doklady-Earth Science Section*, **196**, 197 (1972)].
- Malone, R.D., *Gas Hydrates Topical Report*, DOE/METC/SP-218, U.S. Department of Energy, April (1985).
- Manley, P.L., Flood, R.D., *AAPG Bull.*, **72**, 912 (1988).
- Mann, R., Gieskes, J., *Initial Rep. Deep Sea Drilling Project*, **28**, 805 (1975).
- Markl, R.G., Bryan, G.M., Ewing, J.I., *J. Geophys. Res.*, **75**, 4539 (1970).
- Masuda, Y., Kurihara, M., Ohuchi, H., Sato, T., in *Proc. Fourth International Conference on Gas Hydrates* (Mori, Y.H., ed.), Yokohama, May 19–23, 40 (2002).
- Mathews, M.A., *The Log Analyst*, p. 26, May–June (1986).
- Matsumoto, R., Okuda, Y., Aoki, Y., *Methane Hydrate*, Nikkei Science Publishers, Tokyo (1994).
- Max, M.D., (ed.), *Natural Gas Hydrate: in Oceanic and Permafrost Environments*, Kluwer Academic Publishers, London, 2nd Ed., p. 422 (2003).
- Max, M.D., Johnson, A.H., Dillon, W.P., *Economic Geology of Natural Gas Hydrate*, Springer, New York, p. 338 (2006).
- Mazurenko, L.L., Soloviev, V.A., Belenkaya, I., Ivanov, M.K., Pinheiro, L.M., *Terra Nova*, **14**, 321 (2002).
- McCarthy, J., Stevenson, A.J., Scholl, D.W., Vallier, T.L., *Mar. Pet. Geol.*, **1**, 151 (1984).
- McGrail, B.P., Young, J.S., Martin, P.F., Alexander, M.L., in *Scientific Results from the Mallik 2002 Gas Hydrate Production Research Well Program*, Mackenzie Delta, Northwest Territories, Canada (Dallimore, S.R., Collett, T.S., eds.), Geological Survey of Canada Bulletin 585, including CD , p. 110 (2005).
- McIver, R.D., *Initial Reports, Deep Sea Drilling Project*, **28**, 815 (1975).
- McIver, R.D., *Long-Term Energy Resources* (Meyer, R.F., Olson, J.C., eds.), Pitman, Boston, **1**, 713 (1981).
- McKirdy, D.M., Cook, P.J., *Am. Assoc. Pet. Geol. Bull.*, **64**, 2118 (1980).

- Mienert, J., Posewang, J. Baumann, M., *Gas Hydrates—Relevance to World Margin Stability and Climatic Change* (Henriet, J.-P., Mienert, J., eds.), The Geological Society, London, Special Publication 137, p. 275 (1998).
- Milkov, A.V. *Earth Sci. Rev.*, **66**(3–4), 183 (2004).
- Milkov, A.V., Claypool, G.E., Lee, Y.-J., Diekens, G.R., Xu, W., Borowski, W.S., and ODP Leg 204 Science Party, *Geology*, **31**(10), 833 (2003).
- Milkov, A.V., Xu, W., *Earth Planet Sci. Lett.*, **239**, 162 (2004).
- Miller, J.J., Lee, M.W., von Huene, R., *Am. Assoc. Pet. Geol. Bull.*, **75**, 910 (1991).
- Minshull, T., Singh, S., Pecher, I., Korenaga, J., Yuan, T., in *Proc. 2nd International Conference on Natural Gas Hydrates* (Monfort, J.P., ed.), Toulouse, France, June 2–6, 517 (1996).
- Minshull, T.A., Singh, S.C., Westbrook, G.K., *J. Geophys. Res.*, **99**(B3), 4715 (1994).
- Monfort, J.P., (ed.), in *Proc. 2nd International Conference on Natural Gas Hydrates*, Toulouse, France, June 2–6 (1996).
- Moore, B., Bolin, B., *Oceanus*, **29**, 9 (1989).
- Moore, G.W., Gieskes, J.M., *Initial Reports, Deep Sea Drilling Project 56*, **57**(2), 1269 (1980).
- Moore, J.C., Brown, K.M., Horath, F., Cochrane, G., MacKay, M., Moore, G., *Philosophical Transactions Royal Society of London Series A*, **335**, 275 (1992).
- Mori, Y.H., in *Proc. Fourth International Conference on Natural Gas Hydrates* (2 volumes and CD) Yokohama, May 19–23 (2002).
- Moridis, G.J., Collett, T.S., in *Recent Advances in the Study of Gas Hydrates* (Taylor, C., Kwan, J. eds.), Kluwer Academic Publishers, MA, p. 75 (2004).
- Moridis, G.J., Collett, T.S., Dallimore, S.R., Inoue, T., Mroz, T., in *Scientific Results from the Mallik 2002 Gas Hydrate Production Research Well Program*, Mackenzie Delta, Northwest Territories, Canada (Dallimore, S.R., Collett, T.S., eds.), Geological Survey of Canada Bulletin 585, including CD, p. 140 (2005).
- Moridis, G.J., Collett, T.S., Dallimore, S.R., Satoh, T., Hancock, S., Weatherill, B., in *Proc. of Fourth International Conference on Gas Hydrates* (Mori, Y.H., ed.), Yokohama, May 19–23, p. 239 (2002).
- Moridis, G.J., Sloan, E.D., “Gas Production Potential of Disperse Low-Saturation Hydrate Accumulations in Oceanic Sediments,” *Energy Conversion and Management Journal*, accepted (2006), also as LBNL Report 61446, August 2006.
- Neben, S., Hinz, K., Beiersdorf, H., in *Gas Hydrates—Relevance to World Margin Stability and Climatic Change* (Henriet, J.-P., Mienert, J., eds.), The Geological Society, London, Special Publication 137, p. 255 (1998).
- Normark, W.R., Hein, J.R., Powell, C.L., Lorenson, T.D., Lee, H.J., Edwards, B.D., *EOS, Trans. AGU*, 84(46), Fall Meeting Suppl., Abstract OS51B08555, **F845** (2003).
- Okuda, Y., in *Proc. of Thermal Engineering Symposium of July 7, 1995; Japan Association of Mechanical Engineering*, Tokyo, Japan, 5 (1995).
- Ostrander, W.J., *Geophysics*, **49**, 1637 (1984).
- Paull, C.K., Borowski, W.S., Rodriguez, N.M., and the ODP Leg 164 Shipboard Scientific Party, in *Gas Hydrates—Relevance to World Margin Stability and Climatic Change* (Henriet, J.-P., Mienert, J. eds.), The Geological Society, London, Special Publication 137, p. 153 (1998).
- Paull, C.K., Dillon, W.P., *Natural Gas Hydrates: Occurrence, Distribution and Detection*, American Geophysical Union Monograph 124 (2001).
- Paull, C.K., Lorenson, T.D., Borowowski, W.S., Ussler, W., Olsen, K., Rodriguez, N.M., Wehner, H., in *Proc. Ocean Drilling Program, Scientific Results*, **164**, 67 (1996).

- Paull, C.K., Ussler, W., Borowski, W.S., in (*First International Conference on Natural Gas Hydrates, Ann. N.Y. Acad. Sci.*) (Sloan, E.D., Happel, J., et al., eds.), **715**, 392 (1994).
- Paull, C.K., Ussler, W., Lorenson, T., Winters, W., Dougherty, J., *Geo-Mar. Lett.* **25**(5), 273, Nov. DOI:10.1007/s00367-005-0001-3 (2005).
- Pettigrew, T.L., *The Design and Operation of a Wireline Pressure Core Sampler*, ODP Tech Note 17 (1992).
- Pohlman, J.W., Canuel, E.A., Chapman, N.R., Spence, G.D., Whiticar, M.J., Coffin, R.B., *Org. Geochem.*, **36**, 703 (2005).
- Pooladi-Darvish, M., Hong, H., Bishnoi, P.R., *J. Can. Pet. Technol.*, **42**(11), 45 (2003).
- Posewang, J., Mienert, J., *Geo-Mar. Lett.*, **19**, 150 (1999).
- Prensky, S., in *SPWLA 36th Annual Logging Symposium*, June 26–29 (1995).
- Radler, M., *Oil Gas J.*, **98**(51), 121 (2000).
- Rao, Y.H., Subrahmanyam, C., Rastogi, A., Deka, B., *Geo-Mar. Lett.*, **21**, 1 (2001).
- Rastogi, A., Deka, B., Budhiraja, I.L., Agarwal, G.C., *Mar. Geores. Geotechnol.*, **17**, 49 (1999).
- Rehder, G., Kirby, S.H., Durhan, W.B., Stern, L.A., Peltzer, E.T., Pinkston, J., Brewer, P.G., *Geochim. Cosmochim. Acta*, **68**, 285 doi:10.1016/j.gca.2003.07.001 (2003).
- Rempel, A., *Theoretical and Experimental Investigations into the Formation and Accumulation of Gas Hydrates*, M.S. Thesis, University of British Columbia, Vancouver, B.C., Canada (1994).
- Ripmeester, J.A., Lu, H., Moudrakovski, I.L., Dutrisac, R., Wilson, L.D., Wright, F., Dallimore, S.R., in *Scientific Results from the Mallik 2002 Gas Hydrate Production Research Well Program*, Mackenzie Delta, Northwest Territories, Canada (Dallimore, S.R., Collett, T.S., eds.), Geological Survey of Canada Bulletin 585, including CD, p. 110 (2005).
- Roberts, H.H., in *Natural Gas Hydrates: Occurrence, Distribution and Detection* (Paull C.K., Dillon, W.P., eds.), Geophysical Monograph 124, American Geophysical Union, Washington, DC, p. 145 (2001).
- Sachs, J.D., *The End of Poverty*, Penguin Press, New York (2005).
- Sahling, H., Rickert, D., Lee, R.W., Linke, P., Suess, E., *Mar. Ecol. Prog. Ser.*, **231**, 121 (2002).
- Saltykova, N.A., Soloviev, V.A., Pavlenkin, A.D., *Sevmorgeologiya, Lenigrad*, 119 (1987).
- Sapir, M.H., Khramenkov, E.N., Yefremov, I.D., Ginzburg, G.D., Beniaminovich, A.E., Lenda, S.M., Koslova, V.I., *Geol. Nefti i Gaza*, **6**, 26 (1973).
- Sassen, R., MacDonald, I.R., *Org. Geochem.*, **22**(6), 1029 (1994).
- Sassen, R., MacDonald, I.R., *Org. Geochem.*, **26**, 289 (1997a).
- Sassen, R., MacDonald, I.R., “Thermogenic Gas Hydrates, Gulf of Mexico Continental Slope,” in *Proc. 213th ACS National Meeting*, San Francisco, CA, April 13–17, **42**(2), 472 (1997b).
- Sassen, R., Roberts, H., Milkov, A., DeFreitas, D., Lanoil, B., Zhang, C., *Chem. Geol.*, **205**, 195 (2004).
- Sato, M., *The Earth Monthly*, **16**, 533 (1994).
- Scholl, D.W., Cooper, A.K., *Am. Assoc. Pet. Geol. Bull.*, **62**, 2481 (1978).
- Schulteiss, P., Holland, M., Roberts, J., Druce, M., Humphrey, G. and the Shipboard Scientific Party of IODP Leg 311 nad NGHP Exp 1. “X-ray Images of Gas Hydrates Within Deep Sea Marine Sediment, Retrieved and Analyzed Using HYACINTH Pressure Coring Systems,” Poster at *American Geophysical Union Annual Meeting*, San Francisco, CA, December 14, 2006.

- Selim, M.S., Sloan, E.D., *AIChE J.*, **35**, 1049 (1989).
- Sheshukov, N.L., *Gazov. Delo.*, **6**, 8 (1972).
- Shipboard Scientific Party, Site 796, in *Proc. Ocean Drilling Program, Initial Reports*, **127**, 247 (1990).
- Shipboard Scientific Party, Site 808, in *Proc. Ocean Drilling Program, Initial Reports*, **131**, 71 (1991).
- Shipboard Scientific Party, Site 1041, in *Proc. Ocean Drilling Program, Initial Reports*, **170**, 153 (1997).
- Shipley, T.H., Didyk, B.M., *Initial Reports, Deep Sea Drilling Project*, **66**, 547 (1982).
- Shipley, T.H., Houston, M.H., Buffler, R.T., Shaub, F.J., McMillen, K.J., Ladd, J.W., Worzel, J.L., *American Association of Petroleum Geologists Bulletin*, **63**, 2204 (1979).
- Singh, S.C., Minshull, T.A., *J. Geophys. Res.*, **99B12**, 24, 221 (1994).
- Sloan, E.D., Happel, J., Hnatow, M.A., (eds), in *International Conference on Natural Gas Hydrates, Ann. N.Y. Acad. Sci.*, **715** (1994).
- Soloviev, V.A., *Russian Geol. Geophys.*, **43**(7), 648 (2002).
- Soloviev, V.A., Ginsburg, G.D., *Mar. Geol.*, **137**, 59 (1997).
- Stagg, H.M.J., Symonds, P.A., Exon, N.F., Auzende, J-M., Dickens, G.R., Van de Beuque, S., in G.R. Wood (compiler), *Second Sprigg Symposium, Abstracts, Geological Society of Australia*, **60**, 69 (2000).
- Stern, L.A., Kirby, S.H., Durham, W.B., in *Scientific Results from the Mallik 2002 Gas Hydrate Production Research Well Program*, Mackenzie Delta, Northwest Territories, Canada (Dallimore, S.R., Collett, T.S., eds.), Geological Survey of Canada Bulletin 585, including CD, p. 109 (2005).
- Suess, E., Bohrman, G., Greinert, J., Lausch, E., *Sci. Am.*, **281**(5), 761 (1999b).
- Suess, E., Torres, M.E., Bohrmann, G., Collier, R.W., Greinert, J., Linke, P., Rehder, G., Tréhu, A., Wallmann, K., Winckler, G., Zuleger, E., *Earth Planet. Sci. Lett.*, **170**, 1 (1999a).
- Sumetz, V.I., *Gaz. Prom.*, **2**, 24 (1974).
- Summerhayes, C.P., Bornhold, B.D., Embley, R.W., *Mar. Geol.*, **31**, 265 (1979).
- Takayama, T., Nishi, M., Uchida, T., Akihisa, K., Sawamure, F., Ochiai, K., in *Scientific Results from the Mallik 2002 Gas Hydrate Production Research Well Program*, Mackenzie Delta, Northwest Territories, Canada (Dallimore, S.R., Collett, T.S., eds.), Geological Survey of Canada Bulletin 585, including CD, p. 115 (2005).
- Tamano T, Toba, T., Aoki, Y., in *Proc. 11th World Petroleum Congress*, Wiley, New York, **2**, 135 (1984).
- Taylor, A.E., Wetmiller, R.J., Judge, A.S., in W. Denner (ed.), *Symposium on Research in the Labrador Coastal and Offshore Region*, Memorial University of Newfoundland, p. 91 (1979).
- Taylor, C.E., Kwan, J.T. (eds.), *Advances in the Study of Gas Hydrates*, Springer, New York, p. 225 (2004).
- Thomas, E., Shackleton, N.J., *Correlation of the Early Paleogene in Northwest Europe* (Knox, R.O., Corfield, R.M., et al., eds.), Geological Society (London) Special Publication 101, p. 401 (1996).
- Tohidi, B., Anderson, R., Clennell, M.B., Burgess, R.W., Biderkab, A.-B., *Geology*, **29**(9), 867 (2001).
- Torres, M.E., Wallmann, K., Tréhu, A.M., Bohrmann, G., Borowski, W.S., Tomaru, H., *Earth Planet. Sci. Lett.*, **226**, 225 (2004).

- Torres, M.E., Wallmann, K., Tréhu, A.M., Bohrmann, G., Borowski, W.S., Tomaru, H., *Earth Planetary Sci. Lett.*, **239**, 168 (2005).
- Tréhu, A.M., Glemings, P.B., Bangs, N.L., Chevallier, J., Gracia, E., Johnson, J.E., Liu, C.-S., Liu, X., Riedel, M., Torres, M.E., *Geophys. Res. Lett.*, **31**, L23310, doi:10.1029/2004GL021286 (2004a).
- Tréhu, A.M., Long, P.E., Torres, M.E., Bohrmann, G., Rack, F.R., Collett, T.S., Goldberg, D.S., et al., *Earth Planetary Sci. Lett.*, **222**, 845 (2004b).
- Tréhu, A.M., Ruppel, C., Holland, M., Dickens, G.R., Torres, M.E., Collett, T.S., Goldberg, D.S., Riedel, M., Schultheiss, P., *Oceanography*, **19**(4), 124 (2006).
- Trofimuk, A.A., Cherskiy, N.V., Lebedev, V.S., Semin V.I., et al., *Geol. Geofiz.*, **2**, 3 (1973).
- Trofimuk, A.A., Cherskiy, N.V., Tsarev, V.P., *Future Supply of Nature-Made Petroleum and Gas* (Meyer, R.F., ed.), Pergamon Press, New York, 919 (1977).
- Trofimuk, A.A., Cherskii, N.V., Tsarev, V.P., Nikitin, S.P., *Geologiva i Geofizika*, **23**, 3 (1982).
- Trofimuk, A.A., Makogon, Y.F., Tolkachev, M.V., *Geologiya Nefti i Gaza*, **10**, 15 (1981).
- Tsyplkin, G.G., *Gas Hydrates: Challenges for the Future*, Ann. N.Y. Acad. Sci. (Holder, G.D., Bishnoi, P.R., eds.), **912**, p. 428 (2000).
- Tucholke, B.F., Bryan, G.M., Ewing, J.I., *Am. Assoc. Pet. Geol. Bull.*, **61**, 698 (1977).
- Tulk, C.A., Wright, J.F., Ratcliffe, C.I., Ripmeester, J.A., in *Geological Survey of Canada Bulletin 544* (Dallimore, S.R., Uchida, T., et al., eds.), p. 263 (1999).
- Veerayya, M., Karisiddaiah, S.M., Vora, K.H., Wagle, B.G., Almeida, R., in *Gas Hydrates—Relevance to World Margin Stability and Climatic Change* (Henriet, J.-P., Mienert, J., eds.), The Geological Society, London, Special Publication 137, p. 239 (1998).
- Weaver, J.S., Stewart, J.M., in Roger J.E. Brown Memorial Volume, in *Proc. Fourth Canadian Permafrost Conference*, **1981**, 312 (1982).
- Weitemeyer, K., Constable, S., Key, K., *The Leading Edge*, **25**, 629 (2006).
- Westbrook, G.K., Carson, B., Musgrave, R.J., et al., Scientific Drilling Project in *Proc. Ocean Drilling Program Leg 146*, **146**(1), 301 (1994).
- White, R.S., *Planet. Sci. Lett.*, **42**, 114 (1979).
- Whiticar, M.J., Faber, E., Schoell, M., *Geochim. Cosmochim Acta*, **50**, 693 (1986).
- Whiticar, M.J., Hovland, M., Kastner, M., Sample, J.C., in *Proc. Ocean Drilling Program, Scientific Results*, **146**(1), 385 (1995).
- Wood, W.T., Gettrust, J.F., Chapman, N.R., Spence, G.D., Hyndman, R.D., *Nature*, **420**, 656 (2002).
- Woodside, J.M., Ivanov, M.K., Limonov, A.F., and Shipboard Scientists of the Anaxiprobe Expeditions, in *Gas Hydrates—Relevance to World Margin Stability and Climatic Change* (Henriet, J.-P., Mienert, J., eds.), The Geological Society, London, Special Publication 137, p. 177 (1998).
- Wright, J.F., Dallimore, S.D., in *Proc. Fifth International Conference Gas Hydrates* (Austvik, T., ed.) (paper 5039), 4 volumes and CD, Trondheim, Norway, June 13–15, p. 1699 (2005).
- Wright, J.F., Dallimore, S.D., Nixon, F.M., Dchesne, C., in *Scientific Results from the Mallik 2002 Gas Hydrate Production Research Well Program*, Mackenzie Delta, Northwest Territories, Canada (Dallimore, S.R., Collett, T.S., eds.), Geological Survey of Canada Bulletin 585, including CD, p. 92 (2005).
- Wu, S., Zhang, G., Huang, Y., Liang, J., Wong, H.K., *Marine and Petroleum Geology*, **22**, 403 (2005).

- Xu, W., Ruppel, C., *J. Geophys. Res.*, **104**, 5,081 (1999).
- Yakushev, V.S., Istomin,V.A., "Gas Hydrates Self-Preservation Effect," presented at the *IPC-91 Symposium*, Sapporo, Japan, September (1991).
- Yamano, M., Uyeda, S., in *Proc. ODP. Sci. Results* (Suess, E., von Huene, R., et al., eds.), **112**, p. 653 (1990).
- Yefremova, A.G., Gritchina, N.D., *Geologiya Nefti i Gaza*, **2**, 32 (1981).
- Yefremova, A.G., Zhizhchenko, B.P., *Doklady Akademii Nauk SSSR*, **214**, 1179 (1974).
- Yousif, M.H., Abass, H., Selim, M.S., Sloan, E.D., SPE 18320, in *Proc. 63rd Annual Technical Conference of SPE*, Houston, TX, October 2–5 (1988).
- Yousif, M.H, Sloan, E.D., in *SPE Reserve Engineering*, 452, November (1991).
- Yuan, T., Hyndman, R.D., Spence, G.D., Desmons, B., *J. Geophys. Res.*, **101**, 13655 (1996).
- Zillmer, M., Flueh, E.R., Petersen, J., *Geophys. J. Int.*, **161**, 662 (2005).
- Zonenshayn, L.P., Murdmaa, I.O., Baranov, B.V., Kusnetsov, A.P., Kuzin, V.S., Kuz'min, M.I., Avdeyko, G.P., et al., *Oceanology*, **27**, 795 (1987).